

Runway Pressure Research

The effect of En-Route Delay Absorption
on the runway throughput

Wouter Vermeersch

Technische Universiteit Delft



Runway Pressure Research

The effect of En-Route Delay Absorption on the
runway throughput

by

Wouter Vermeersch

in partial fulfillment of the requirements for the degree of

Master of Science
in Aerospace Engineering

at the Delft University of Technology,

Student number: 1396048
Project duration: January 1, 2015 – September 30, 2015
Supervisor: Prof. dr. R. Curran
Thesis committee: Dr. ir. J. Ellerbroek, TU Delft
Ir. G. A. Mercado Velasco, To70
Dr. ir. D. Mijatovic, LVNL
Ir. P. C. Roling, TU Delft

An electronic version of this thesis is available at <http://repository.tudelft.nl/>.

Preface

During a guest lecture of the course Airport Operations, I made contact with dr. ir. D. Mijatovic to apply for an internship at Air Traffic Control the Netherlands (LVNL). During this internship, I had the opportunity to work out a research proposal which lead to this Master's Research Project. Special thanks goes out to ir. P. C. Roling for the inspiring lectures that lead to my internship and graduation project at LVNL. I would also like to thank him for the supervision and feedback throughout this project.

A warm thank you to all the members of LVNL and the Strategy department in particular, to make this research project such an unique experience. Special thanks goes out to dr. ir. D. Mijatovic and ir. E. Westerveld for their supervision and guidance and to the operational experts R. Pauptit and D. Noordam for sharing their knowledge about the complex world of air traffic control. The cover picture of this report is provided by LVNL and shows a series of aircraft lined up for landing on runway 18C of Schiphol airport [1].

I would like to thank To70 for the opportunity to work with a professional simulation software package and I specially thank ir. G.A. Mercado Velasco for his support and feedback with the simulations.

Last, but not least, I would like to thank my psychologist, MSc. M. Broekmans, for her understanding, patience and support during the final moments of my student life.

*Wouter Vermeersch
Schiphol, October 2015*

Summary

Major airports in Europe experience a number of arrivals close to the maximum of their capacity throughout the day. Multiple aircraft arrive at the airport in a short time window and often have to be delayed in the airspace surrounding the airport before they are cleared to land. A higher fuel burn and costs for the airlines is the result, but it also has a negative effect on the environment in terms of additional pollution and noise. The Cross-border Arrival Management (XMAN) project, which is part of the Single European Sky program, tries to reduce the negative effects of delay in the proximity of airports. The main idea is to shift the necessary delay in the Terminal Manoeuvring Area (TMA) or holding towards the cruise flight phase by reducing the speed of aircraft. If an aircraft is inbound for an airport and the expected arrival time is too close to the arrival time of a leading aircraft, the trailing aircraft can be asked to slow down such that it arrives at the airport when the runway is available. The speed reduction or gaining additional flight time is referred to as 'delay absorption'.

Although the shift of delay absorption from the TMA to the en-route phase shows promising results for fuel consumption and reduced emissions, the question rises whether this En-Route Delay Absorption (ERDA) can also have a negative impact on the runway efficiency. If aircraft are delayed too much in an earlier flight phase due to e.g. inaccuracy of the expected arrival times, so called gaps appear in the landing sequence. As a result, the total number of aircraft that actually landed per time period decreases.

The idea is that in order to maintain an optimal runway throughput, some expected delay should be left in the TMA for the approach controller to absorb. In that case, the approach controller can fine-tune a tight landing sequence without any gaps that would result in an underused runway when the demand for landings is high. This phenomenon is defined as Runway Pressure.

The main goal of this research project is to investigate the effect on the runway throughput when the expected delay is absorbed in the en-route phase. To achieve this goal, different fast time simulations are performed with a model of both Schiphol and Charles de Gaulle airport.

The amount of expected delay that needs to be absorbed in an earlier flight phase is calculated in analogy with the working principles of the inbound planning system of both Schiphol and Charles de Gaulle airport. The expected arrival time at the runway is given for an aircraft and compared with the expected arrival time and minimum required separation time of the previous aircraft in the inbound planning. If the trailing aircraft is expected to arrive too soon at the runway, it has to be delayed prior to passing the Initial Approach Fix (IAF). How the aircraft is delayed, is not researched in this project. However, a maximum of five minutes delay absorption in an earlier flight phase is set, based on previous research on this topic.

One simulation scenario consists of a period of two hours where the amount of demand for arrivals changes throughout the inbound peak. The demand exceeds the maximum runway capacity for a certain period of time in each arrival peak. The landing sequence order does not change. A comparison is made between scenarios with the same amount of demand throughout the inbound peak, but with all aircraft either experience En-Route Delay Absorption or not. The outcome of the simulations is the average amount of delay in the \bar{T} per 20 minutes and the amount of landings per rolling hour. A rolling hour consists of three consecutive time periods of 20 minutes.

Based on the simulation outcomes, it can be concluded that ERDA can result in a small decrease of runway throughput, with a maximum of one aircraft per rolling hour. However, a decrease does not always occur. By the end of the inbound peak, the actual landing time of an aircraft with ERDA is between 30 and 90 seconds later than the same aircraft with no ERDA. So the inbound peak is extended in time and shifted backwards with approximately one extra landing when ERDA is applied. The benefit is that aircraft have to spend up to four minutes less in the TMA.

An important parameter that determines the runway throughput, is the inter-arrival separation. This separation between different aircraft wake vortex categories is translated from distance to a time based separation. The same time interval at the threshold is used for the interval times between aircraft passing the IAF. The required passing time at the IAF can be calculated by one average flight time for each aircraft category, where a distinction has to be made between the flight time of jet and turboprop engine aircraft. If the total flight time in the TMA between aircraft categories deviates more than one minute, it can be necessary to use different approach paths to the final approach fix for each aircraft category, in order to maintain safety and a sufficient runway throughput.

It is important that the calculations of the inter-arrival times at the threshold and IAF are as accurate as possible. If the inter-arrival time for each aircraft is wrongly increased by five to ten seconds, the throughput decreases with two landings per hour. It is meaningful to take this into account when a dynamic time based separation for the threshold is calculated and compensated for strong headwinds.

The definition of runway pressure suggests that there is a minimum amount of delay that should be left for the approach controller to absorb, in order to guarantee sufficient runway throughput. From the results of this research, it can be concluded that there will always be a minimum amount of delay that needs to be absorbed in the TMA to optimize the landing sequence. However, the minimum amount of delay in the TMA is a consequence of the difference in flight time between aircraft types and the accuracy of the actual time passing the IAF. If the inter-arrival times at the IAF are set correctly, a minimum amount of delay is not required to maintain sufficient runway throughput.

Although a minimum amount of delay in the TMA is not required to maintain runway throughput, not all delay can always be absorbed in earlier flight phases. Therefore, it is recommended to investigate the effect on the workload of air traffic controllers and the delay absorption capacity of the different airspace sectors along the route. If the expected delay is divided and absorbed in the different flight phases along the trajectory towards the airport, the arrival process is easier to manage for all controllers involved.

Contents

Summary	v
1 Introduction	1
2 General research project information	3
2.1 Research objectives and questions	3
2.2 Available data	4
2.3 Simulation program	5
2.4 Definitions	5
3 Landing procedures	9
3.1 Schiphol airport landing procedures	9
3.1.1 Airspace structure around Schiphol airport	9
3.1.2 Arrival management and inbound planning	10
3.1.3 Trajectory predictor and approach paths	11
3.1.4 Fleet mix	12
3.1.5 Current separation standards	13
3.1.6 Time based separation values	14
3.1.7 Flight times in the TMA	16
3.1.8 Arrivals, runway capacity and delay	18
3.2 Charles de Gaulle airport landing procedures	21
3.2.1 Airspace structure around CDG airport	21
3.2.2 Trajectory predictor and routes in TMA	22
3.2.3 Arrival management system MAESTRO	23
3.2.4 Inbound peaks and runway capacity	23
4 Simulation Set-up	25
4.1 AirTop Simulation Software	25
4.2 Important elements of the simulated environment	26
4.2.1 Flight plans, trajectory predictor and arrival management	26
4.2.2 En route delay absorption in AirTop	26
4.3 Schiphol airport simulation model	28
4.3.1 En-route simulation environment	28
4.3.2 TMA structure and different parameters	28
4.3.3 Variables and scenarios	31
4.3.4 Verification of Schiphol airport model	33
4.4 Charles de Gaulle airport simulation model	37
4.4.1 TMA structure and important parameters	37
4.4.2 Variables and scenarios	39
4.4.3 Verification of CDG airport model	40
5 Simulation results and discussion	43
5.1 Schiphol airport simulation results	43
5.1.1 Results of demand and the relationship with delay	43
5.1.2 Results of En-Route Delay Absorption with a single approach leg	49
5.1.3 Results of ERDA for two merging approach legs	54
5.1.4 Discussion Schiphol airport simulation results	56
5.2 Charles de Gaulle airport simulation results	58
5.2.1 Effect on demand, delay and throughput	58
5.2.2 Effect when there is an offset between two IAFs	62
5.2.3 Discussion CDG airport simulation results	64

6	Conclusions & Recommendations	65
6.1	Conclusions	65
6.1.1	Conclusions related to the research questions	65
6.1.2	Other conclusions	66
6.2	Recommendations	67
	Bibliography	69
A	Additional Schiphol airport information	71
A.1	Reference flight times of the simulation	71
A.2	Fleet mix, landing sequence and capacity	72
A.3	STAR routes Schiphol airport	72
B	Additional Charles de Gaulle airport Information	77
C	Overview additional results	79
C.1	Remaining results of Schiphol airport	79
C.2	Remaining results of CDG airport	80
	Acronyms	83

1

Introduction

Major airports in Europe experience a number of arrivals close to the maximum of their capacity throughout the day. Multiple aircraft arrive at the airport in a short time window and often have to be delayed in the airspace surrounding the airport before they are cleared to land. A higher fuel burn and costs for the airlines is the result, but it also has a negative effect on the environment in terms of additional pollution and noise. The Cross-border Arrival Management (XMAN) project, which is part of the Single European Sky program, tries to reduce the negative effects of delay in the proximity of airports. The main idea is to shift the necessary delay in the Terminal Manoeuvring Area (TMA) or holding towards the cruise flight phase by reducing the speed of aircraft. If an aircraft is inbound for an airport and the expected arrival time is too close to the arrival time of a leading aircraft, the trailing aircraft can be asked to slow down such that it arrives at the airport when the runway is available. The concept is illustrated in figure 1.1.

The XMAN Heathrow trials: the delay sharing strategy between London Terminal (LATC), London ACC (LACC) and Reims UAC (En-route)

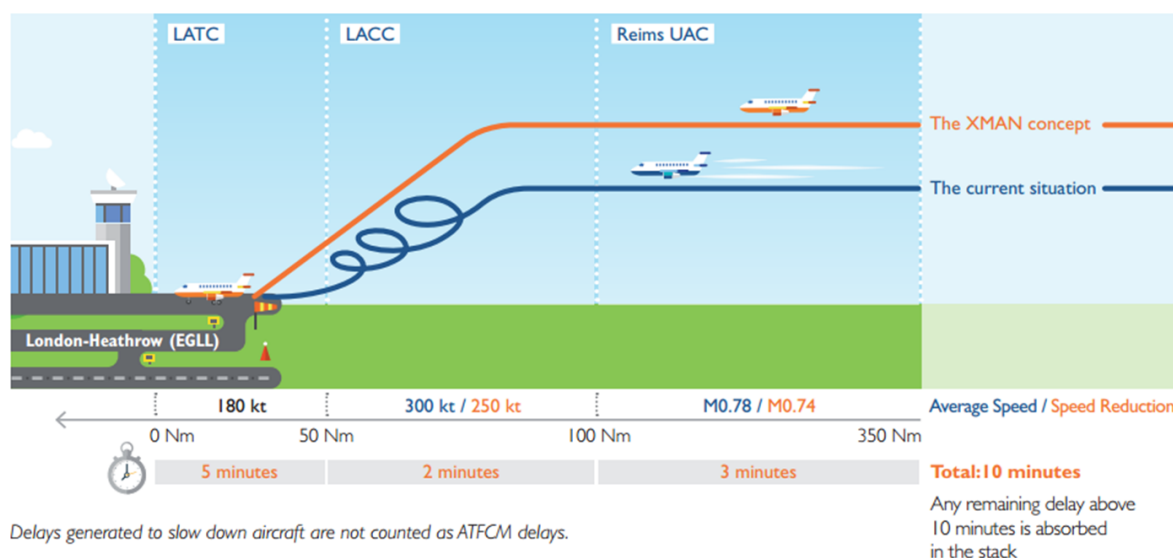


Figure 1.1: Illustration of the XMAN concept for Heathrow airport [2].

The goal is to implement the XMAN concept at five main airports in Europe; London Heathrow, Paris Charles de Gaulle, Frankfurt, Munich and Schiphol airport [3]. Live trials for Heathrow airport started in April 2014 in cooperation with the English (NATS) and French (DSNA) Air Navigation Service Providers (ANSPs) [2]. Although the shift of delay absorption to the en-route phase shows promising results for

fuel consumption and reduced emissions, the question rises whether this shift can also have a negative impact on the runway efficiency.

If aircraft are delayed too much in an earlier flight phase due to e.g. inaccuracy of the expected arrival times, so called gaps appear in the landing sequence. As a result, the total number of actual landing slots decreases. Such a decrease in runway throughput is not acceptable by many stakeholders. The idea is that in order to maintain an optimal runway throughput, some expected delay should be left in the TMA for the approach controller to absorb. In that case, the approach controller can create a tight landing sequence without any gaps in the landing sequence that would result in an underused runway when the demand for landings is high. This phenomenon is defined as Runway Pressure [4]. However, research on the working principles and parameters behind Runway Pressure has not been performed so far in the academic world.

If the amount of Runway Pressure is known for each airport mentioned above, the benefits of XMAN can be used without the negative side effect of a decreased runway throughput.

The main goal of this research project is to investigate the effect on the runway throughput when the expected delay is absorbed in the en-route phase. To achieve this goal, different fast time simulations will be performed with a model of both Schiphol and Charles de Gaulle airport.

Structure of the report

The research objectives and questions are described in chapter 2, together with the most important definitions. The landing procedures of both Schiphol and Charles de Gaulle airport are explained in chapter 3. These procedures and relevant parameters will be implemented in the simulation program in order to create a realistic model of both airports. Chapter 4 describes the simulation program and set-up, as well as the verification of the models. The results of the simulations and the discussion on those results are mentioned in chapter 5, followed by the recommendations and conclusions of this research in chapter 6.

2

General research project information

In this chapter, the main goal and objectives of this project are described, followed by the different research questions that are related to these objectives. Because the reader is confronted with specific terms and abbreviations in this report, an overview of important definitions is given in section 2.4. The chapter ends with additional background information on the available data during the research and the decision to use a specific simulation program.

2.1. Research objectives and questions

At the beginning of the project, certain objectives and goals are created to give guidance to the project. As stated in the introduction, the main goal of this research project is to investigate the effect of the absorption of congestion delay in the en-route phase on the runway throughput.

The sub-goal is to get insight in the working principles behind the definition of Runway Pressure, which is defined as the amount of delay that shall be left for the approach to be absorbed. This will guarantee an optimum use of the runway and avoiding 'gaps' in the landing sequence [4].

Both goals can be achieved by developing a model that represents the current landing procedures of an airport runway system and identifying the relevant parameters that have an effect on runway throughput and congestion delay. The model must be applicable for different airport systems.

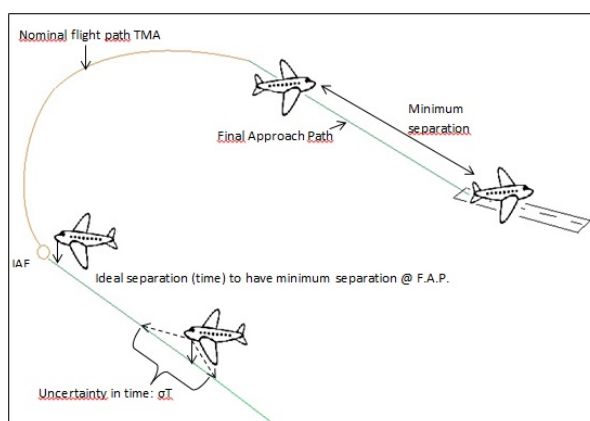


Figure 2.1: Illustration of the expected relation between the time separation at the threshold and the required time separation at the IAF.

Another sub-goal that will assist in achieving the main goal of this project is to formulate a relationship between the optimal minimum (time) separation at the threshold and the interval time of two aircraft passing the Initial Approach Fix (IAF) when flying a fixed arrival path. An illustration is given in figure 2.1. It is expected that this relationship will result in a set of Controlled Time Over (CTO) IAF values

for different aircraft types in the scheduled landing sequence. A distinction in different approach paths will be made between one IAF to one runway and two IAFs merging in the TMA to one runway.

The final research objective is to perform a fast-time simulation and investigate the effect of changing demand, fleet mix, nominal flight paths, etc. on the congestion delay and runway throughput of the system.

Research questions

The following research questions are related to the goals and objectives mentioned earlier. The main research question is formulated as:

What is the effect on the actual runway throughput if the expected delay in the TMA is absorbed in the en-route phase? R.Q. 1

The sub-questions that support the main question are defined as:

What is the CTO IAF for each aircraft in the landing sequence to obtain minimum separation at the runway threshold? R.Q. 2

Which parameters have a substantial effect on the CTO mentioned in R.Q. 2 R.Q. 3

How many aircraft, in different fleet mix combinations, can be offered to the TMA of the airport for a certain runway capacity without causing any congestion delay? R.Q. 4

What is the development of the delay in time when the demand exceeds the maximum arrival capacity? R.Q. 5

What is the margin of the demand such that no unacceptable delays (or gaps in the landing sequence) occur? R.Q. 6

What is the Runway Pressure value of different IAF - runway combinations to guarantee a certain runway throughput? R.Q. 7

What is the standard deviation of each Runway Pressure value? R.Q. 8

Which parameters used in the simulations have a significant effect on the runway throughput and delay? R.Q. 9

By answering these research questions, information will become available to support stakeholders in their decision to shift a certain amount of congestion delay towards the en-route flight phase.

2.2. Available data

Air Traffic Control the Netherlands provides access to the database of their ATM system, containing radar tracks and all other relevant historic data from airplanes flying into the Amsterdam Flight Information Region (FIR). Estimated Time of Arrival (ETA) and Actual Time of Arrival (ATA) as well as estimated and actual times over waypoints are available, together with wake-vortex category, airspeed and altitude information. The assigned Standard Arrival Route (STAR), IAF and actual used runway information is also available. Furthermore, details on actual agreed capacity of the runway for certain time periods can be obtained as well. This is important, because the runway capacity is sometimes limited due to equipment restrictions, taxiway maintenance, etc. This could have an effect on the results and has to be checked.

Data from Charles de Gaulle airport was only available at the end of the research project. As a result, the verification of the simulation model for this airport could not be tested as thorough compared to the model of Schiphol airport.

2.3. Simulation program

There are three different options to acquire a (fast-time) simulation program for this research; Either use a commercial simulation package, modify and use an existing simulation program from the Control and Simulation department of the Aerospace Faculty or create a new simulation algorithm. A commercial program is often too expensive and can be limited in its inputs and outputs. As a result, there is a chance the user cannot perform the analysis as intended. The same is true for an existing simulation program from the TU Delft, except for the cost price. Creating a new algorithm on the other hand is time consuming and acceptance of the results by the general public can be a problem, even if the validation of the program is done thorough.

In the thesis of van der Klugt [5], an overview of different simulation programs is composed. From all available commercial programs, AirTOP has the best properties for this research. It has the tools to design every required airspace structures to simulate incoming traffic, it can perform Monte-Carlo simulations and can simulate time based separations standards between aircraft [6]. Furthermore, this program is also used by EUROCONTROL, NLR, To70 and other European research and consultancy firms, which increases the acceptancy level of the results from this research. An agreement between the researcher and To70 is constructed such that AirTOP can be used for this research under the supervision of To70. Due to limited time and resources, a normal set-up of the simulation procedures cannot be performed. This means that the researcher will have to make a simulation plan, put the simulation environment into the software package and perform a validation of the results by himself. Feedback on the processed work will be given, but in normal simulation work, different experts would perform checks and validations. On the other hand, it is in the interest of the Master student to show he possesses these professional working methods.

2.4. Definitions

Throughout the air traffic industry, similar terms are often used which can be interpret by the reader differently than intended by the author(s). To avoid this, some key terms related to this project are described in table 2.1 and 2.2 .

This research will investigate the absorption of congestion delay in the en-route phase, excluding the holding sub-phase. Although holding is officially part of the en-route phase, it will often only be provoked due to congestion delay in the TMA where the approach flight phase takes place. Therefore, holding is considered as part of the approach phase in this research.

Table 2.1: List of important terms and abbreviations.

Terms & abbreviations	Description	Described by
Runway Pressure 'P'	<i>The Runway Pressure P is defined by the amount of delay that shall be left for the approach controller to be absorbed.</i> This is to guarantee an optimum use of the runway and avoiding "holes" in the sequence. This value may vary with "physical" parameters such as IAF, Runways in use, Type of Aircraft, Wind, etc.	Regniaud [4]
En-route flight phase	<i>From completion of Initial Climb through cruise altitude and completion of controlled descent to the Initial Approach Fix.</i> This flight phase has the following three sub-phases that are important for this research: Cruise, Descent and Holding.	ICAO[7]
Cruise flight phase	A sub-phase of the en-route flight phase defined as: Any level flight segment after arrival at initial cruise altitude until the start of descent to the destination.	ICAO
Descent flight phase	<i>Descent from cruise to either Initial Approach Fix (IAF) or VFR pattern entry.</i>	ICAO
Holding	<i>Execution of a predetermined manoeuvre (usually an oval racetrack pattern) which keeps the aircraft within a specified airspace while awaiting further clearance.</i> Holdings are often executed at or close to the IAFs. This phase is officially part of the en-route phase, but will be treated as part of the approach phase.	ICAO
Approach flight phase	<i>From the Initial Approach Fix (IAF) to the beginning of the landing flare.</i>	ICAO

Table 2.2: (Continued) List of important terms and abbreviations.

Terms & abbreviations	Description	Described by
ETA	<p>Estimated Time of Arrival: the time computed by the FMS for the flight arriving at a point related to the destination airport. (SESAR definition)</p> <p>In this research the ETA will be calculated by a Trajectory Predictor (TP) of the ground ATM system and not by the FMS. However, the principle stays the same: the estimated time of touchdown on the runway (or passing the threshold), which is calculated by the relevant information that is available at that moment.</p>	EUROCONTROL [8]
ATA	<p><i>Actual Time of Arrival: the time an aircraft has touchdown on the runway.</i></p> <p>The available radar data from LVNL gives the ATA time value when the aircraft passes the runway threshold.</p> <p>EUROCONTROL uses the term ATA in flow management documents for estimated time of arrival taking into account real time updates for flow management. The term Actual Landing Time (ALDT) is used for touchdown time. However, at LVNL and in other literature the abbreviations ATA is used as defined here and will be used as such during this research.</p>	Author/LVNL
ETO	<p><i>Estimated Time Over: estimated time over a significant point.</i></p> <p>Similar to the ETA, but instead of the runway threshold a different report or waypoint is used.</p>	EUROCONTROL
ATO	<p><i>Actual Time Over: the time at which a flight will actually arrive over an area based on flight plan activation information.</i></p> <p>In this research only the arrival or passing time over a significant point is used.</p>	EUROCONTROL
CTO	<p><i>Controlled Time Over: an ATM imposed time constraint over a point.</i></p> <p>For example a time constraint at which an aircraft has to pass the IAF to maintain an optimal arrival sequence.</p>	EUROCONTROL
Nominal flight path	<p><i>A 3D flight path determined by a set of waypoints which serves as a reference flight path to use 4D trajectory predictions.</i></p> <p>The nominal flight path is used for the calculation of the ETA and ETO by a Trajectory Predictor and serves as a reference flightpath. It is not the same as a Fixed Arrival Route.</p>	Author
Bunching effect	<p><i>The arrival of multiple aircraft at an entry point of an airspace area in a relative short time period.</i></p>	Author
ERDA	<p><i>En-route Delay Absorption: an ATM procedure to increase the flight time of an aircraft in the en-route flight phase as a purpose to absorb the expected delay in the approach phase.</i></p>	Author

3

Landing procedures

Each airport has a specific lay-out and surrounding airspace structure which results in a specific way of handling air traffic. The most important landing procedures and relevant parameters for the research on runway throughput at both Schiphol and Charles de Gaulle airport are described in this chapter.

3.1. Schiphol airport landing procedures

The different elements that are important for the understanding of the landing procedures at Schiphol airport are explained in this section. The information that is given here, will be used to create the simulation environment which is further described in the next chapter. This section starts with a description of the airspace around Schiphol airport and the runway lay-out. Chapter 3.1.2 explains the working principles of the inbound planning tool used by the air traffic controllers, followed by an explanation of the Trajectory Predictor (TP). The fleet mix used in this research is elaborated in chapter 3.1.4 and chapter 3.1.5 describes the current standards separation values, followed by the time based Separation standards. These separation standards are related to the flight times of aircraft in the TMA of Schiphol airport, which is explained in chapter 3.1.7. This section ends with a description of the arrival peaks and runway capacity in section 3.1.8.

3.1.1. Airspace structure around Schiphol airport

Aircraft inbound for Schiphol airport will in general be guided from one of the five main upper airways towards one of the three Initial Approach Fixes (IAFs); RIVER, SUGOL or ARTIP. Figure 3.1 (a) shows an illustration of the main airways in blue and the Standard Arrival Routes (STARs) in red. Outbound traffic will follow the green routes. There are large military airspaces in the north and south of the Netherlands, which can be used for civil aviation if there are no military activities taking place. The exact STAR chart retrieved from the Aeronautical Information Publication (AIP) is given as a reference in appendix A.

When aircraft are under control of an APP controller inside the TMA, they are guided towards the glideslope of the assigned runway by radar vectoring. The TMA of Schiphol airport has a radius of approximately 30 NM. Although any route towards the runway can be instructed to the pilots, most aircraft will be guided along the same and possibly shortest approach path. An example of actual radar tracks of a morning inbound peak on 1 June 2014 is given in figure 3.1 (b), together with a location of the three IAFs. Figure 3.4 in section 3.1.3 gives an overview of all the common approach paths relevant for this research project.

Schiphol airport has six runways in different directions of which three runways are parallel. Figure 3.2 gives an overview of all the runways at Schiphol airport. Depending on the wind direction, the preferred main runway for landing is either 18R or 06 and the secondary runway is 18C or 36R. During an inbound peak, at most two runways are available for landings due to regulations and agreements with surrounding communities and the government [9] [10]. The number of landings on these four runways represent 80% of all landings at Schiphol airport (based on the summer period from April to

October 2014). To limit the amount of work for analysis and simulations during this research, only landings on those four runways are investigated and simulated.

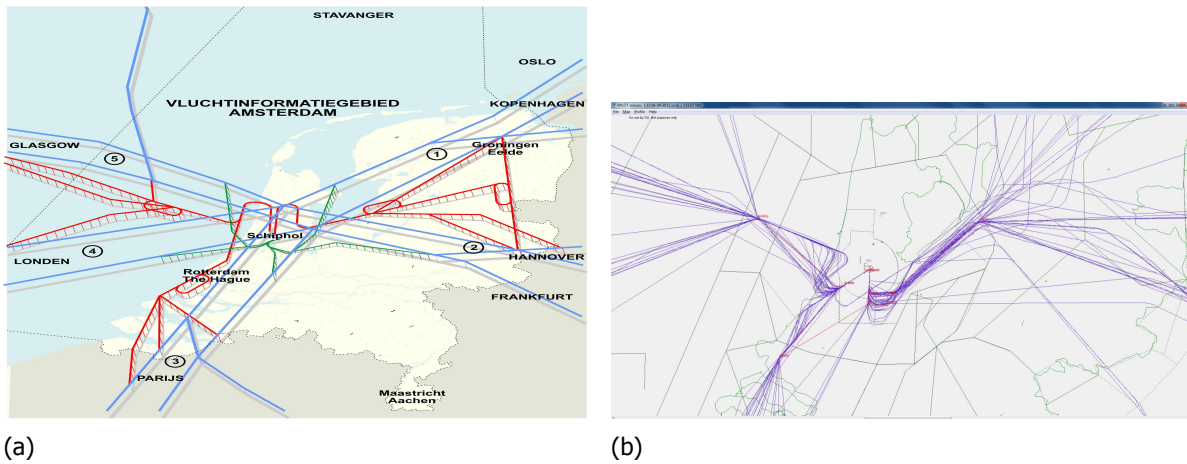


Figure 3.1: (a) Schematic overview of the routes towards Schiphol airport [11] and (b) radar tracks inside the Schiphol TMA with landings on runway 06 and 36R.



Figure 3.2: Runway configuration at Schiphol airport. Source: www.schiphol.nl.

3.1.2. Arrival management and inbound planning

Air traffic controllers at LVNL use the Amsterdam Advanced ATM system (AAA) to get the necessary information regarding flight tracks and information to guide and separate aircraft from each other. AAA is a collection of hard- and software connected by a local area network, like controller work places, surveillance equipment, external information sources and central processing units. The Arrival Management (AMAN) tool and inbound planning process is part of this AAA system. The information described in this section is retrieved from the Operations and Instructions Manual (OIM) and other internal documents of Air Traffic Control the Netherlands (LVNL) [12].

Inbound planning is the process in which traffic inbound for the TMA of Schiphol airport is regulated by an approach planner, usually the approach supervisor (APP-SUP), in order to get an optimised traffic flow towards the runways. The inbound planning will calculate the landing slots of aircraft based on the separation settings, allocate a runway, provide controllers with an Estimated Approach Time (EAT)¹ for each flight and last but not least, calculate any delay.

¹The estimated approach time is the time an aircraft has to leave the stack or arrive at the assigned IAF to be handed over from the ACC to an APP controller. It is similar to the definition of the CTO.

When there is a correlation between a radar track and the system flight plan of an aircraft in the AAA system, some relevant times for the inbound planning are calculated: the Estimated Time Over (ETO) FIR, the ETO IAF and ETA. A system flight plan contains amongst other things the IAF an aircraft is heading to. The three IAFs are assigned to one of the available runways. When two runways are available during an inbound peak, by default traffic coming from ARTIP in the east will be assigned to runway 18C or 36R. Traffic coming from RIVER in the South and SUGOL in the west will be planned to land on runway 18R or 06. The approach planner can change the assigned runway for an individual flight or for all flights coming from one IAF, in which case all calculations of the flight times and estimated arrival times are redone. A detailed description of the flight times along different approach paths is given in section 3.1.7.

Fourteen minutes before the ETO IAF of a flight, a landing slot is allocated based on the latest assigned slot (LAS) and the required separation interval. The sum of the LAS and the required interval time is the first available landing slot, which is compared with the calculated ETA. If the ETA is earlier than the earliest available landing slot, the new landing slot is the earliest available one. The difference between ETA and the new landing slot is the required delay that needs to be absorbed. This is illustrated in figure 3.3.

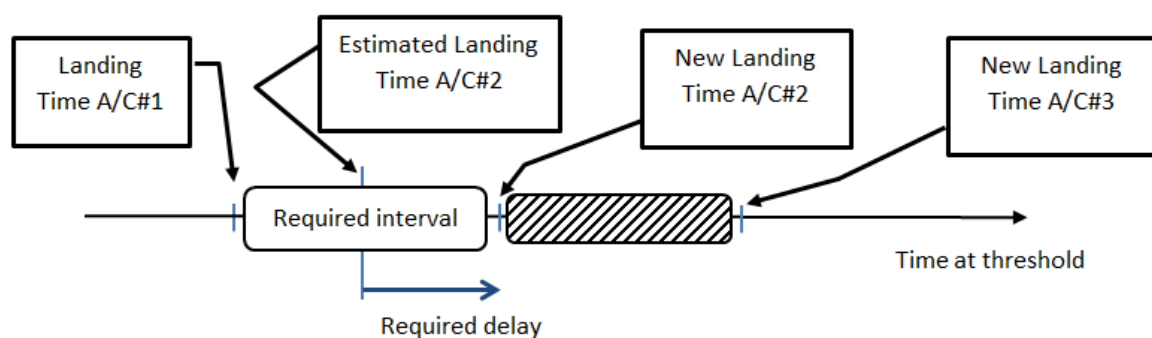


Figure 3.3: Overview of the required delay and shift in the landing times of the aircraft in function of the separation and expected landing time.

The predicted flight time between the IAF and the runway threshold is added to the landings slot to form the EAT (or CTO IAF). The current margin in which aircraft have to be at the IAF on this EAT is ± 120 seconds. The next sections describe all the relevant parameters that are important for the understanding of the inbound planning system.

3.1.3. Trajectory predictor and approach paths

LVNL's AAA system has a trajectory predictor which calculates the expected time an aircraft would pass the planned waypoints. The TP is fed with data like the system flight plan, operating airline, aircraft performance, current speed, heading and altitude, meteorological data, etc. The exact algorithm of TP calculations will not be given in this report, but the predictor takes all previously named parameters into account as well as a descent profile to calculate the remaining flight time to the IAF and the threshold. The STAR filed in the system flight plan is the reference trajectory to calculate the remaining flight time to the IAF. An example of the approach paths used as a reference to calculate the flight time in the TMA of Schiphol airport is given in figure 3.4. The figure shows the two approach paths from ARTIP to runway 18C and 36R, the paths from SUGOL to 18R and 06 and the routes from RIVER to those four runways.

The actual flight tracks given in figures 3.1 and 3.4 show that most aircraft passing over an IAF follow these reference flight paths (red), unless they need to perform a vectoring manoeuvre to increase separation. Only flights that are passing RIVER and have to land on 18C often have a different approach path that the one displayed in figure 3.4 (a). The radar tracks in this figure show that those flights get a direction towards the airport and fly over it so that they can fly a downwind leg on the east side of runway 18C and merge with the approach path coming from ARTIP.

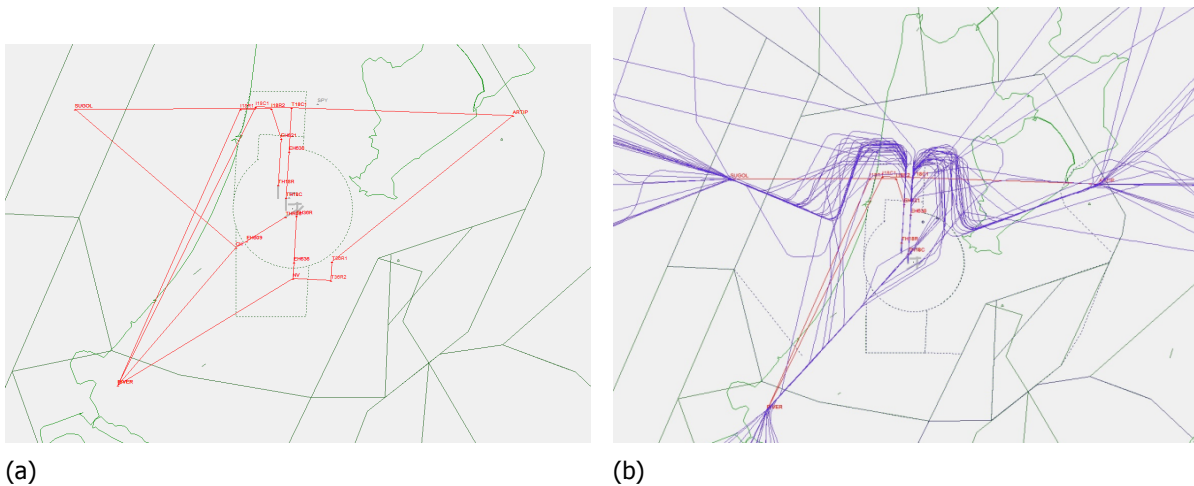


Figure 3.4: (a) Overview of the approach paths in the TMA used for the TP calculations and (b) radar tracks inside the Schiphol TMA with landings on runway 18C and 18R.

3.1.4. Fleet mix

At the initial stage of the research, an analysis is performed on the different aircraft types arriving at Schiphol airport. This analysis will help to determine which aircraft types have to be taken into account when creating the different fleet mixes for the simulation. Furthermore, different aircraft types can result in different flight times in the TMA due to a difference in approach speed and aircraft performance. To limit the amount of required calculations, it is good to have an analysis on the fleet mix at Schiphol airport to determine which aircraft types to focus on in the first place.

The fleet mix research is done on the arrivals at Schiphol airport landing at the four aforementioned runways in the summer period of 2014 between 1 April and 15 October. The group does not contain any light aircraft, which only represent 0,07% of the amount of landings on those four runways. There are three categories of aircraft, based on the wake vortex they produce: super, heavy and medium aircraft. Throughout the day, only one super aircraft lands at Schiphol per day and the landing is planned in the afternoon. Recently, in the summer of 2015, a second A380 coming from Beijing lands at Schiphol airport in the early morning before the first inbound peak [13]. If this airplane is delayed for two three hours, which is not uncommon from long intercontinental flight, it will arrive during one of the busiest inbound peaks (see section 3.1.8). It can be interesting to take this into account when designing the fleet mix for the simulations.

Around 17% of the aircraft landed in the summer of 2014 are heavy aircraft. This number is mainly caused by the amount of heavy cargo aircraft landing during the night. Throughout the day, on average ten to fifteen percent of the fleet mix is heavy. The gross of aircraft types are medium class airplanes with 85% to 90% of the landings during the day. A distinction can be made between jet and turboprop medium aircraft. There is a big difference in aircraft performance and flight speed between both types, which has an effect on the flight time along the approach path in the TMA.

Most medium aircraft arriving at Schiphol airport have jet engines. Only four turboprop aircraft land per hour throughout the day, at most. However, during the morning or evening inbound peak, most of the time only two aircraft per hour land at Schiphol.

If the two busiest inbound peaks throughout the day (see section 3.1.8) are compared in terms of fleet mix composition, differences can be observed. The morning peak (between 05.00 and 07.00 hours UTC) consists of 15% heavy and 85% medium aircraft, whereas the evening peak (± 15.30 to 17.30 hours UTC) mainly consists of medium aircraft and only one or two heavies per peak.

The arrivals at the three IAFs are divided almost equally during the morning inbound peak. However, more aircraft pass ARTIP (45%) during the evening peak than RIVER (28%) and SUGOL (27%).

The actual aircraft type percentages of flight arriving at Schiphol airport and land on one of the four

runways is given in table 3.1². It is no surprise that the Airbus and Boeing family is well represented. Within the medium aircraft type class, Embraer represents almost 20%, followed by Fokker with 11%. Not all different types that land at Schiphol are shown in this table, but only the most common which will be used in the simulation program³. The aircraft types given in table 3.1 represent more than 95% of all types landed at Schiphol airport in the summer of 2014.

Table 3.1: Overview of the fleet mix types with relevant data like wake vortex (WTC) and approach speed category (APC). The approach speed data is retrieved from various sources [14][15].

WTC	type	amount	subratio	V_app (IAS)	APC	WTC	type	amount	subratio	V_app (IAS)	APC
J	total	198				M	total	106673			
	A388	198	100,0%	138	C		A319	9041	8,5%	130	C
							A320	9893	9,3%	130	C
H	total	21348					A321	2502	2,3%	135	C
	A310	3256	15,3%	130	C		AT43-AT76	241	0,2%	115	B
	A333	2619	12,3%	130	C		B733-737	14687	13,8%	133	C
	A343	504	2,4%	135	C		B738/9	29183	27,4%	141	D
	B742/4/8	5125	24,0%	150	D		B752/3	822	0,8%	140	C/D
	B763	2547	11,9%	145	D		CRJ2-9	1145	1,1%	132	C
	B772	3412	16,0%	136	C		E135-190	20789	19,5%	130	C
	B77L	1133	5,3%	140	C		F50/70	11817	11,1%	120	B
	B77W	1394	6,5%	149	D		RJ85	2760	2,6%	125	C
	MD11	813	3,8%	153	D		DH8D	1559	1,5%	125	C

3.1.5. Current separation standards

The vertical separation between aircraft inside the FIR must be at least 1000ft. The horizontal separation expressed in distance is based on the available radar equipment. In general, a Minimum Radar Separation (MRS) of three nautical miles must be maintained inside the TMA and five nautical miles in the Control Area (CTA) [9]. When visibility conditions are good, pilots can be asked to maintain separation on the final approach path with the leading aircraft on a visual basis and the separation can be reduced to 2,5 NM if the wake vortex is not an issue.

The required horizontal separation between aircraft flying over or crossing the same flight path within 1000ft vertical distance is also determined by the wake vortex a leading aircraft produces. International Civil Aviation Organisation (ICAO) has determined four different classes of aircraft and a minimum distance based separation between each class. An aircraft is divided in a certain class based on the maximum take-off weight. An overview of the different aircraft types used in this research and their wake vortex classification is given in table 3.1. LVNL has adopted these wake vortex separation and are shown in table 3.2. The separations for light aircraft are omitted in this table. The minimum separation for an A380 super aircraft trailing another super or heavy is determined to be four nautical miles instead of the minimum radar separation as ICAO describes. This is done to keep some consistency (a heavy aircraft behind another heavy also maintains 4 NM separation) and takes into account the extra time a super or heavy aircraft needs to clear the runway [9]. So there is no need to maintain additional spacing for runway occupancy time and it is assumed that all aircraft can leave the runway and the trailing aircraft can get a landing clearance in time with the given separations.

Wake vortex decays in time and the values in table 3.2 can also be expressed in the required time a certain wake vortex has to decay before a trailing aircraft can pass the same position of the leading aircraft. The time based separation according to the air traffic controllers manual of LVNL is given in table 3.3 and is also based on ICAO standards. ICAO does not recommend a certain time based

²The letter 'J' for the wake vortex category refers to an A380 aircraft. this letter that needs to be filled in at an ICAO flight plan to indicate the wake vortex category of an A380. In radio transmissions, the pilot has to mention 'super' instead of heavy.

³The B757 aircraft is a special one in terms of wake vortex. This aircraft is classified as a heavy when it is flying in front of a medium aircraft, but it is a medium when trailing a heavy. Because this type does not land at Schiphol frequently, it is decided to exclude this type of aircraft from the research and to replace it as a heavy type in the simulation if necessary.

separation for heavy and super aircraft, so LVNL has obtained its own values based on available data [9]. In every day practice, Air Traffic Controllers (ATCOs) will not use time as a separation tool, but rely on distances visual on the radar screen to separate aircraft.

Table 3.2: Wake vortex separation standards retrieved from LVNL documentation [9].

Lead\trail	SUPER	HEAVY	MEDIUM
SUPER	4 NM	6 NM	7 NM
HEAVY	4 NM	4 NM	5 NM
MEDIUM	MRS	MRS	MRS

Table 3.3: Time based wake vortex separations retrieved from LVNL documentation [9].

Lead\trail	SUPER	HEAVY	MEDIUM
SUPER	4 min	4 min	4 min
HEAVY	-	-	3 min
MEDIUM	-	-	-

Currently, different studies are performed both in the USA and Europe to investigate new wake vortex separation standards to update the somewhat outdated ICAO standards [16][17]. Other projects look at the ability to decrease the required separation distance between aircraft when strong headwind are present, which requires a transition from distance based to time based separation values [18]. Because there are no time based separation values available at LVNL for all different wake vortex combinations⁴, it is decided to do an analysis on the required minimum time separation at the threshold between different aircraft types. This analysis can also be helpful to determine the required interval times at the IAFs and to simulate the inbound planning tool of the AAA system (see section 3.1.2 and figure 3.3).

3.1.6. Time based separation values

When the minimum required distance between two aircraft is translated to a time based interval, the approach speed near the threshold becomes an important parameter. Apart from wake vortex categories, aircraft can also be divided in different categories based on their average approach speed. This speed is always expressed in Indicated Air Speed (IAS), because the aircraft needs a certain wind flow over the wings to be in balance with the current landing weight.

ICAO has determined five different approach speed classes, A to E, of which only category B to D is relevant for the fleet mix presented in table 3.1. Aircraft with an approach speed between 91 and 120 knots are divided in category B, which are some light medium aircraft like the F70 and all medium turboprop aircraft considered in this research. Aircraft with an approach speed between 121 and 140 knots are divided in category C and when the approach speed is between 141 and 160 knots, an aircraft belongs to category D. Both medium and heavy aircraft can have approach speeds in the range of 121 to 160 knots, although most Airbus aircraft have a category C approach speed whereas Boeing aircraft often have a higher wing loading which results in a category D classification[14][15].

The actual approach speed of each aircraft can vary depending on weight, so there is some variation in the time each aircraft from the same approach class travels its required separation. When wind is not taken into account together with standard atmospheric conditions, it can be assumed that the indicated airspeed equals the ground speed when the aircraft are on the glideslope (<2000ft altitude). With a given average ground speed for each approach class, the time to cover the minimum separation shown in table 3.2 can be calculated. The MRS is set to three nautical miles and the average ground speed of for approach category B, C and D is 110, 130 and 150 knots, respectively. The calculations of the corresponding separation times are given in table 3.4.

⁴The inbound planning tool uses time based intervals for landing slot allocation when a dynamic landing interval setting is active, but the values of those intervals could not be retrieved from the available documents.

Table 3.4: Time based separation matrix for different aircraft types with different approach speeds.

Approach speeds [Knots]	130	130	150	110	130	150
Lead\trail [seconds]	SUPER C	HEAVY C	HEAVY D	MEDIUM B	MEDIUM C	MEDIUM D
SUPER C	110	166	144	230	196	168
HEAVY C	110	110	96	163	138	120
HEAVY D	110	110	96	163	138	120
MEDIUM B	83	83	72	98	83	72
MEDIUM C	83	83	72	98	83	72
MEDIUM D	83	83	72	98	83	72

This table shows that the difference in minimum time separation within the medium aircraft category is the largest. A medium class D aircraft can pass the threshold behind an A380 after roughly 170 seconds, while a slower medium turboprop aircraft need an extra minute to cover the same minimum separation distance. This makes the wake vortex time separation matrix more complex and difficult to set one average separation time between each wake vortex category.

The required separation behind a leading aircraft due to wake vortex, addressed by ICAO, is to guarantee that the produces vortex is decayed enough in time before a smaller/lighter aircraft passes the same spot. So if a medium aircraft of approach class D, trailing a heavy aircraft, can safely pass the threshold after 120 seconds, it can be assumed that the wake vortex is decayed enough. So it should not pose a problem for a medium aircraft with approach class C to have the same time separation of 120 seconds behind a heavy, even if this result in a separation distance lower than five nautical miles. Of course, this proposed time separation of 120 seconds must allow that the lightest medium aircraft can still handle the most severe wake vortex produced by a heavy. It is hard to determine if the lowest calculated time separation of a certain wake vortex category provides enough time to handle the vortex. Research by Gerz *et al.* [19] describes different methods to calculate wake vortex and calculate the time needed to encounter it, but it is outside the scope of this research to do this for all different aircraft combinations. The same paper states that the ICAO separation standards used for the calculation of the time separation in table 3.4 are considered over-protective or not fully adequate [19]. So the calculated time separations can be assumed to be over-protected as well and the lowest calculated time separation of each wake vortex category should provide enough separation for a safe approach.

Aircraft trailing a medium are not affected by wake vortex, but have to maintain enough separation due to radar equipment limitations. If aircraft with a ground speed of 130 knots would fly 72 seconds behind another one, the distance between them is only 2,6 NM. To keep the time separation consistent for all aircraft that only require a minimum radar separation, it is decided to set that time separation to 90 seconds. This is also in line with the standard dynamic landing interval setting on the inbound planning, which corresponds to a minimum time separation between 94 and 100 seconds [9]. Table 3.5 shows the time separation matrix in seconds for each wake vortex combination and taking into account minimum radar separation as well. The values are rounded off per ten seconds. Only the separation of medium aircraft trailing a super is somewhat increased to comply with the ICAO guidance regarding the wake vortex of an A380-800 [20].

Table 3.5: Simplified time based minimum separation standards.

Lead\trail	SUPER	HEAVY	MEDIUM
SUPER	110 s	140 s	180 s
HEAVY	110 s	100 s	120 s
MEDIUM	90 s	90 s	90 s

The same time separation used at the threshold can also be used at the IAF. Although different atmospheric conditions are present at 10.000 feet, it is assumed that all wake vortex will decay in the same time as near the threshold [21].

The minimum radar separation is 5 NM at the IAF, which could be violated if aircraft maintain the same 90 seconds separation as near the threshold. The speed at which aircraft pass the IAF is higher than the approach speed, so the distance covered in 90 seconds is also larger. The maximum IAS at the IAF is 250 knots, but some turboprop medium aircraft will enter the TMA at 220 knot. So the distance covered in 90 seconds with an IAS of 220 knots should be larger than five nautical miles. To calculate the covered distance at that altitude, the true airspeed (which is the same as the ground speed if no wind factor is taken into account) should be taken⁵. The true airspeed at FL100 in international atmospheric conditions is 256 knots, which results in a covered distance of 6,4 NM in 90 seconds [22]. So the time separations of table 3.5 do not violate the minimum radar separation are assumed save with respect to wake vortex turbulence.

Although the same time separations do not pose a problem in terms of wake vortex or minimum radar separation, there is one extra parameter that needs to be taken into account. If a faster aircraft is trailing a slower aircraft, it will catch up if both airplanes are flying the same trajectory towards the runway and will violate the minimum separation standards. So an additional time buffer is needed to compensate for the difference in flight time towards the threshold.

Slower aircraft trailing a fast one will result in a different outcome when both aircraft fly the same fixed approach path. The interval time between them will increase and result in a larger separation at the threshold, which decreases the runway throughput. But it is not possible to decrease the interval time at the IAF to compensate for this, so it is essential to keep the difference in TMA flight time as low as possible. To investigate how big the differences in flight time are or could be, an analysis on the flight times is performed and described in the next section.

3.1.7. Flight times in the TMA

The time it takes to fly between the IAF and the threshold depends on the approach path and speed development along the trajectory. The approach paths on which the estimated flight times are based are given in figure 3.4. The first analysis of the reference flight times calculated by the TP showed much variation in flight times between the same aircraft types. Factors like wind, airline behaviour and current speed, but also speeds of leading aircraft are taken into account when the TP calculates expected flight times towards the threshold. This made it hard to determine one average flight time for each wake vortex or engine class and to see if there were large differences in flight time between each class. This is important for the calculation of the additional time buffer for the time separation at the IAF. To have an idea of the flight time in the TMA along each approach path per aircraft category without aforementioned factors like wind, own calculations are performed.

Flight times based on calculations without wind

Analysis of the approach procedures in the TMA during inbound peaks has shown that the speed instructions given by the Air Traffic Controller (ATCO) will follow a similar pattern for all jet aircraft. All speeds mentioned in this part are indicated airspeeds. Aircraft will enter the TMA at 250 knots and will get a speed reduction instruction to 220 or even 200 knots if traffic is in front and vectoring is required. Before aircraft are intercepting the glideslope, a speed reduction to 190 or 180 knots is instructed, which is further decreased to 160 knots when they are stabilized on the glideslope. When an aircraft is further down on that glideslope, the pilot will reduce the speed and maintain the right approach speed according to the weight and type of the aircraft.

It can occur that heavy aircraft need more time to lose their speed and energy, where medium aircraft can obtain the instructed speed in a shorter time. As a consequence, heavy aircraft need to decrease their speed earlier to be sure that the right speed around 180 knots is obtained when intercepting the glideslope. Medium jet aircraft can fly somewhat faster and lose the speed just before the glideslope if necessary. As a result, jet medium aircraft can have a shorter flight time in the TMA compared to heavy or super aircraft.

⁵The deviation between calibrated and indicated airspeed is not significant for these calculations where airspeed and altitudes are relatively low.

By using the speed settings described above, the flight time along the approach paths can be calculated. Table 3.6 gives an example of the speeds and altitude settings for each aircraft wake vortex and approach category along the approach path between ARTIP and runway 18C. Each approach path consist of waypoint and it is assumed that aircraft fly in a straight line from one waypoint to another and have a linear descent rate between the assigned altitude. Furthermore, it is assumed that the speeds decrease linear as well and that the reference speeds are just obtained when passing the waypoints. The indicated airspeeds are translated to the corresponding true airspeeds according to the waypoint altitude and no wind is assumed.

Table 3.6: Overview of the indicated airspeed and altitude at each waypoint of the approach path between ARTIP and runway 18C for the calculation of the flight time per aircraft type.

Waypoint	SUPER C	HEAVY C	HEAVY D	MEDIUM B	MEDIUM C	MEDIUM D	Altitude (feet)
ARTIP	250	250	250	240	250	250	10000
T18C1	180	180	180	170	200	200	3000
EH630	160	160	160	160	160	160	2000
TH18C	138	134	155	120	130	148	50

The first waypoint after the IAF (T18C1) is already the intersection with the extended centreline of the runway. Therefore, heavy and super aircraft will need a speed of 180 knot when they arrive at this point. The medium B category represents the turboprop engine aircraft and it is assumed that the average speed is lower for those aircraft compared with jet aircraft. Waypoint EH630 is the point on the glideslope where aircraft have an altitude of 2000ft and it is assumed that all aircraft will have a speed of 160 knots there before they further reduce the speed to their reference approach speed. The interception of the glideslope has to occur at 2000ft altitude for all studied runways according to the procedures, expect for runway 18C where the interception takes place at 3000ft to create a vertical off-set with traffic for the parallel approach to runway 18R.

The estimated flight times for each aircraft category along this approach path is given in table 3.7. The flight time of the medium aircraft with approach speed category B has obviously the longest flight time, which is approximately a minute longer than the flight time of a medium jet aircraft. The difference in flight time between jet engine aircraft is limited to a maximum of 32 seconds.

The difference between jet aircraft (and between jet and turboprop aircraft) increases with increased approach path length. However, the deviation between jet aircraft is at most 40 seconds for the longest route between RIVER and runway 18C. The difference between a turboprop and jet aircraft along this approach path varies between one and 1,5 minutes.

Table 3.7: Overview of the calculated flight times per aircraft type for the approach path between ARTIP and runway 18C.

Flight time (seconds)	SUPER C	HEAVY C	HEAVY D	MEDIUM B	MEDIUM C	MEDIUM D
Approach leg part 1	447	447	447	469	428	428
Approach leg part 2	122	122	122	126	116	116
Approach leg part 3	143	145	135	152	147	138
Total (seconds)	712	714	704	746	690	682
Total (h:mm:ss)	0:11:52	0:11:53	0:11:44	0:12:26	0:11:30	0:11:21

As it was mentioned at the beginning of this section, a comparison with calculated flight time of the TP is hard to make due to external factors like wind. Data from days with low wind⁶ showed that estimated flight times of the TP had similar results with a difference less than 30 seconds for some aircraft. However, other aircraft from the same category had completely different estimated flight times and there was too much deviation in estimated flight time in order to conclude that the calculations of the flight times were a good estimate for a reference flight time in the TMA. Therefore, a more detailed

⁶The days with low wind in this case are 28-05-2014 and 03-06-2014

analysis of the Trajectory Predictor calculations is performed.

Flight times based on TP calculations

The calculations of the TMA flight time by the TP are based on data files containing aircraft speed profiles and expected descent rates, as described shortly in section 3.1.3. It is observed from these data files that medium jet aircraft and some turboprop aircraft like the AT45 and AT72 are classified as 'fast aircraft'. The reference speed in the TMA is 215 knots IAS and the speed at the final approach fix is 160 knots for these aircraft. Other turboprop aircraft like the F50 or DH8D have a reference speed of 200 and 180 knots in the TMA, respectively. Their speed on final is between 155 and 165 knots.

The Embraer aircraft, which represent a large portion of the medium jet aircraft of the fleet mix (see table 3.1), have a reference speed of 201 knots in the TMA and 160 knots at the final approach fix. This is significantly lower than other medium jet aircraft. This result in a longer estimated flight time for the Embraer aircraft, compared to the other medium ones like the A320 or B737.

All heavy aircraft have approximately the same speed profiles in the TMA and on the final approach fix, 200 and 165 knots, respectively. One exception is the A332, with reference speeds of 217 and 151 knots. The A380 has approximately the same reference speeds as medium jet aircraft.

Conclusions on the flight times in the TMA

Conversations with experts in the field have revealed that the data files with aircraft characteristics used by the TP can be somewhat outdated or do not represent the current speeds in the TMA for all aircraft. Furthermore, a discussion with an air traffic controller confirmed that the speed instructions given to pilots in the TMA rarely pose any problems for the aircraft itself. The difference in flight time or speed profile is often determined by airline policy or the flying behaviour of the pilot. Taken these opinions in account, jet aircraft should be able to maintain a very similar speed profile in TMA until the glide slope, which limits the difference in flight time. Therefore, it is decided to assume that all jet aircraft will have the same flight time in the TMA and no additional time has to be taken into account for the time separation at the IAF. After initial tests with flight times in the simulation program, it appeared that all jet aircraft had the same optimal flight time in the TMA within a range of ± 15 seconds. This is further described in chapter 4.2.2 and appendix A has an overview of all reference flight times of the different approach paths in the simulation.

The difference between jet and turboprop aircraft however, is still there. In daily practice, ATCOs take the speed difference into account by maintaining a larger distance behind a slower aircraft or by given a more direct route towards the final fix if a slower aircraft is trailing. The difference in flight time between a turboprop and faster jet aircraft will be taken into account in the simulation when determining the passing time over the IAF. Jet aircraft will have a larger separation after a slower turboprop equipped aircraft. When a slower aircraft trails a faster one, the ideal separation time to maintain runway throughput will be lower than the minimum required separation given in table 3.5. To overcome this problem in the simulation, aircraft will be able to enter the TMA on different flight levels and be spaced sufficiently along different vectoring patterns towards the Final Approach Fix (FAF).

It is therefore decided to use the minimum time separations as given in table 3.5 at both the threshold and at IAFs.

3.1.8. Arrivals, runway capacity and delay

In this part, background information is given about the numbers of arrivals at Schiphol airport throughout the day and the occurrence of inbound peaks. The capacity of the runways is discussed as well. The relation between capacity and the number of landings can be described as delay and is explained at the end of this section.

Arrival peaks

Schiphol airport functions as the main hub airport for KLM (as part of Air France – KLM) and is characterized by a relatively high amount of transfer passengers. 40% of the passengers visiting Schiphol airport in 2014 had a connecting flight towards a different airport [23]. To limit the connection time between two flights, airlines like KLM wants all of their passengers towards the hub airport to arrive at the same time to transfer them on an outbound flight towards their destination. As a result, throughout the day a high amount of landings in the shortest possible time is followed by a high amount of departures [24]. Figure 3.5 illustrates this phenomenon by showing the amount of landings and take-offs

on Friday 28 August 2015. From the figure two arrival peaks can be distinguished that have a higher amount of landings, one in the morning ($\pm 05:00$ to $07:00$ UTC) and one in the evening ($\pm 16:00$ to $18:00$ UTC). The amount of landings is close to or above 70 landings, for all active runways combined. These numbers are close to or even above the declared capacity of the runway system, which is further described below.

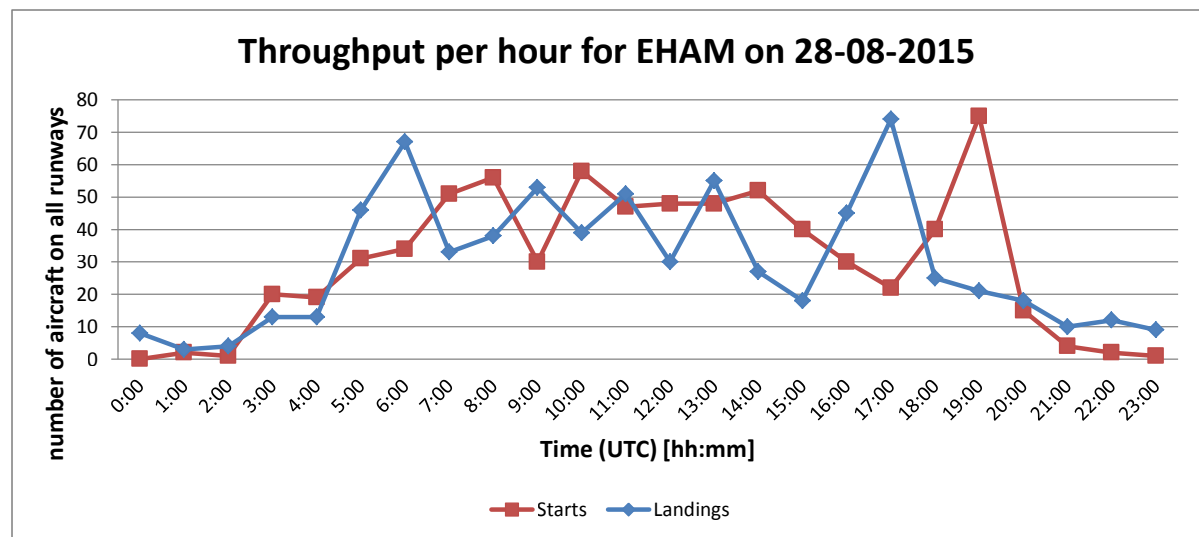


Figure 3.5: Illustration of the number of arrivals and departures at Schiphol airport throughout the day. Source: LVNL, S&P/PERF - CS/ICT.

Runway capacity

The earlier performed literature review on runway capacity, which is part of this research project, described a paper by Poldy [25] which gives some relatively simple models to address the runway capacity under different demand conditions. The parameters that have an influence on the runway capacity can be divided in five main factors. The most important one is the standard (time) separation between aircraft, but the capacity is also dependent on aircraft characteristics, runway configuration and lay-out, composition of the fleet mix and ATC operational strategies [25]. The capacity calculations based on these parameters are called maximum declared capacity.

LVNL has composed its own technical report that describes the maximum declared capacity of movements in and around Schiphol airport [10]. The document motivates the ATC operational strategies in more depth and provides a clear set of capacity numbers for every possible variation of runway usage in different weather conditions. In addition to the paper by Poldy [25], safety, efficiency and environmental agreements are always taken into account to determine the runway capacities at Schiphol airport. The declared hourly capacity during an inbound peak with normal weather conditions is 68 inbound, which have to be divided over two runways. During the simulation, it will be assumed that a maximum of 34 aircraft per hour can land on one runway.

It can occur that the number of landings is actually higher or lower than the declared capacity, due to the sequence and composition of the fleet mix. If for example only medium aircraft would land during an hour with a separation of 90 seconds in between, 40 aircraft could land on the runway. The theoretical capacity which is based on the time separation standards and fleet mix order is referred to as actual runway capacity in this research. As an example the actual runway capacities for the fleet mix combinations used in the simulation can be found in appendix A.2.

Delay

In section 3.1.2, it was mentioned that if multiple aircraft are planned in the inbound planning system to land at the same time on the same runway, measurements have to be taken to sequence each aircraft safely after each other. These measurements can be either a reduction in speed or an extended flight path, but the result is often a longer flight time towards the runway than originally planned in the

arrival system⁷. The longer flight time is referred to as delay and can be described as the deviation between the planned flight time between two points and the actual flight time. There are different types of delay, depended on the main source that caused it, described in literature [26]. The type of delay this research is focussed on is related to the capacity of the runway system.

The literature review described various papers that explained the relationship between the demand for arrivals, the capacity of the runway system [27]. According to classical stochastic queuing models, the delay in the queue system (or inbound system in this case) increases exponentially when demand increases towards the maximum capacity [28][29]. This is illustrated in figure 3.6. These stochastic models tend to overestimate the amount of delay, for high congested runway system. A different model is developed that is similar to the classical queuing models, but has better results when demand reaches the runway capacity. The model is called a Pre-Scheduled Random Arrival (PSRA) model and has a better fit with the actual measured delays, because it takes into account flow control by Control Flow Management Unit (CFMU) [30]. This model by Guadagni *et al.* [30] is validated with data from Rome Fiumicino airport and a case study for London Heathrow [31]. Both researches determined the delay related to congestion in a different way.

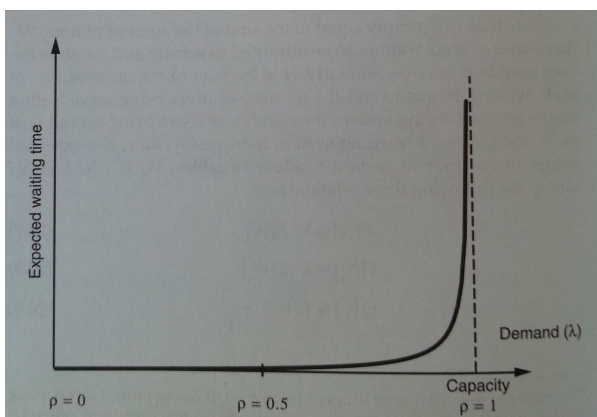


Figure 3.6: Illustration of the expected exponential waiting time in the queue when demand increases to the maximum capacity of the system [29].

To determine the delay, a reference time is always needed and can also be called the optimal flight time. Research by Guadagni *et al.* [30] used the computed scheduled approach time and compared this with the actual approach time. No further explanation on the source or accuracy of the data is given and the authors acknowledge that they had difficulties with determine the time spent in the queue. The case study with Heathrow airport determined the optimal flight time by choosing the shortest flight time of the data set along a STAR. The down sight of this approach is that the reference flight time depends very much on the wind speed and direction and can have a big impact if this varies throughout the dataset. Furthermore, if that particular reference flight got a shorter flight path due to minor congestion, the delay of the other flights would be larger compared to a reference flight following a determined nominal flight path [27].

For this research, the reference flight time is determined by the flight paths used for the TP calculations (see figure 3.4). These flight paths are also constructed in the simulation program and a reference flight time is calculated by the program for each aircraft type in the fleet mix. The flight time is always measured between the passage at the IAF and the threshold. As explained in section 3.1.7, it is chosen to have one reference flight time per trajectory for jet engine and one for turboprop engine aircraft. An overview off all relevant reference flight times used in the simulation can be found in appendix A.1.

The delay in this research is the difference between the reference flight time and the actual flight time in the TMA. The delay also includes any time spend in the holding, because holding time is also related to congestion. In this report, delay is always related to the delay in TMA, unless mentioned otherwise.

⁷Aircraft can also receive a request to speed up and arrive earlier than planned, although most aircraft will experience a longer flight time than originally planned when runway capacity issues occur.

3.2. Charles de Gaulle airport landing procedures

The relevant elements for the handling of inbound traffic towards Charles de Gaulle airport (CDG) are described in this section. The same lay-out of the section is used as much as possible and a comparison with Schiphol airport is made, if relevant. The airspace structure around CDG and the runway configuration is described in chapter 3.2.1, followed by a detailed description of the approach routes in the TMA in chapter 3.2.2. Charles de Gaulle airport uses a different AMAN than Schiphol airport, which is explained in chapter 3.2.3. The section ends with an overview of the arrival peaks throughout the day and the maximum runway capacity.

3.2.1. Airspace structure around CDG airport

Charles de Gaulle airport is located north-east of Paris and has four parallel runways of which two are used for landings and the other two for departures in normal conditions. Figure 3.7 gives an overview of the runways at CDG. There are two runways on the north side of the terminals and two on the south side. They are referred to as 'doublets' or more specific, 'le doublet nord' and 'le doublet sud'. The two runways on the outside of the airport are the ones used for landings only, so arriving aircraft have to cross the inner runways dedicated to departing traffic. All runways can be used in both directions and the runway designations are 09L-27R, 09R-27L, 08L-26R, 08R-26L. In this research, only landings in the eastern direction are considered, so landing on 26L or 27R.

There are two airports in the vicinity of CDG airport, le Bourget and Orly airport. Le Bourget is situated approximately eight kilometres south-west of Charles de Gaulle, but serves mainly business and other general aviation traffic. Orly airport is situated in the south of Paris. Traffic towards le Bourget is also handled by the approach controllers of CDG airport, which is illustrated by the overview of the approach paths inside the TMA of the Paris region in figure 3.9. A detailed description of the relevant approach paths is given in the next section.

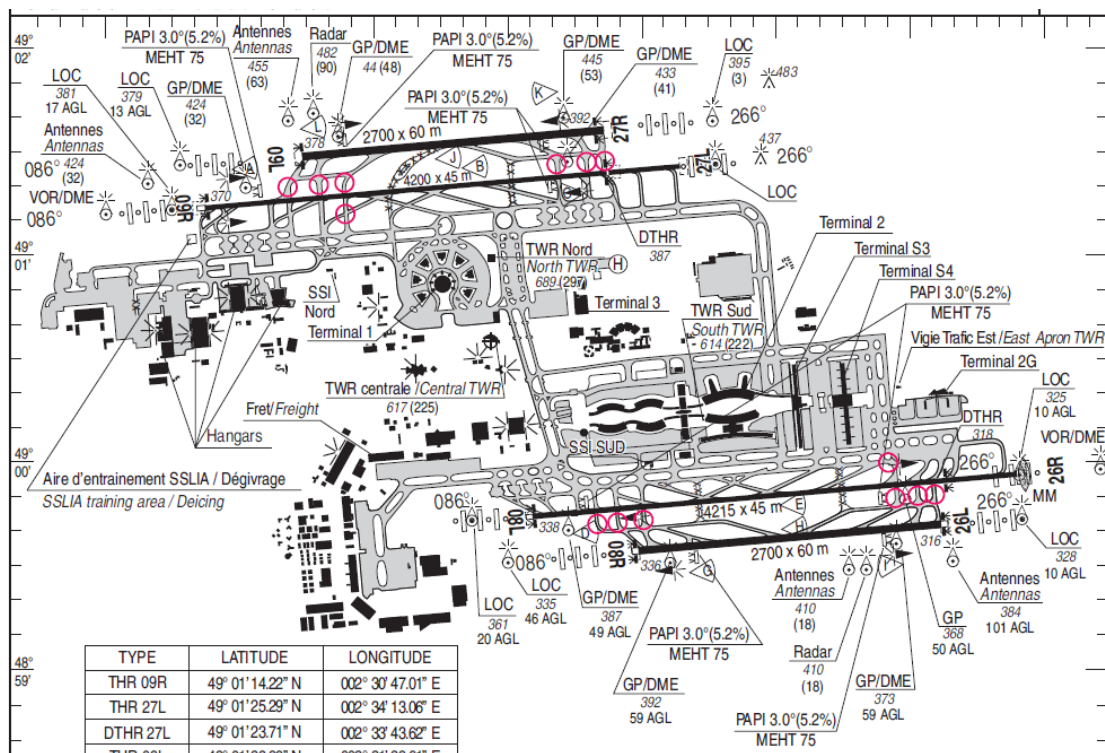


Figure 3.7: Airport lay-out with runways of Charles de Gaulle airport [32].

The TMA of the Paris region covers a distance of approximately 45 to 55 nautical miles between CDG and the IAFs. This is substantially larger than the TMA of Schiphol airport. There are four main IAFs for inbound traffic to Charles de Gaulle (and le Bourget), somewhat evenly spread in the four corners of the TMA. The location of the fixes together with the contours of the TMA used in the simulation

program is given in figure 3.8. During an inbound peak, aircraft arriving at one of the two fixes in the north will be guided to land on the northern runway and aircraft arriving from the south will land on the southern runway. In other circumstances when traffic permits, aircraft will land on the runway closest to the assigned terminal to minimize taxiing time.

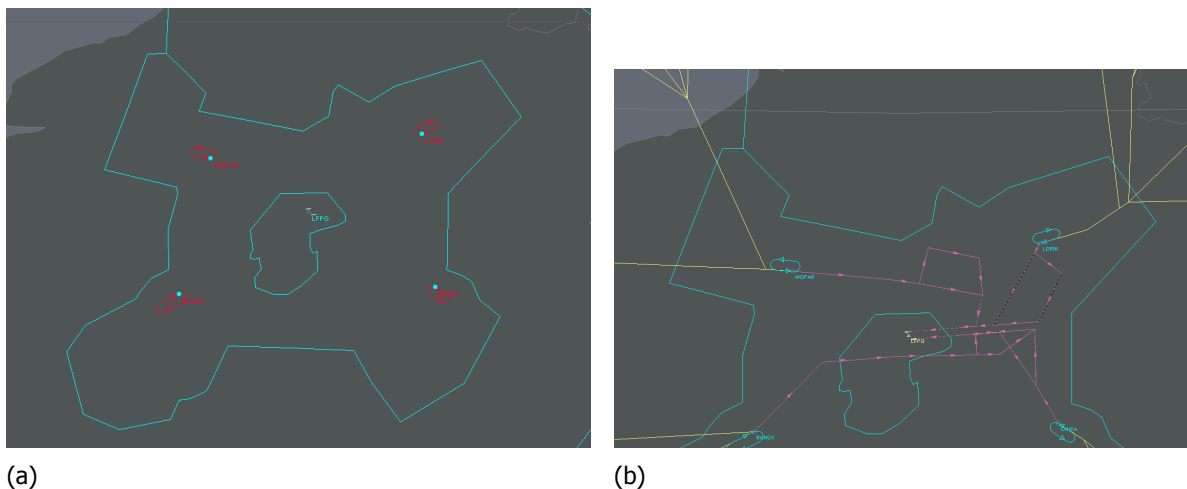


Figure 3.8: (a) TMA structure around Charles de Gaulle airport and (b) approach paths used in the simulation, retrieved from AIP data.

3.2.2. Trajectory predictor and routes in TMA

Figure 3.9 shows the approach paths in the TMA when a western wind blows. The red lines with waypoints or reference 'PG' are the routes towards CDG and the blue ones with reference 'PB' to Le Bourget airport. Propeller aircraft (given letter 'H') can have a different route and IAF than jet aircraft (given the letter 'R')⁸. There are four IAFs for jet aircraft: MOPAR, LORNI, OKIPA and BANOX. The relevant information regarding speed and altitude is also given in this figure. Inbound aircraft coming from the west have to maintain a certain altitude to allow outbound traffic (black thinner lines) to pass underneath. This is different than the separation between inbound and outbound traffic at Schiphol airport, where outbound traffic climbs over inbound traffic. The thinner red lines indicate that controllers can use vectoring manoeuvres along this part of the route to sequence traffic from different IAFs towards the extended centreline of the assigned runway. The glideslope for the runway in the north (27R in this figure), will intercept the glideslope at a height of 5000ft. Traffic for runway 26L will intercept the glideslope at 4000ft altitude. As a result, the distance to cover on the final approach path is five to seven nautical miles longer compared to the distance of the final approach paths at Schiphol airport. The outer marker is eight nautical miles from the threshold.

The routes given in figure 3.9 are also used as reference for the Trajectory Predictor of the arrival management system of Charles de Gaulle airport. There are differences in calculations of the predicted flight time in the TMA between this TP and the one used at Schiphol airport.

The flight times are predicted for the route between the IAF and the outer marker, instead of the threshold, so the difference in landing speed between aircraft is of less importance. There is no automated link with meteorological data, so wind is not taken into account⁹. Furthermore, all jet aircraft have the speed profiles used for the calculation of the flight times. As a result, all the predicted flight times of (jet) aircraft between one IAF and the outer marker of the assigned runway are the same. An overview of the reference flight times and a comparison with the flight times in the simulation, is given in chapter 4.4.3.

⁸Propeller aircraft are called 'avion à hélices' and jet aircraft are 'avion à réaction'.

⁹Values for headwind can manually be set as an input for the separation of aircraft on the final approach fix. This is to overcome a decrease in throughput due to strong headwinds and unnecessary additional separation between aircraft due to a lower groundspeed. Although the (time based) separation on final takes into account wind and this separation is used as a reference for the inbound planning, the calculation of the flight times itself do not take wind conditions into account.

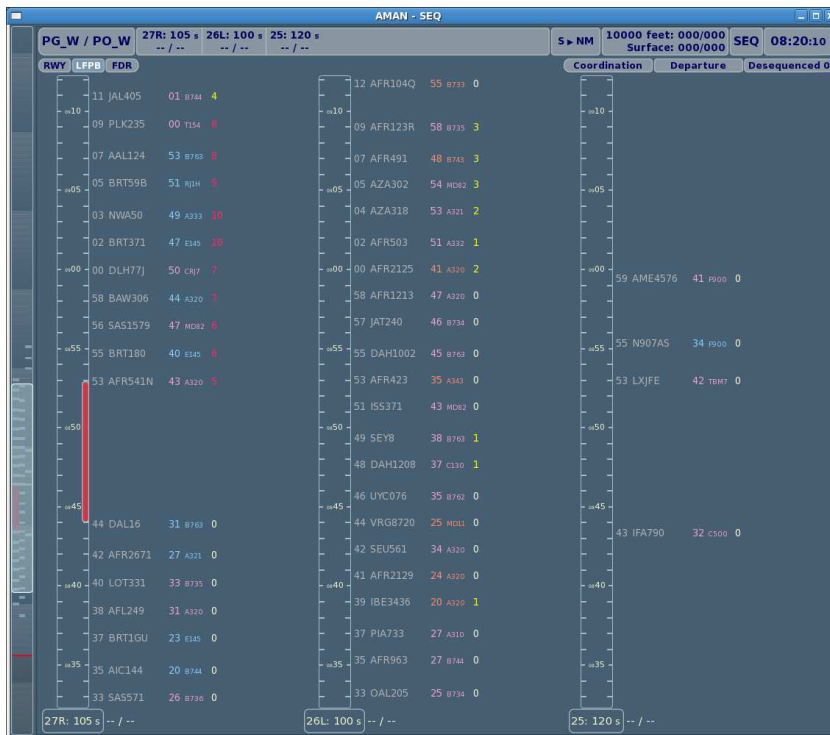


Figure 3.10: Example of the AMAN interface used by the planning controller at CDG airport [33].

Although this figure indicates that there is a constraint of 62 landings per hour, an arrival planner at CDG mentioned that the maximum declared capacity is 72 arrivals per hour, divided over two runways. So an average of 36 arrivals per runway is the maximum declared capacity which will be used throughout this research. The time separation standards are similar to the ones calculated for Schiphol airport in section 3.1.6 and the same separation standards will also be used for the runway throughput research of Charles de Gaulle airport.

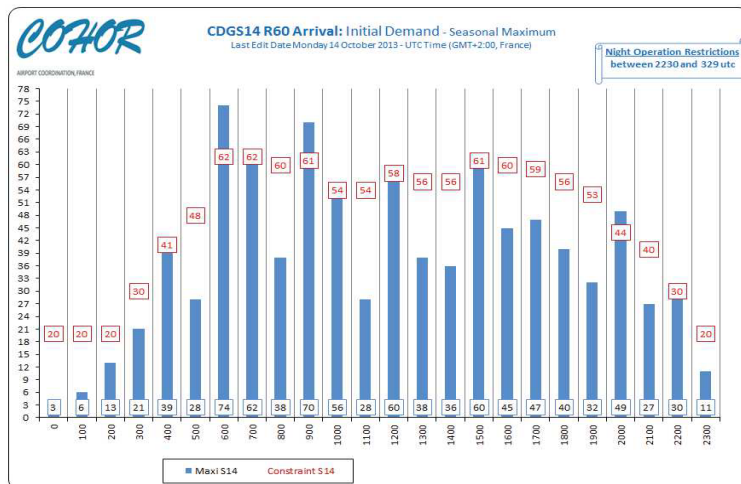


Figure 3.11: Expected amount of arrivals per hour for the summer of 2014 at CDG airport. Source: www.cohor.org

4

Simulation Set-up

The simulation program used for this research and the simulation set-up is described in this chapter. The first section elaborates on the software package AirTop, followed by an explanation of two important elements for the simulation in chapter 4.2. The simulation set-up and the different scenarios for Schiphol airport are described in chapter 4.3, which also contains the verification of the model. This chapter ends with a description of the simulation set-up of Charles de Gaulle airport.

4.1. AirTop Simulation Software

For the fast-time simulation parts, there are different options; Either use a commercial simulation package, modify and use an existing simulation program from the Control and Simulation department of the Aerospace Faculty or create a new simulation algorithm. A commercial program is often too expensive and can be limited in its inputs and outputs. There is a chance the user cannot perform the analysis as intended. The same is true for an existing simulation program from the TU Delft, except for the cost price. Creating a new algorithm on the other hand is time consuming and acceptance of the results by the general public can be a problem, even if the validation of the program is done thorough.

From all available commercial programs, AirTOP has the best properties for this research. It has the tools to design every required airspace structures to simulate incoming traffic, it can perform Monte-Carlo simulations and can simulate time based separations standards between aircraft [6]. Furthermore, this program is also used by EUROCONTROL, NLR, To70 and other European research and consultancy firms, which increases the acceptancy level of the results from this research.

An agreement between the researcher and To70 is constructed such that AirTOP can be used for this research under the supervision of To70. Due to limited time and resources, a normal set-up of the simulation procedures cannot be performed. Feedback on the processed work will be given, but in normal simulation work, different experts would perform checks and validations.

AirTop version 2.3.15 is used during this research, which unfortunately has no dynamic en-route AMAN and flow management module. A solution for this problem is further described in section 4.2.2.

Aircraft performance

AirTop has the ability to import Base of Aircraft Data (BADA) files in order to use realistic aircraft performance data during the simulations. This database is developed by EUROCONTROL in cooperation with aircraft manufacturers and airline operators to create aircraft performance models which can be used for research and development activities [34]. BADA version 3.12 is used for the simulations of this project.

Assumptions

A model is always a representation of the real world and is limited to some assumption to make the development of the model and the complete research feasible. for example, the approach procedure at Schiphol airport in which traffic from three IAFs is divided over two runways is too complex to simulated simultaneously for this research. In order to find answers for the research questions, certain approach

procedures have to be split in different simulation scenarios such that they cannot interfere with each other. Furthermore, when a high amount of traffic is simulated with AirTOP, unwanted events and aircraft behaviour can occur that affects the outcome of the research. To prevent this from happening, the following assumptions will be applicable for all simulation scenarios:

- Normal weather conditions are assumed to calculate the parameters (weather does not affect arrival demand, runway capacity or air traffic handling by controllers).
- No wind model is implemented in AirTOP.
- Nominal flight paths and standard arrival routes will be flown, with some deviation (vectoring) if necessary during the simulation sessions.
- One runway is at most served by two IAFs.
- One runway is active per simulation scenario to limit the amount of traffic that needs to be simulated simultaneously.
- No outbound and transfer traffic is simulated.
- General aviation traffic is excluded in this research, because they often do not land on the main landing runways during an inbound peak.
- Jet aircraft have the same average speed to calculate the flight time in the TMA. The same holds for propeller aircraft¹.

4.2. Important elements of the simulated environment

There are two main elements that are important for both the simulations of Schiphol and Charles de Gaulle airport. The first one is the way flights are imported and handled in the simulated environment, which is described in section 4.2.1. Section 4.2.2 explains how the En-Route Delay Absorption (ERDA) technique is used within the simulation program.

4.2.1. Flight plans, trajectory predictor and arrival management

Each simulated aircraft requires a flight plan with basic essential information about the aircraft type, the route, cruise altitude and a reference time. This reference time must be linked to a departure, arrival or a specific waypoint time along the route². Depending on the accuracy settings of the simulation, an aircraft will depart, arrive or pass the waypoint at the specified reference time. Although an arrival time seems the most convenient choice for this arrival related research, a reference time at the IAF waypoint is used. An initial simulation test revealed that there is a large difference between the planned and actual simulated arrival time, while a waypoint reference time is more accurate (approximately ± 10 seconds). A bunching effect at the IAF can be created by adjusting the interval times between consecutive flight plans.

The build in trajectory predictor calculates the time an aircraft will pass the waypoints along the trajectory (up to the IAF) based on the filed reference time, cruise altitude, route and aircraft performance. 20 minutes before the planned arrival time, an aircraft is listed in an arrival sequence list and assigned to a runway. Each scenario is created as such, that only one arrival runway is available at the time, as mentioned in the assumptions.

4.2.2. En route delay absorption in AirTOP

The used version of AirTOP did not include the sophisticated dynamic AMAN module, which automatically adjusts the en-route trajectories and speeds of aircraft such that an optimised sequence at the IAFs is created. In order to investigate the effect of en-route delay absorption, an algorithm is created that adjust the reference times at the IAFs, such that the required inter-arrival times at the IAF (and

¹This assumption is based on the flight times per approach leg for the most common aircraft types at Schiphol and Charles de Gaulle airport. See chapter 3.1.7 and 4.4 for a detailed description on the flight times inside the TMA.

²Only en-route waypoints are allowed as reference waypoints for time in AirTOP, no waypoints on the approach path after the IAF.

the threshold) are obtained. The algorithm works in analogy with the principles of the AMAN system of Schiphol airport (see chapter 3).

Figure 4.1 shows a schematic view of the shift in the landing time and required delay in function of the expected landing time and separation between aircraft. The reference time of the flight plan is considered as the ETO IAF. Based on the average flight time along the approach path of either a jet or propeller aircraft, a landing time (#1) is calculated. The required interval time at the threshold is added to the landing time to create the earliest available landing time. If the calculated landing time of the trailing aircraft (landing time #2) is earlier than the earliest available landing time, landing time #2 is moved further on the timeline. As a result, the required passage time at the IAF of aircraft #2 is later as well, compared to the original planned reference time. The difference between this original ETO IAF and the new required time (or CTO) is the additional time or delay that needs to be 'absorbed' in an earlier flight phase.

If the ETA of the third aircraft falls within the interval time after the second one, a new landing and CTO IAF is established and the required delay can grow or decrease, depending on the interval time between aircraft #2 and #3.

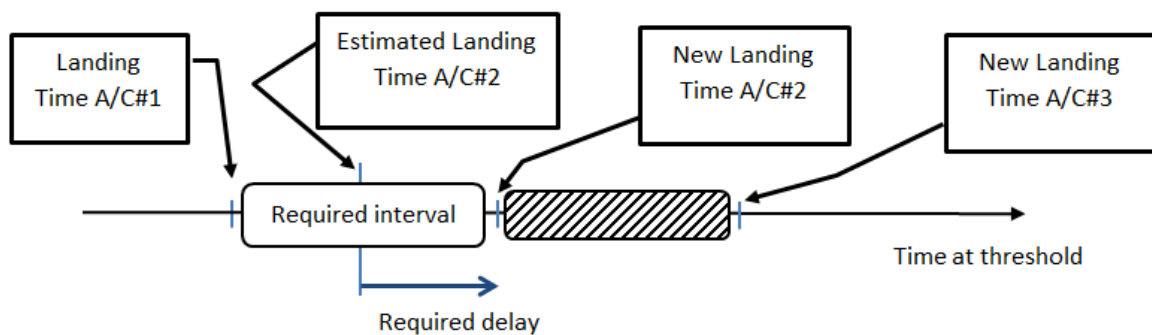


Figure 4.1: Overview of the required delay and shift in the landing times of the aircraft in function of the separation and expected landing time.

Table 4.1 gives an example of the new calculated reference time at the IAF, based on the calculated ETA and the required wake vortex separation. 'ETA_CALC' is the estimated time of arrival and the demand for arrivals is ten aircraft per 20 minutes, hence the interval time is two minutes. 'Separation' is the separation time between the 'new ETA' of the first aircraft and the planned 'ETA_CALC' of the trailing one. If the difference between 'separation' and 'required separation' is negative, the trailing aircraft arrives too early and has to be delayed en-route. If the amount of required delay (the 'difference') is smaller than five minutes, all delay will be absorbed en-route and the 'New ETA' is such that the required wake vortex arrival interval is achieved. A new CTO IAF is calculated based on the engine type of the aircraft and the assigned fix. The algorithm will only create a new CTO for the IAF if delay is required. If there is a gap in the landing sequence (e.g. aircraft #21 has a separation of 2:00 minutes instead of the required 1:40 minutes), the new CTO will be the same as the original planned reference time.

Table 4.1: Example of the en-route delay absorption algorithm calculations for Schiphol airport

callsign	Engine type	WTC	IAF	ETA_CALC	separation	required sep	difference	new ETA	new sep	new ref time IAF
14	Jet	SuperHeavy	SUGOL	10:17:43				10:17:43	0:02:00	10:07:10
15	Jet	Medium	SUGOL	10:19:43	0:02:00	0:03:00	-0:01:00	10:20:43	0:03:00	10:10:10
16	Jet	Heavy	RIVER	10:21:43	0:01:00	0:01:45	-0:00:45	10:22:28	0:01:45	10:07:42
17	Jet	Medium	SUGOL	10:23:43	0:01:15	0:02:00	-0:00:45	10:24:28	0:02:00	10:13:55
18	Jet	Medium	SUGOL	10:25:43	0:01:15	0:01:45	-0:00:30	10:26:13	0:01:45	10:15:40
19	Jet	Medium	SUGOL	10:27:43	0:01:30	0:01:45	-0:00:15	10:27:58	0:01:45	10:17:25
20	Jet	Heavy	RIVER	10:29:43	0:01:45	0:01:45	-0:00:00	10:29:43	0:01:45	10:14:57
21	Jet	Heavy	RIVER	10:31:43	0:02:00	0:01:40	0:00:20	10:31:43	0:02:00	10:16:57

The amount of maximum delay absorption is somewhat arbitrarily chosen, but with preliminary knowledge on maximum achievable delay absorption taken into account. Research on the delay absorption

capabilities of Maastricht Upper Airspace Control Centre (MUAC) airspace shows that additional flight times in upper airspace of 60 to 105 seconds per 150 NM can be achieved by applying speed reductions or altitude changes. If detouring is considered with 25 NM of additional flight path along a route, up to 200 seconds can be gained [35]. So 300 seconds of delay absorption is achievable when an extended AMAN horizon of 150 up to 200 NM from the IAF is chosen. Especially when small detours on the STARs are possible as well to absorb some expected TMA delay.

Jet aircraft have shorter flight times in the TMA than turboprop aircraft. The algorithm takes this into account when the new reference time at the IAF is calculated. However, the consequence is that a turboprop aircraft will arrive closer behind its predecessor jet aircraft at the IAF. A wake vortex problem at this point can occur, unless both aircraft enter the TMA at a different altitude and follow a different approach path in the vectoring area until the speed difference between the two result in enough spacing. The rules for entering the TMA in AirTOP are designed as such that aircraft are allowed to enter the TMA at different flight levels between FL70 and FL100. An overview of all reference flight times of the different approach paths in the simulation is given in appendix A.

4.3. Schiphol airport simulation model

The simulation environment consists of two main parts. The first one is the en-route part and includes all the routes up to the Initial Approach Fixes. The second part is the most important one for this research and contains the TMA area where aircraft are lined up towards the glideslope to land. Both parts with their relevant parameters are described in this section below before the different variables that are subject to change in the different scenarios are described in section 4.3.3. The verification of the Schiphol model is given in section 4.3.4.

4.3.1. En-route simulation environment

The implementation of all relevant objects and airspaces around Schiphol airport are based on the information that is available in the AIP, which is readily accessible and the information is consulted in May 2015 [36]. Small deviations from the exact AIP are applied when it obviously does not affect any outcome of the simulation. An example is the FIR boundary at the German and Belgian border, which follow only roughly those borders in the simulated environment. In real life, aircraft are not handed over from one FIR region to another at the border exactly. There is a buffer area near the border in which aircraft have to maintain speed and altitude of execute the instruction of the first controller, until they are contacted by a the controller of the new airspace they enter [9]. Figure 4.2 shows an overview of the different airspaces and sector blocks used in the simulation. The airspaces around the Netherlands represent the upper airspace, but are not a replication of the MUAC or English Air Navigation Service Provider (ANSP) (NATS) airspace. These airspaces are created to make a controlled airspace for en-route aircraft up to 250 NM distance from Schiphol airport. However, the distance of the en-route flight paths are chosen somewhat arbitrarily to give an impression of the extended AMAN horizon. It is explained in section 4.2 that the simulated aircraft will enter the simulation at the beginning of the route, depending on the reference time of the flight plan. So it does not matter if the beginning of a route is 100 or 500 NM from the planned IAF, as long as the en-route flight path length is long enough to comply with certain simulation rules. The routes and distances are created to be compatible for future research with an upgraded AirTOP version in which en-route arrival management and flow control is possible.

The STARs used for routing between the FIR boundary and the IAFs of Schiphol airport are the same ones used for real inbound traffic handling. The speed and altitude restrictions for the holdings and entering the TMA are implemented as well. A detailed chart of the STARs, retrieved from the AIP, can be found in appendix A. Additional rules that are specific for the handling of traffic towards Schiphol are based on the operating instructions manual of LVNL (in Dutch: Voorschriften Dienst verkeersleiding) [9]. The most important rules for this simulation are already described in chapter 3.

4.3.2. TMA structure and different parameters

The TMA is the most important part of the simulation in this research. To give the reader a good understanding of the simulation program and set-up, the most relevant parameters are described in more detail below.

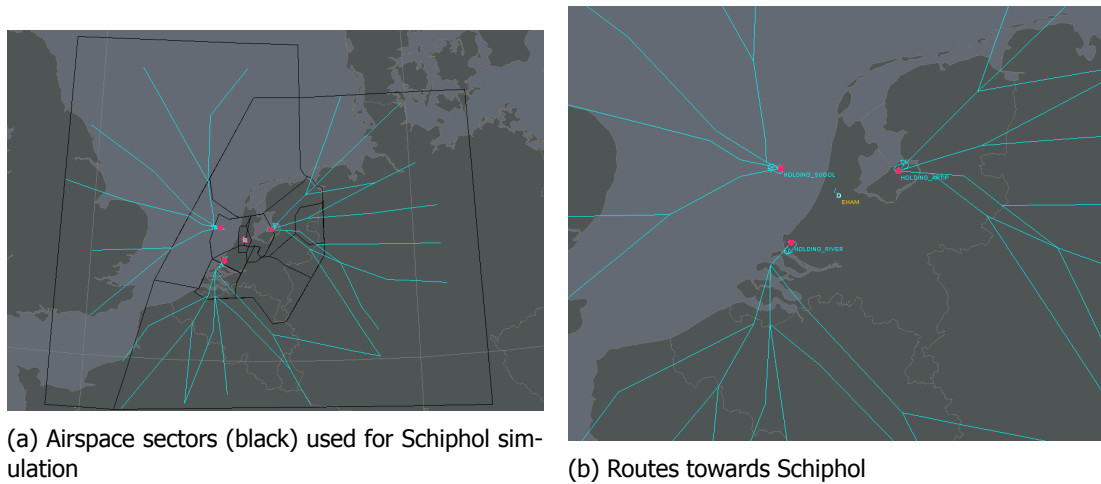


Figure 4.2: Sectors (black) and route structure (cyan) of the Schiphol simulation model

Approach paths

Aircraft will enter the simulation at the beginning of an assigned route and fly towards the IAF related to that route. Aircraft will continue their flight towards one of the assigned runways on an approach leg and land on the runway. Once the maximum allowable speed exit speed is reached, the aircraft leaves the simulation and the runway is cleared for the next one.

To land an aircraft on a runway in AirTop, an approach path between the IAF and Final Approach Fix have to be created. An approach path consists of one or more approach legs formed by waypoint locations. So the most basic approach path is a straight line between the IAF and the FAF and the glideslope connects the FAF with the runway threshold. At each waypoint of an approach leg, a range of IAS and altitude can be given such that the aircraft can descent to the right altitude with a certain speed. Instead of one straight approach leg, the approach path can also be divided in several smaller approach legs. By connecting two approach legs, a vectoring area can be created in the space between them. This allows the simulation to alter the flight time of an aircraft in the approach phase by a speed adjustment (within the predefined range) or a different trajectory from one approach leg to another. An overview of the approach paths between the three IAFs and the designated runways is given in figure 4.3. An example of a vectoring area is the one between ARTIP and runway 18C, which is on the north side of the line between ARTIP and the intersection with the glideslope of runway 18C (dotted lines).

Each aircraft type in the simulation has an approach profile, based on the available approach path towards the assigned runway. The approach profile allows AirTop to calculate the estimated arrival times at the threshold and other points along the approach path. The principle of optimising the approach sequence and interval times at the threshold is the same in AirTop as with the real life situation. If an aircraft's estimated arrival time is too close to the (estimated) arrival time of the aircraft in front of it to maintain sufficient wake vortex separation, this second aircraft will have to add additional flight time (delay) by reducing its speed, extending its flight path or both. A speed reduction can be executed along the entire approach path, but is limited to the minimum flight speed of the aircraft. An extension of the flight trajectory is only possible in the vectoring area of the approach path.

runway arrival rate

The runway arrival rate parameter limits the amount of landings per hour on the assigned runway. The arrival rate is set to be 34 landings per hour on one runway for Schiphol airport. This is the declared capacity in normal operating conditions when two runways for landing are in use [10]. By adding this extra rule in AirTop, the minimal time based wake vortex separation values will be changed to comply with the runway arrival rate. This is further explained in the next paragraph.

Time based wake vortex separation values

The inter-arrival separations at the threshold between the different wake vortex classes are given in table 4.2. The formulation of the values is already described in chapter 3. These values are the



Figure 4.3: Approach legs in the simulated TMA environment around Schiphol airport.

minimal separations between aircraft that cannot be exceeded and is an addition on standard 3NM radar distance that needs to be maintained inside the TMA. However, because the maximum arrival rate per hour is set to be 34 landings, AirTop will increase the required time separation for each aircraft trailing a medium aircraft from 1:30 to 1:45 minutes during the simulation. This new separation needs to be taken into account in the ERDA algorithm, else the aircraft arrive at the IAF too early after each other and additional delay in the TMA will be applied by AirTop. Table 4.1 shows that the increased required separation between medium-medium aircraft is already corrected.

Table 4.2: Time based separation values based on the required wake vortex separation between aircraft types. The formulation of the values is given in chapter 3.

Time based separation [m:ss]		Trailing		
		S	H	M
Leading	S	1:50	2:20	3:00
	H	1:50	1:40	2:00
	M	1:30	1:30	1:30

Accuracy of the actual time over the IAFs

The agreement today between Area Control Centre (ACC) and Approach (control centre) (APP) controllers is that aircraft will be delivered at the IAF within ± 120 seconds of the planned arrival time (EAT). To facilitate the use of fixed arrival routes in the TMA, the accuracy of the actual time over the IAF should be reduced to ± 30 seconds. LVNL's goal is to implement new tools that should realise an accuracy of the actual time over the IAF with a ± 30 seconds margin [37][38]. For this reason it is chosen to run all the Schiphol simulations with the same conditions: the Actual Time Over (ATO) IAF is random for each aircraft within ± 30 seconds margin around the reference time.

Another reason to keep the variation of the reference time within 30 seconds, is to keep the conflicts and separations inside the TMA during the simulations manageable and the sequence stable. If aircraft

in the flight plans are separated two minutes apart, but the first aircraft arrives 1:15 minutes later at the IAF and the second one 1:30 minutes too early, a re-sequence of the traffic flow occurs. As a result, a different wake vortex separation could be needed and the calculated times of the ERDA algorithm are no longer valid.

4.3.3. Variables and scenarios

In this section, the different variables that are subject to change in the simulation scenarios are described. The different scenarios that are created to test the effect of en-route delay absorption on the delay and throughput are given at the end of this section.

Demand profiles

Initial tests of different traffic flows revealed that delay in the TMA only occurs when the demand for arrivals for a certain period of time is higher than the runway capacity (see chapter 5.1.1). The runway capacity is based on the required safe inter-arrival times between aircraft³. Delay develops when the planned inter-arrival time between two aircraft is smaller than the required inter-arrival time. If more than one aircraft arrives too closely after another at the TMA, each following aircraft has to deviate from the optimal approach path towards the runway in order to increase the distance (and time) between one another. In real life, flow management tries to avoid that more aircraft arrive at an airport per 20 minutes than the declared capacity[9]. However, if most aircraft arrive in the first five minutes of the 20 minutes period, delay will still occur. This 'bunching' effect must be created in the simulation in a realistic way such that delay occurs, but does not create unrealistic conflicts like two aircraft arriving at a waypoint along the STAR at the same time.

To investigate the effect of ERDA on the throughput and delay, three different demand profiles are created for the Schiphol scenarios; a high, medium and low demand peak. Each inbound peak contains 68 aircraft that are planned to land within two hours. Only the third inbound peak has a longer inbound peak of 2:20 hours because the overall demand is lower and a total of 68 landings are maintained. The demands per 20 minutes are presented in table 4.3. The maximum declared capacity is 34 aircraft per hour or 11,3 per 20 minutes.

Table 4.3: Different demand profiles for the simulations at Schiphol airport

Time period [H:MM]	0:20	0:40	1:00	1:20	1:40	2:00	2:20
High demand	10	11	13	12	11	11	
Medium demand	11	11	12	12	11	11	
Low demand	10	10	11	11	10	10	6

The reference time at the IAFs of each aircraft is distributed evenly over this 20 minutes time period to avoid unrealistic bunching effects. In other words, when the demand is ten aircraft per 20 minutes, the interval time at the IAF is two minutes. Bunching effect can still occur in those 20 minutes, because the accuracy of passing the IAF is set to be ± 30 seconds and the required separation can be larger than two minutes if the fleet mix consists of different wake vortex categories.

Fleet mix

It is mentioned in chapter 3, that the fleet mix at Schiphol airport is not the same for each inbound peak. To investigate the effect of en-route delay absorption with different fleet mixes, three different ones are chosen. An exact overview of each fleet mix and the corresponding aircraft types can be found in appendix A.2.

The first fleet mix is based on a busy morning inbound peak in the summer at Schiphol airport, containing seven heavies, two turboprops and 25 medium aircraft per hour. The second fleet mix is based on an evening inbound peak and contains only medium aircraft of which two aircraft per hour are turboprops. The third fleet mix includes no turboprops, but one super (A380), seven heavy and 26 medium aircraft per hour. In an overview, the fleet mixes for the Schiphol airport scenarios are:

³In the simulations, the actual runway capacity is determined by the wake vortex separation values. If a maximum arrival rate is set, AirTOP will increase the wake vortex separation values of the lowest ones during the simulation to comply with the maximum arrival rate, as described earlier.

- FM 1: 7 Heavy, 2 Medium Turboprop and 25 Medium Jet aircraft per hour,
- FM 2: 2 Medium Turboprop and 32 Medium Jet aircraft per hour,
- FM 3: 1 Super, 7 Heavy and 26 Medium Jet aircraft per hour.

All fleet mixes are randomly ordered per hour and differently for each of the two hours. However, the sequence of each fleet mix is not changed between the three demand profiles in each scenario and when ERDA is applied.

Approach legs and complex runway system at Schiphol airport

At Schiphol airport, three initial approach fixes have to be divided over two active runways for arrivals during an inbound peak. In real life, ARTIP and SUGOL each have a dedicated runway set in the AMAN tool, whereas the traffic coming from RIVER is divided over the two runways. To keep the simulations somewhat clear, the use of two runways with three IAFs is split up in a part with one IAF (ARTIP) to one runway and a part with the two remaining fixes where the traffic merges in the TMA to another runway (see figure 4.3).

Simulation scenarios

The scenarios for the simulations of Schiphol airport are designed as such, that the change in demand, fleet mix and approach legs can be analysed against each other. There are two main simulations for Schiphol airport: a simulation where traffic flies from ARTIP to one runway and a simulation where traffic from RIVER and SUGOL merge in the TMA and land on runway 18R. When traffic arrives at ARTIP, it will fly to runway 18C in one simulation and to runway 36R in another, to see the difference when traffic flies over a longer approach path. For each of the three scenarios described, a simulation run is performed with all three demand profiles for each of the three fleet mixes, so:

- 1 IAF to 1 runway
 - ARTIP to 18C
 - ◊ FM 1 with Demand 1, 2, and 3 and no en-route delay absorption
 - ◊ FM1 with D1, 2 and 3 but with ERDA
 - ◊ FM2 with D1, 2 and 3, both no ERDA and ERDA
 - ◊ FM3 with D1, 2 and 3, both no ERDA and ERDA
 - ARTIP to 36R
 - ◊ FM1 with D1, 2 and 3, both no ERDA and ERDA
 - ◊ FM2 with D1, 2 and 3, both no ERDA and ERDA
 - ◊ FM3 with D1, 2 and 3, both no ERDA and ERDA
- 2 IAFs to 1 runway (RIVER and SUGOL to 18R)
 - FM1 with D1, 2 and 3, both no ERDA and ERDA
 - FM2 with D1, 2 and 3, both no ERDA and ERDA
 - FM3 with D1, 2 and 3, both no ERDA and ERDA

In addition to the scenario of two IAFs to one runway, an extra scenario is simulated where the accuracy of the ATO RIVER is different than the one over SUGOL. This could occur due to external factors like errors in the wind predictions models or wrong flight data. The scenario of the first fleet mix with the three demand profiles and applied ERDA is taken as the reference scenario, the following two off-sets in ATO accuracy between RIVER and SUGOL are simulated:

- Off-set 1: The accuracy at RIVER is between -60 and -30 seconds (too early), at SUGOL between +30 and +60 seconds (too late).
- Off-set 2: The accuracy at RIVER is between +30 and +60 seconds (too late), at SUGOL between -60 and -30 seconds (too early).

To investigate the deviation of the throughput and delay, 25 simulation runs are performed for each scenario. Because the accuracy of the actual arrival time at the IAF is randomly determined within a ± 30 seconds range, each run can have different results for the throughput and delay.

4.3.4. Verification of Schiphol airport model

In order to verify if the constructed AirTop model of Schiphol airport behaves the same as if the traffic would be handled by real ATCOs, AAA traffic data is implemented in the model. The actual landing times, throughput, flight time and TMA congestion delay measured with AirTOP are compared with the actual radar track data. Because wind can have a large impact on the flight time inside the TMA and it is not simulated in the model, only a limited amount of days with low wind conditions are suitable for verification. Furthermore, other factors like a reduction of runway capacity or different runways in use due to maintenance and rainy days limit possible candidate inbound peaks considerably. Nonetheless, at least two inbound peaks are found to verify the model: The busy morning peak on 28-05-2014 for traffic towards runways 18R and 18C and the inbound peak on the same day in the evening towards runways 06 and 36R. Three scenarios are verified; one scenario with traffic flying from ARTIP to runway 18C and one scenario with traffic to runway 36R. The third verification is the scenario with traffic from RIVER and SUGOL merging in the TMA and landing on runway 18R.

The most important part of the model is the TMA environment. The main idea of the verification is to implement the Actual Time Over the IAFs in the flight plans as reference time and to compare the simulated ATA with the real ATA. The congestion delay is compared as well. However, such a comparison between simulated and actual delay is harder to make, because the real TMA delay is based on the estimated flight time of the TP. It is explained in chapter 3 that the estimated flight time in the TMA, and therefore the calculated delay, is not always correct for all aircraft types. As a result, the average delay from the simulation can deviate much from the calculated average delay of the AAA data if the aircraft performance models deviate too much. The reference flight time in the TMA, calculated by the simulation, determines the amount of simulated delay. The reference flight time in the simulation is not always exactly the same as the reference time of the real TP for all approach paths. As a result, a bias can occur when delay is compared between real and simulated scenarios. As mentioned before, an overview of all reference flight times of the simulated approach paths and the comparison with real TP reference flight times is given in appendix A.

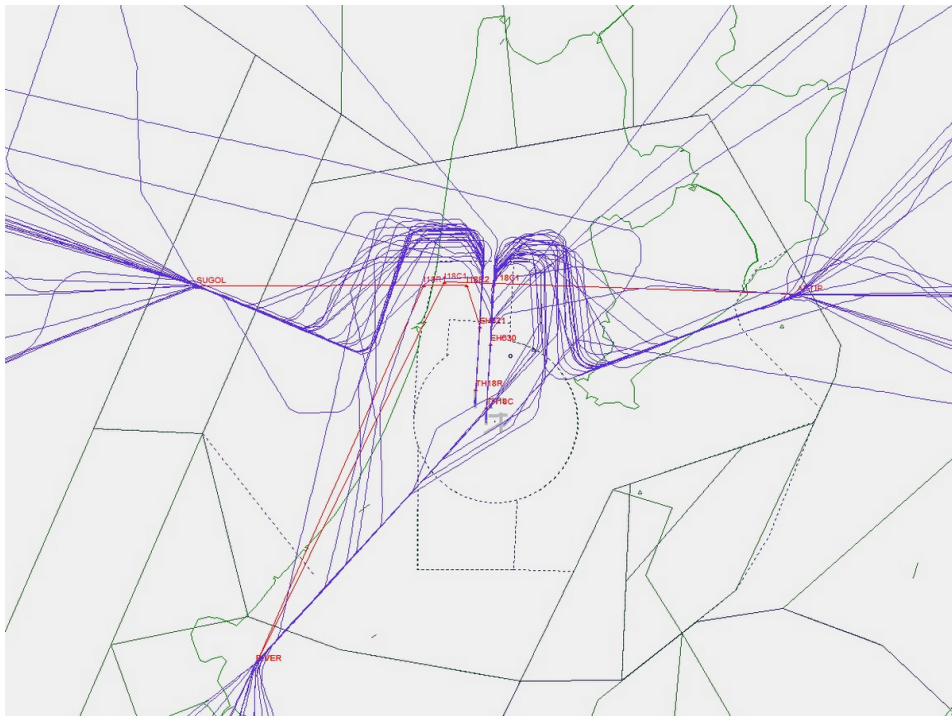


Figure 4.4: Flight radar tracks (blue) of the morning inbound peak (0500 to 0700Z) at Schiphol airport.

In real life, some aircraft are given a direct route towards the glideslope of the runway, without passing the assigned IAF, which is shown in figure 4.4. As a result, the ATO is registered as the time when the aircraft had the closest distance to the IAF⁴. Therefore, not all ATOs can be implemented in a flight

⁴For this reason, it is also difficult to perform a good analysis of the actual congestion delay inside the TMA if the reference

schedule as reference time for the simulations without some small modification. Luckily, during busy inbound peaks, the amount of aircraft not passing the IAF within reasonable distance is limited. The reference time of the aircraft in question are adjusted such that they will pass the IAF in the simulated environment between the two aircraft of the real landing sequence.

During an inbound peak, some aircraft that arrive at SUGOL or ARTIP are guided to the other runway than the designated one, if necessary. For the verification of aircraft landing on 18C, all aircraft that pass ARTIP are not modified (unless they did not pass the IAF within reasonable distance) and aircraft that passed SUGOL or RIVER have an adjusted reference time at ARTIP in the simulation so that it fits the landing sequence. The same method is applied for landings on runway 36R. For the landings on runway 18R, no aircraft passed ARTIP and only one aircraft's reference time had to be adjusted because it entered the TMA in the North through the available military airspace.

Verification of the model for traffic from ARTIP to 18C and 36R

Figure 4.5 shows the difference in TMA flight time between the simulation model and the actual flight time for traffic arriving at ARTIP and landing on 18C. The flight times include holding times as well. The delay experienced by aircraft in the TMA, including any holding delay, is given at the lower side of graph. Only the flight times and delays of the aircraft that passed ARTIP according to the flight data of AAA, are shown in figure 4.5, otherwise, fluctuations in the flight times would be visible which is too distracting.

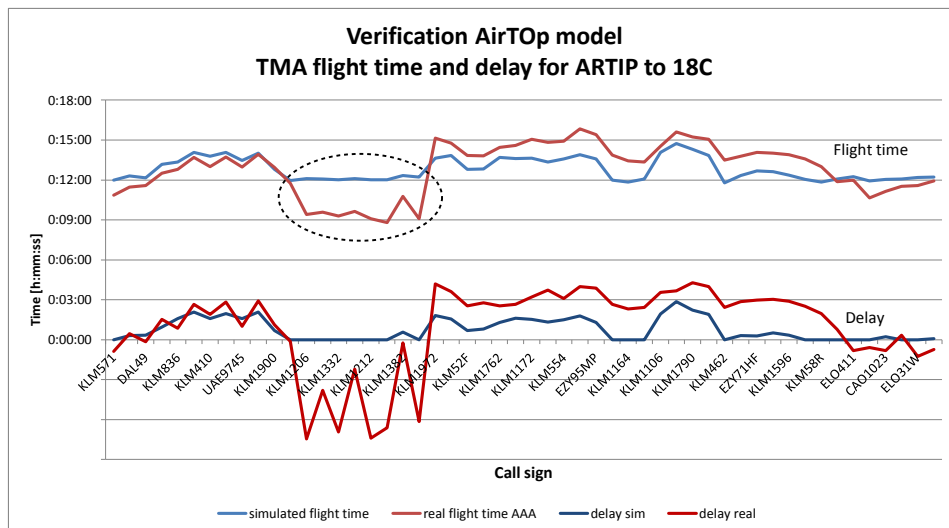


Figure 4.5: Comparison of the flight times and delays between the simulated and actual flight data for traffic from ARTIP to 18C.

The actual flight time graph in this figure (top red line) shows a sudden decrease for six consecutive flights, indicated with the black circle. The reason for this decrease is that those flights entered the TMA in the North instead of passing over ARTIP directly. As a result, their actual flight time is shorter and deviates significantly from the estimated flight time based on the route passing ARTIP. For the same reason, the calculated delay is substantially negative. The remaining of the flights show that the propagation of the flight time and delay is the same, but that there is an off-set between the simulation and the real data. The longer flight time in real life could be explained by an additional buffer that is applied by the ATCOs to separate the aircraft. With this verification scenario, the model did not take into account a maximum arrival rate of 34 aircraft per hour.

Figure 4.6 shows the simulated flight times and delay when a maximum arrival rate of 34 aircraft per hour is applied. The difference in flight time and delay is now decreased until aircraft 'KLM1106' and some trailing aircraft had to perform a holding turn (black circle). In real life, a holding turn was

flight time of the TP is used. Each aircraft flight track in such analysis must be checked to see if it does pass the IAF within a reasonable distance; else the actual flight time could deviate too much from the estimated flight time, which has an effect on the calculated delay.

not necessary because some of the aircraft came from RIVER and delay could be absorbed along two approach paths instead of only one in the simulation. The actual throughput during this part of the inbound peak was 35 landings, which explains the extra flight time and delay when the simulation has a maximum arrival rate of 34 aircraft per hour. The throughput per 20 minutes and per rolling hour for the last verification scenario is given in table 4.4.

Table 4.4: The throughput per 20 minutes and per rolling hour for the verification scenario of ARTIP to 18C.

Throughput	per 20 min sim	per 20 min real	rolling hour sim	rolling hour real
4:40	3	3		
5:00	10	10		
5:20	9	10	22	23
5:40	10	10	29	30
6:00	11	12	30	32
6:20	12	11	33	33
6:40	11	12	34	35
7:00	10	8	33	31

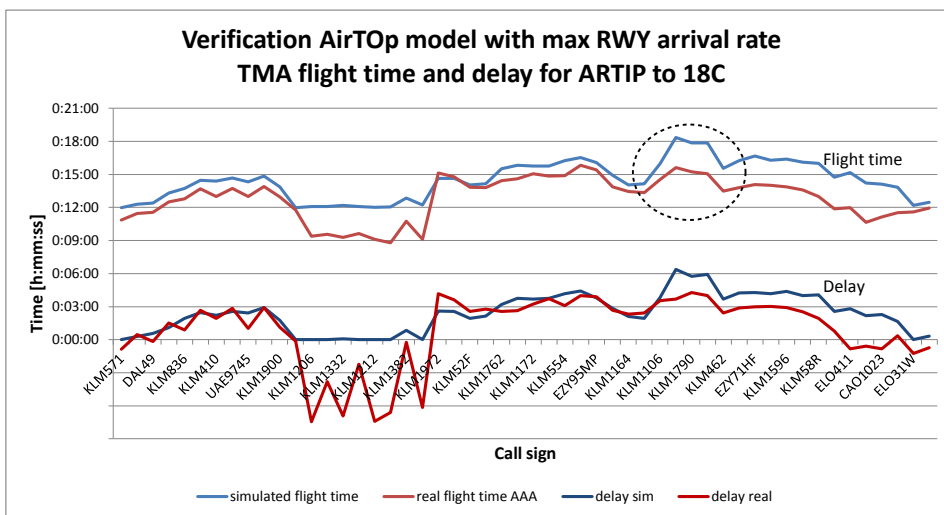


Figure 4.6: Comparison of the flight times and delays between the simulated and actual flight data for traffic from ARTIP to 18C, but with a maximum arrival rate of 34 aircraft per hour.

The verification of the model for the approach path from ARTIP to runway 36R is presented in figure 4.7. The flight times and delays from the simulation and actual data do not deviate much and the values for the throughput, given in table 4.5, are almost the same. No aircraft’s reference time had to be adjusted because they did not pass ARTIP within reasonable distance. Only seven aircraft arrived at RIVER and landed on runway 36R during this inbound peak. The black circle in figure 4.7 indicates a small difference between the model and how traffic was handled in real life. Flight KLM62R performed the first necessary holding turn both in real life and in the simulation. However, the trailing flight, KLM1576, did not require a holding turn in the simulation, but did perform one in real life.

Verification of the model for traffic from SUGOL and RIVER to 18R

The final verification for the Schiphol model is traffic arriving at RIVER and SUGOL and landing on runway 18R. The comparison between the flight times and delays is shown in figure 4.8. The approach path from RIVER to 18R is longer than the one from SUGOL. Therefore, the graph shows some spikes each time an aircraft approaches from RIVER. There are two interesting differences between the simulation and the real aircraft data. The first one is a shorter flight time of flight KLM1196, due to a direct given at the beginning of the inbound peak. The second one is the lower delay that occurred in the simulation, but not in real life. In the simulation, the landing sequence is switched between

Table 4.5: The throughput per 20 minutes and per rolling hour for the verification scenario of ARTIP to 36R.

Throughput	per 20 min sim	per 20 min real	rolling hour sim	rolling hour real
16:00	1	1		
16:20	10	10		
16:40	10	10	21	21
17:00	11	11	31	31
17:20	12	11	33	32
17:40	8	9	31	31

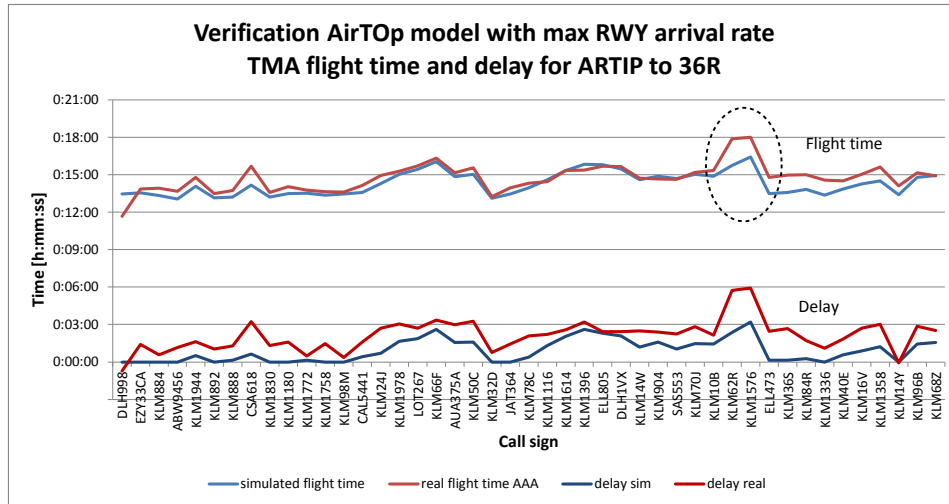


Figure 4.7: Comparison of the flight times and delays between the simulated and actual flight data for traffic from ARTIP to 36R, with a maximum arrival rate of 34 aircraft per hour.

KLM1260 coming from RIVER and KLM1184 passing SUGOL. In real life, KLM 1184 had to encounter up to 7,5 minutes of delay to allow KLM1260 in front of it. In the simulation, KLM1184 arrives first which results in lower total delay of both aircraft: eight minutes instead of 10,5 minutes⁵. The values for the throughput are given in table 4.6.

Table 4.6: The throughput per 20 minutes and per rolling hour for the verification scenario of RIVER and SUGOL to 18R.

Throughput	per 20 min sim	per 20 min real	rolling hour sim	rolling hour real
4:40	1	1		
5:00	5	5		
5:20	1	1	7	7
5:40	7	6	13	12
6:00	11	13	19	20
6:20	12	11	30	30
6:40	8	8	31	32
7:00	6	6	26	25

Based on the graphs and data comparison of the three different approach paths, it can be concluded that the AirTOP model handles the traffic inside the TMA in a similar way as real air traffic controllers, if the assumptions of the model are taken into account.

⁵Although the simulation model handled the traffic somewhat better in this situation, it is wrong to conclude that all air traffic controllers must be replaced by computer models. For example, other factors that could have influenced the decision of the controller, like outbound traffic or transfer traffic, are not taken into account in this model.

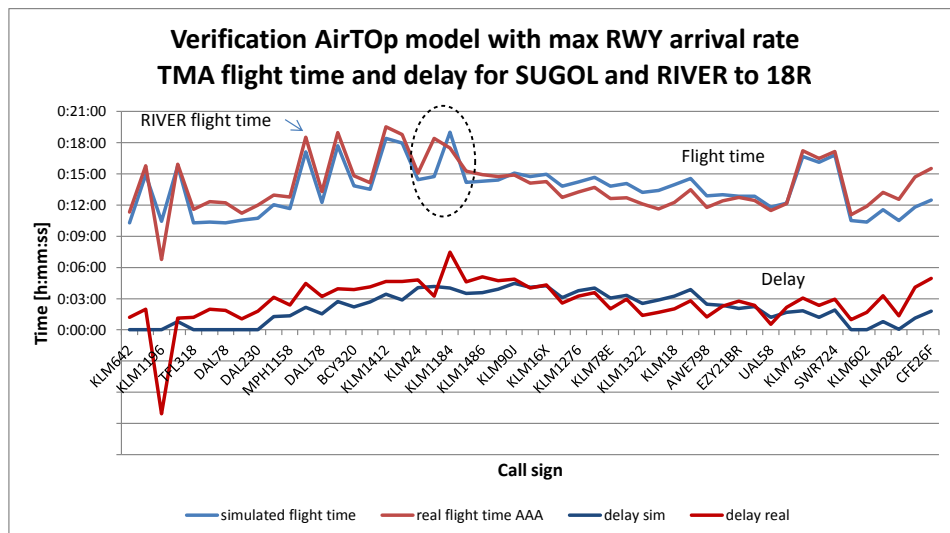


Figure 4.8: Comparison of the flight times and delays between the simulated and actual flight data for traffic from RIVER and SUGOL to 18R, with a maximum arrival rate of 34 aircraft per hour.

4.4. Charles de Gaulle airport simulation model

The simulation model of Charles de Gaulle airport is created with the same analogy as for the model of Schiphol airport. The structure of the airspace and relevant air traffic management procedures described in chapter 3.2 are created in AirTOP. The most important parameters and differences with the Schiphol model are given in the next section. Chapter 4.4.2 explains the variables used in the simulation and the different scenarios. The verification of the model is described in chapter 4.4.3.

4.4.1. TMA structure and important parameters

The simulation environment of the airspace around Charles de Gaulle airport and all other relevant waypoints, routes and runways are based on the French AIP [32]. The consulted version of the AIP is the version of 8 January 2015. In a similar way as with the model for Schiphol, certain airspace sectors at the border of the French FIR are designed somewhat roughly in order to create controlled airspace for descending aircraft. An overview of the designed airspaces and routes towards CDG is given in appendix B. The most important aspects of the TMA structure of CDG are explained in more detail in the next paragraphs.

Approach legs

The approach paths at CDG are to some extent mirrored along a longitudinal line between the main landing runways. During an inbound peak, Aircraft approaching the TMA from the North pass either the IAF MOPAR or LORNI and are guided to the Northern runway. The same holds for aircraft passing IAF OKIPA or BANOX in the South: they are guided towards the Southern runway. If the wind blows from the West, aircraft will normally land on either runway 26L or 27R. Because both approach paths in the North and in the South are very similar, only approaches from the North on runway 27R are simulated.

Figure 4.9 presents the approach paths between the IAFs towards the assigned runway. In real life, the merging happens somewhere along the extended centreline of the runway. Two different concepts for this merging are tried. The first concept is shown by the approach paths from BANOX and OKIPA in the South, where the manoeuvring areas of both approach paths overlap. This procedure did not work, because too many conflicts occurred and aircraft were flying over each other. The second concept, shown with the two approach paths in the North, worked out better. Each manoeuvring area needs to start at approximately the same distance from the merge point, in order to prevent aircraft from overtaking each other on the final approach path.

Conflicts with merging aircraft and distance based wake vortex separation

Because the applied rules and settings in the Schiphol model for merging approach paths worked out well, the same rules were applied for Charles de Gaulle at first. However, when the demand for



Figure 4.9: Approach paths inside the simulated TMA airspace of CDG.

landings was close to the runway capacity, too many conflicts and loss of separation occurred on the final approach path. AirTOP could not find solutions to merge aircraft when too many aircraft were on the approach legs inside the TMA. When no solution is found, strange things happen, like aircraft overtaking each other on the glideslope. Trial and error with different settings learned that when a distance based wake vortex separation is used instead of a time based separation, the merging and landing sequence behaved more stable. However, when the ICAO distance based wake vortex rules are used⁶, the actual throughput rises to 39 or 40 aircraft per hour. This is not realistic when a standard maximum declared capacity of 36 aircraft per hour is used at Charles de Gaulle Airport. Setting a maximum arrival rate of 36 or 37 aircraft results again in strange behaviour and conflicts inside the TMA.

To prevent an unrealistic high throughput when only a distance based wake vortex separation rule is set, an additional arrival buffer is needed between the aircraft. By selecting such an additional arrival buffer of 0,5 NM in the settings of the TMA controller of AirTOP, the throughput decreased towards 36 landings per hour without conflicts on the final approach path.

Accuracy of the actual time over the IAFs

Because this model has difficulties with merging approach legs when demand is high, the reference time at the IAF cannot varied as much as with the Schiphol model. According to the manual of AirTOP, the accuracy of the used Trajectory Predictor in the simulation is ± 10 seconds. However, a comparison between the filed reference times at the IAF and the actual time over the IAF during simulations revealed that the accuracy is more in the range of ± 15 seconds.

En-route delay absorption

The same technique and algorithm for the en-route delay absorption is used for the simulations at CDG. The inter-arrival separation times are the same that would be used when time based wake vortex separation would be applied, except that each arrival get an additional eight seconds to compensate for the 0,5 NM arrival buffer that is in place to get a more realistic throughput. Table 4.7 gives an example of the ERDA technique that modifies the reference times at the IAFs.

The maximum amount of delay absorption that can happen in the en-route phase is increased from five to ten minutes. Due to the additional buffer in separation, the amount of required en-route delay absorption rises to ten minutes for the first inbound peak demand profile (which is further described in the next paragraph). Not all ten minutes of delay will be absorbed in upper airspace. The current AMAN tool at CDG already ask for an absorption of delay in the French CTA up to seven or eight minutes

⁶see chapter 3 for an overview of the distance based wake vortex values

Table 4.7: Example of the en-route delay absorption algorithm calculations for Charles de Gaulle airport

callsign	Engine type	iaf	WTC	ETO_IAF	ETA_CALC	separation	required sep	difference	new time slot	new sep	new ref time IAF
673	Jet	MOPAR	Heavy	2:23:23	2:42:51	0:00:05	0:01:38	-0:01:33	2:44:24	0:01:38	0,100648
674	Jet	MOPAR	Medium	2:24:49	2:44:17	-0:00:07	0:02:08	-0:02:15	2:46:32	0:02:08	0,10213
675	Jet	MOPAR	Heavy	2:26:15	2:45:43	-0:00:49	0:01:38	-0:02:27	2:48:10	0:01:38	0,103264
676	Jet	MOPAR	Medium	2:27:41	2:47:09	-0:01:01	0:02:08	-0:03:09	2:50:18	0:02:08	0,104745
677	Jet	LORNI	Medium	2:35:31	2:48:34	-0:01:44	0:01:38	-0:03:22	2:51:56	0:01:38	0,110336
678	Jet	LORNI	Medium	2:36:57	2:50:00	-0:01:56	0:01:38	-0:03:34	2:53:34	0:01:38	0,11147
679	Jet	LORNI	SuperHeavy	2:38:23	2:51:26	-0:02:08	0:01:38	-0:03:46	2:55:12	0:01:38	0,112604
680	Jet	LORNI	Medium	2:39:48	2:52:51	-0:02:21	0:03:08	-0:05:29	2:58:20	0:03:08	0,11478

(see chapter 3.2.3 for additional information). The additional three minutes of delay absorption can be achieved at upper airspace, if detouring or en-route holding techniques are applied [35].

4.4.2. Variables and scenarios

The demand profiles used for the Schiphol airport simulation need to be adapted for the different runway capacity of Charles de Gaulle airport. There is also a difference in fleet mix between the two airports. Both variables are further described in the next two paragraphs. The section ends with an explanation of the different scenarios for the simulation.

Demand profiles

Similar to the Schiphol case, three different demand profiles are determined to create delay inside the TMA. Because the declared capacity at CDG is set to be 36 aircraft per hour, the demand profiles used for Schiphol had to be increased. An overview of the three profiles is given in table 4.8. The fleet mix order does not change between each demand profile.

Table 4.8: Different demand profiles for the simulations at CDG airport

Time period [H:MM]	0:20	0:40	1:00	1:20	1:40	2:00	2:20
High demand	10	12	14	13	12	11	
Medium demand	11	12	13	13	12	11	
Low demand	10	11	12	12	11	10	6

Fleet mix

There is only one fleet mix used for the CDG simulations and it is based on the current (winter 2014 -2015) overall fleet mix. It consists of one A380, eight heavy and 27 medium aircraft per hour. The sequence of aircraft in the first hour of the inbound peak is different than the second hour and is determined randomly. A detailed overview of the fleet mix with the used aircraft types can be found in appendix B.

Based on the limited data of one inbound peak at CDG, the ratio of arrivals at LORNI and MOPAR is 60% against 40%, respectively. Because there is only one fleet mix which will be simulated, this research also looked at scenarios where there is a variation in arrival distribution between both IAFs. The different scenarios are a distribution of 50-50, 60-40, 70-30 and 30-70 percent for arrivals at LORNI and MOPAR, respectively. However, due to a change in distributions, the fleet mix sequence also changed, which changed the actual runway capacity. A good and reliable comparison between the different scenarios described above is difficult to make and therefore it is decided to leave the results of these simulation out of the report. The scenarios with reported results are further explained in the next paragraph.

Scenarios

There are two main scenarios for Charles de Gaulle airport. The first one investigates the effect on throughput and delay when en-route delay absorption is applied for one fleet mix and three demand profiles. The ratio between arrivals at LORNI and MOPAR is changed to investigate if there is a difference in delay and throughput. Because there is no variation in the reference time at the IAFs, only one run per scenario is performed.

The second part investigates the effect on throughput and delay when there is an off-set in the accuracy on the ATO IAF between LORNI and MOPAR. A ratio of 60-40 for arrivals at LORNI and MOPAR is used as a reference.

In an overview, the following scenarios are simulated:

- 1 Different distributions of arrival at LORNI and MOPAR
 - 50 % arrivals at LORNI and 50% at MOPAR
 - 60 % arrivals at LORNI and 40% at MOPAR
 - 70 % arrivals at LORNI and 30% at MOPAR
 - 30 % arrivals at LORNI and 70% at MOPAR
- Off-set in accuracy of arrival at the IAFs
 - Off-set 1: The accuracy of passing MOPAR is between -20 and 0 seconds (too early), the accuracy at LORNI is between 0 and +20 seconds (too late).
 - Off-set 2: The accuracy at MOPAR is between -40 and -20 seconds, at LORNI between +20 and +40 seconds.
 - Off-set 3: The accuracy at MOPAR is between -70 and -50 seconds, at LORNI between +50 and +70 seconds.

4.4.3. Verification of CDG airport model

Prior to the simulation sessions for Charles de Gaulle, no data was available from CDG in order to compare the simulation model with an actual inbound peak. The limited provided data contains ATO IAF of the four stacks and actual times passing the outer marker for one morning inbound peak in the summer of 2014. The data also provides information on the reference flight time between the IAF and outer marker of the assigned runway, but the runway itself is not given. If the actual runway is not given, it is hard or even impossible to know the actual separation between aircraft at the outer marker. Furthermore, no aircraft type or wake vortex category is included in the data set, only a call sign. Unfortunately, online databases did not stored call signs and aircraft types that far back in the past to retrieve a wake vortex category. The only verification that could be made is a comparison between the reference flight time in the TMA calculated by the TP and the optimal flight time determined by the simulation. Table 4.9 gives a comparison of both simulated and calculated reference flight times.

Table 4.9: Comparison of the reference flight time in the TMA calculated by the TP and the optimal flight time determined by the simulation.

Flight time comparison [u:mm:ss]	LORNI 27R	MOPAR 27R
Min	0:12:45	0:19:12
Max	0:13:16	0:19:40
Average	0:13:03	0:19:28
Reference flight time TP	0:11:10	0:17:35
Difference	0:01:53	0:01:53

As explained in chapter 3.2.2, the TP of CDG's inbound planning system uses one speed profile for all jet aircraft. Because the fleet mix does not contain any turboprop aircraft and does not take any wind into account, there is only one flight time for each acIAF – runway combination. The actual reference flight time is calculated for the approach part between the IAF and outer marker of the runway, whereas the simulation calculates the flight time until the touchdown. The flight time between the outer marker and runway is determined manually from the simulation. The average flight time on the glides slope for all aircraft of the fleet mix is three minutes \pm 10 seconds. So the difference in approach speed between

aircraft types is not that large. The three minutes are already concluded in the actual reference flight time given in table 4.9.

The optimal flight time in the TMA is almost two minutes slower in the simulation than the reference flight time predicted by the TP. The difference in optimal flight times is the same for both the route between LORNI to 27R and MOPAR to 27R, although the route from MOPAR is significantly longer. It is hard to determine which part of the approach path causes the difference in flight time between the model and the TP. Most likely, the aircraft speed range settings along the approach leg where vectoring occurs is different for the TP and simulation model. This could also explain that the difference in flight time is the same for a longer or shorter approach path. Both vectoring areas of each approach path start from the same distance of the outer marker towards runway 27R.

Another reason for the difference in reference flight times could be that the TP calculates the time over a different route than the one given in figure 3.9 of the previous chapter. This route is implemented in the simulation model and the routes are shown in figure 4.9. However, the difference in approach path used by the TP would only be the part where vectoring is applied. Figure 4.10 shows the actual radar flight tracks from a couple of days in July 2014. Although the figure gives the flight tracks towards both landing directions, it is clear that aircraft from MOPAR and LORNI to 27R are using a fixed approach path for the first part inside the TMA and are only vectored closer to the fix with the extended centreline of the runway.

Despite the difference in reference flight time and the lack of sufficient data to do more verification of the model, it is assumed that this simulation model is accurate enough to test the effect of En-Route Delay Absorption on the runway throughput of CDG airport.

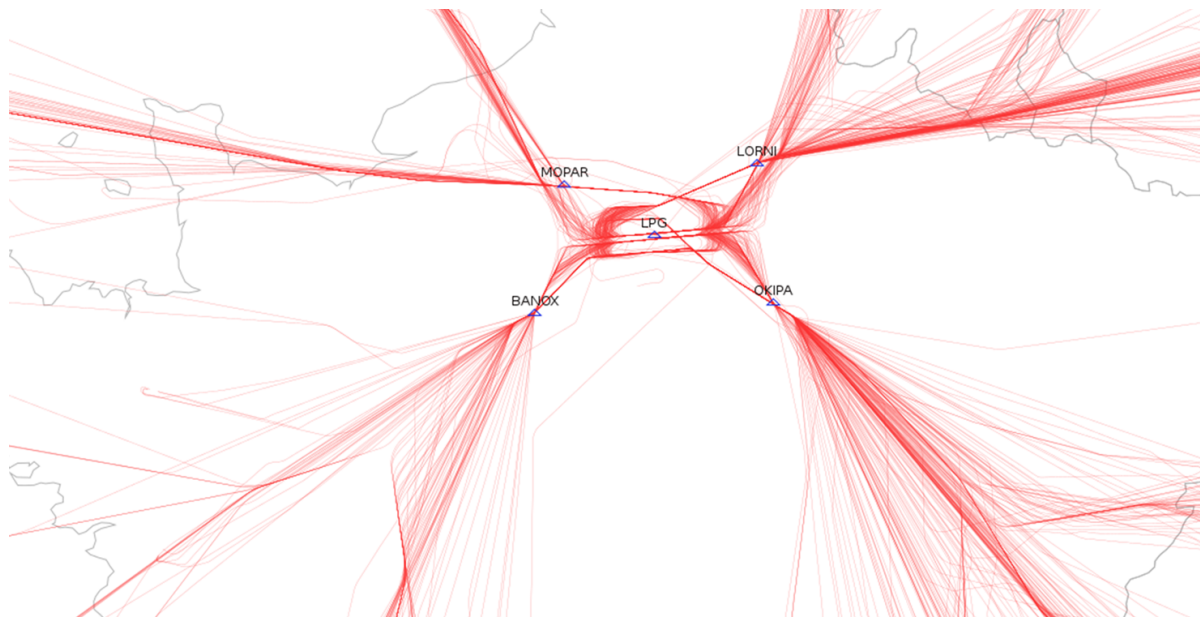


Figure 4.10: Real radar tracks of inbound traffic to CDG airport in July 2014.

5

Simulation results and discussion

The results of the different simulations described in the previous chapter are presented below. First, the results of the simulations for Schiphol airport are given, followed by the results of Charles de Gaulle airport in chapter 5.2.

5.1. Schiphol airport simulation results

The results of the Schiphol airport simulations are presented in the three following subsections. The first one describes the increase of congestion delay in the TMA with respect to the amount of demand for landing. Section 5.1.2 presents the effect of En-Route Delay Absorption (ERDA) on the throughput and congestion delay for a single approach leg in . Section 5.1.3 shows the effect on throughput and delay when two approach legs merge to one runway. The section ends with a discussion of the Schiphol simulation results.

5.1.1. Results of demand and the relationship with delay

The relationship between demand for arrivals, runway capacity and delay found with the AirTop simulations of Schiphol airport, is described in the following section. Next, the results of the change in demand for each inbound peak and the different simulated scenarios are given.

The relationship between demand and delay

Initial tests of the simulation environment revealed that little to no delay occurred in the TMA of Schiphol airport when the demand for landings was close to but lower than the arrival capacity. The used time intervals between aircraft passing the IAF for the initial test is based on the wake vortex separations values described in chapter 3, which means that the aircraft are already spaced properly and no significant bunching effect occurred. Such a scenario of perfect spacing between aircraft at the entrance of the TMA is unlikely to happen with the current operations in air transportation. Therefore, variations of the arrival time at waypoints and bunching effects have to be implemented in the simulation model to create a more realistic air traffic environment. As already described in chapter 4.3.3, this is achieved by increasing the demand above the maximum arrival capacity for a certain period of time in combination with a certain random variation of the actual time passing the IAF.

To investigate how the delay would increase when the maximum arrival rate decreased (and the arrival flow kept constant), different simulation tests are executed. These simulations are performed to answer the sub research question:

'What is the development of the delay in time when the demand exceeds the maximum arrival capacity?'

The demand is set to have 33 aircraft per hour arriving at ARTIP. The fleet mix consists of seven heavies and 26 medium aircraft of which two are turboprops. The fleet mix order changed for each hour of simulation. The maximum arrival rate is decreased from 35 to 30 with steps of one landing per hour. Each simulation run with a setting for the maximum arrival rate is continued for six simulation hours to

investigate the delay propagation over a longer period of time. Expect for the simulation runs with a maximum arrival rate of 31 and 30 aircraft per hour, because the delay increased too much after three hours of simulation with this setting. As a result, the maximum number of stack flight levels exceeded and aircraft had to enter the stack at a higher Flight Level (FL) than the maximum service ceiling, which caused a simulation error.

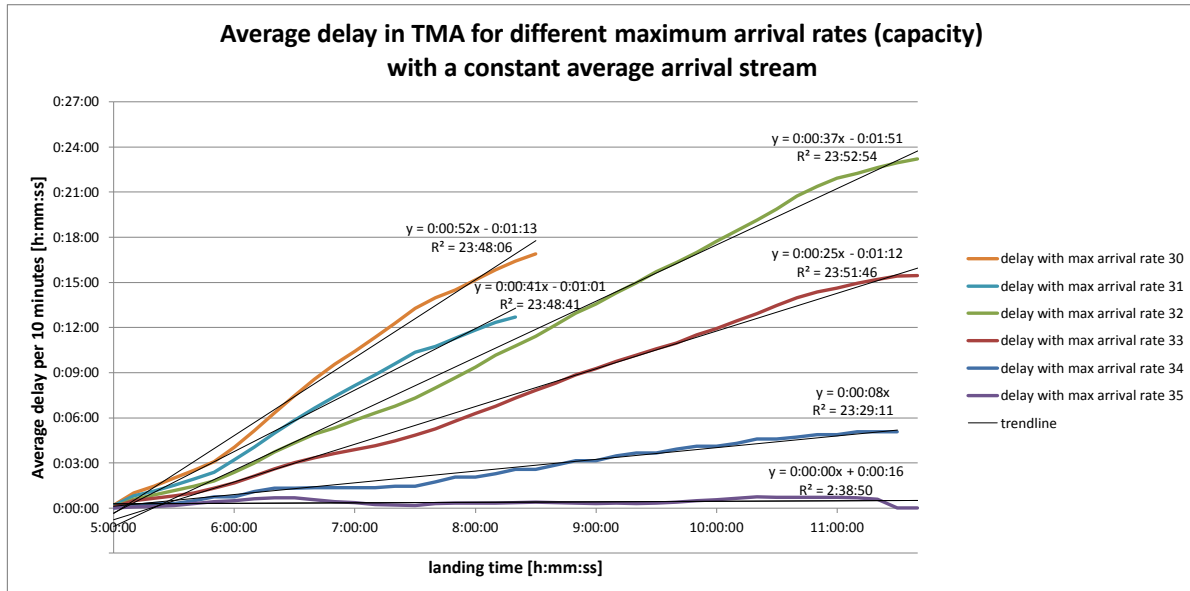


Figure 5.1: Linear delay development over a period of time with different maximum arrival rate settings. The trendline equations are given in a time format. R^2 values closer to 24:00:00 hour represent a value closer to 1.

Figure 5.1 gives an example of the delay development over a large period of time with different maximum arrival rates. From the graphs and the calculated trend lines, it is clear that delay increases linear over time when the ratio demand/capacity is constant. The results suggest that when demand exceeds the runway capacity with a certain ratio for a period of time, the average delay can be calculated with a linear equation.

When the amount of delay is presented against the demand/capacity ratio for different hours of the simulation, the outcome is not as expected. This can be observed in figure 5.2. Based on the performed literature study on delay, described in chapter 3.1.8, it is expected that delay would increase exponentially when demand reaches capacity [29]. But the relation between delay and demand/capacity ratio is clearly linear in this case. Apparently, the conditions for exponential delay increase are not present in this case, because there is no stochastic random demand. The demand is not random, because it is already sequenced in earlier flight phases and made more predictable by EUROCONTROL's flow management. When demand is not random, but constant for a certain period of time, delay grows linear in time for the same demand/capacity ratio.

During an additional literature study, no research on the behaviour of delay with current AMAN systems could be found. Although it is interesting to do further research on this topic, it is decided not to focus on this matter any further during the research and to focus on the main research question: the effect on throughput when En-Route Delay Absorption (ERDA) is applied.

The effect on demand

Due to different separation standards between aircraft, different fleet mixes, demand profiles and applied ERDA, the amount of aircraft entering the TMA per time period is different for each scenario. Such a change in demand has an effect on delay, as explained above, but it will also have an effect on the throughput. To see the effect of ERDA on the demand of various scenarios, the amount of arrivals entering the TMA are shown in a graph together with the maximum arrival rate. The demand, throughput and average delay are measured and shown per 20 minutes time period.

In figure 5.3, the three graphs show the amount of aircraft passing the IAF (ARTIP) per 20 minutes. There are three arrival peaks, each with a different demand profile; high, medium and low (see chapter

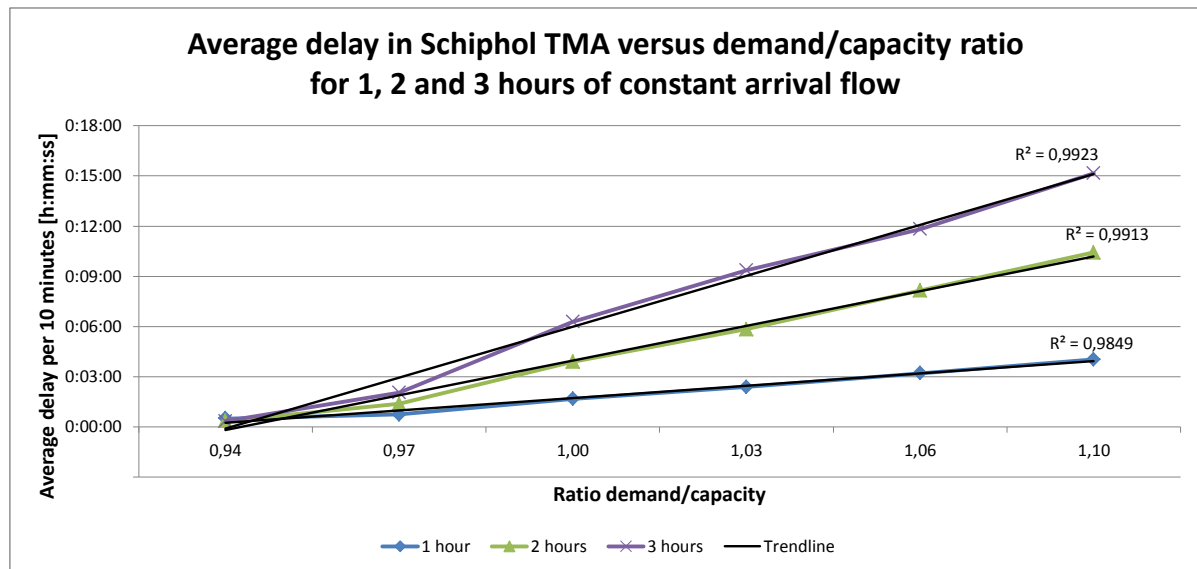


Figure 5.2: Delay versus demand/capacity ratios.

4.3.2 for a detailed description of the demand profiles). The fleet mix order is the same for each arrival peak and both scenarios with and without En-Route Delay Absorption. The maximum arrival capacity throughout each peak is therefore the same. The maximum arrival capacity in figure 5.3 shows the amount of aircraft that can land in 20 minutes, taken into account the required separation after the leading aircraft. In the first 20 minutes, twelve aircraft can land, but this decreases to eleven aircraft per 20 minutes during the remaining of the inbound peak.

The effect of ERDA on the demand can clearly be observed from arrival peak 1 and 2. With ERDA, the demand is lowered such that it does not exceed the maximum capacity. However, at the end of the first arrival peak (starting at 3:00 hour), the demand still exceeds the capacity. The reason is that the required amount of delay absorption at that time is higher than the maximum five minutes of allowed ERDA. Therefore, the required optimal separation at the IAF cannot be achieved and on average slightly more aircraft will arrive and have to be delayed in the TMA or holding stacks to achieve the required amount of separation at the threshold.

The demand can also be presented as an average per rolling hour. In that case, the amount of arrivals is summed for three consecutive time periods of 20 minutes. The graph then looks like figure 5.4. The first two 20 minute periods are not taken into account. So the first column shows the amount of aircraft passing the IAF between 1:40:00 and 2:39:59 hour, the next one between 2:00:00 and 2:59:59 hour, and so on. Although at first it looks like both figures are the same, there is a clear difference between them. With a rolling hour representation, the aircraft that arrive near the 20 minute marker (2:20:00 hour, 2:40:00 hour, etc.) will be taken into account as well, either in the first rolling hour or in the next one. This gives a 'smoother' representation of the demand. A second difference is the amount of demand that exceeds the capacity. It is clearer in figure 5.4 that the demand in the first inbound peak exceeds the hourly capacity until the end of the arrival peak and the amount of demand is larger than the second and third arrival peak. This analysis is difficult to make from figure 5.3. Certain conclusions can be drawn more easily when the results are given per rolling hour. This is also the case for the representation of the throughput, which will be shown in the next section. A final reason is that often in literature, the maximum capacity and the relationship between demand and capacity is expressed in (rolling) hourly capacity, which makes it easier to compare the results from this research with other literature.

Therefore, the graphs for demand and throughput will be shown per rolling hour for the rest of this chapter. The maximum arrival capacity is determined in this graph by the amount of aircraft that can land in the two hour inbound peak, based on the time based separation values. That number is divided by two to get the average hourly (arrival) capacity of the fleet mix. This shows that the capacity for the first fleet mix is 67 aircraft in two hours (34 in the first and 33 in the second), or 33,5 aircraft per

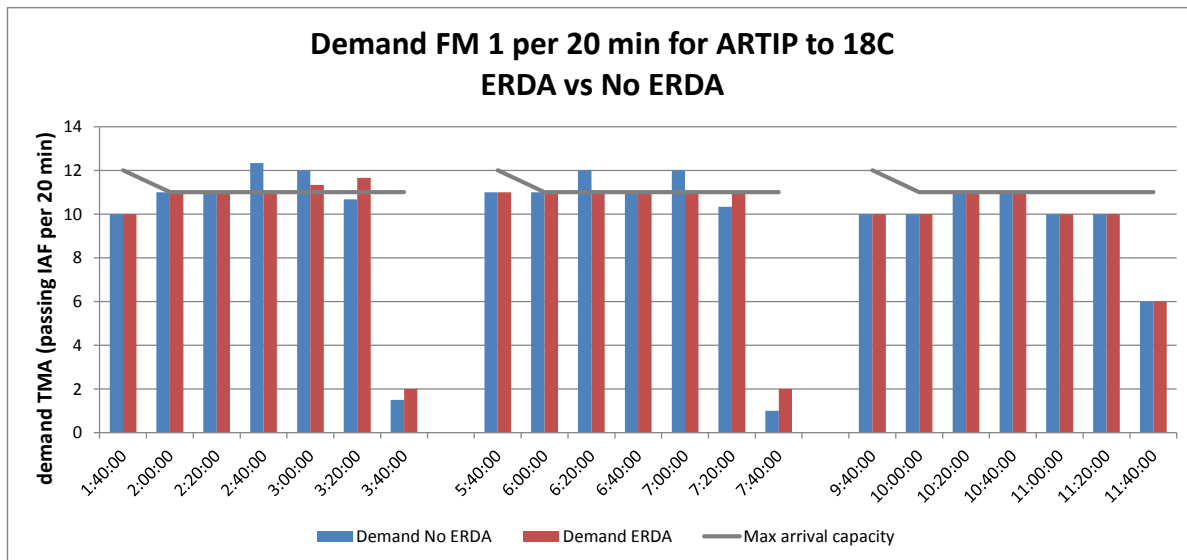


Figure 5.3: Fleet mix 1 demand per 20 minutes for three arrival peaks at ARTIP to 18C. Both the demand with (red) and without (blue) En-Route Delay Absorption is given, together with the maximum arrival capacity based on the fleet mix order and required separation.

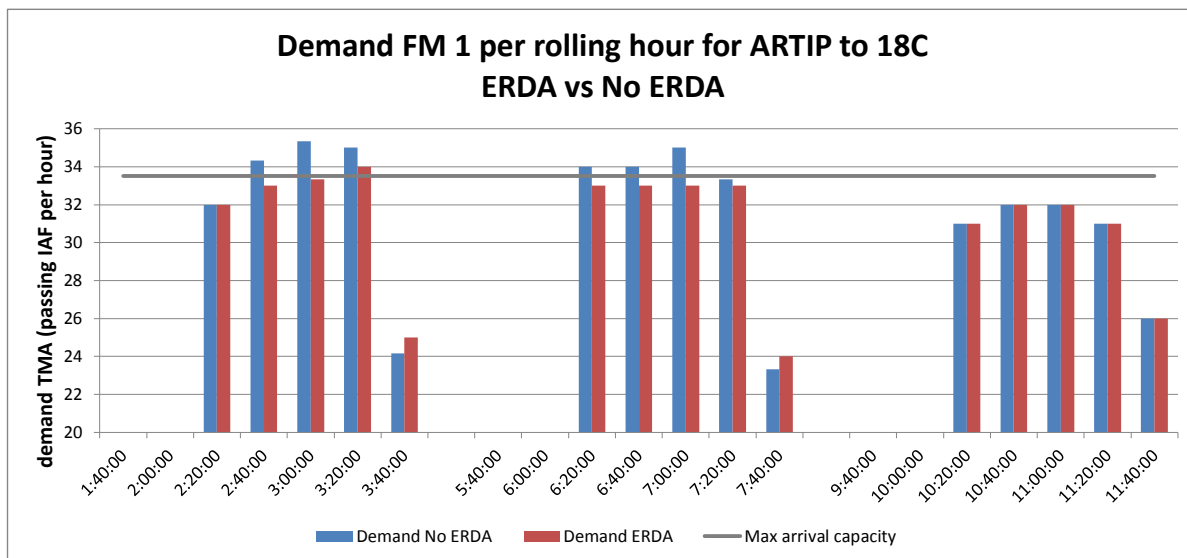


Figure 5.4: Fleet mix 1 demand per rolling hour for three arrival peaks at ARTIP to 18C. Both the demand with (red) and without (blue) En-Route Delay Absorption is given, together with the maximum arrival capacity based on the fleet mix order and required separation.

hour.

Figure 5.5 shows the demand per rolling hour for fleet mix 2. The average maximum arrival capacity for this fleet mix is 34,5 aircraft per hour, which is higher compared fleet mix 1. The reason is that fleet mix 2 consist of only medium aircraft, so the total amount of wake vortex separation is lower. A time separation of 105 seconds between medium aircraft allows 69 landings per two hours, or an average of 34,5 aircraft per hour. Due to a higher capacity, less delay will occur compared to the same demand profile of fleet mix 1, which will be shown in the next section when the results of throughput and delay are given. The demand for the ERDA scenario in the first and second arrival peak of figure 5.5 shows an en extra bar at 3:40 and 7:40 hours. Due to the en-route delay absorption algorithm, the arrivals at the IAF are shifted backwards and one aircraft in each inbound peak arrived just in the 3:40 and 7:40 hour time period.

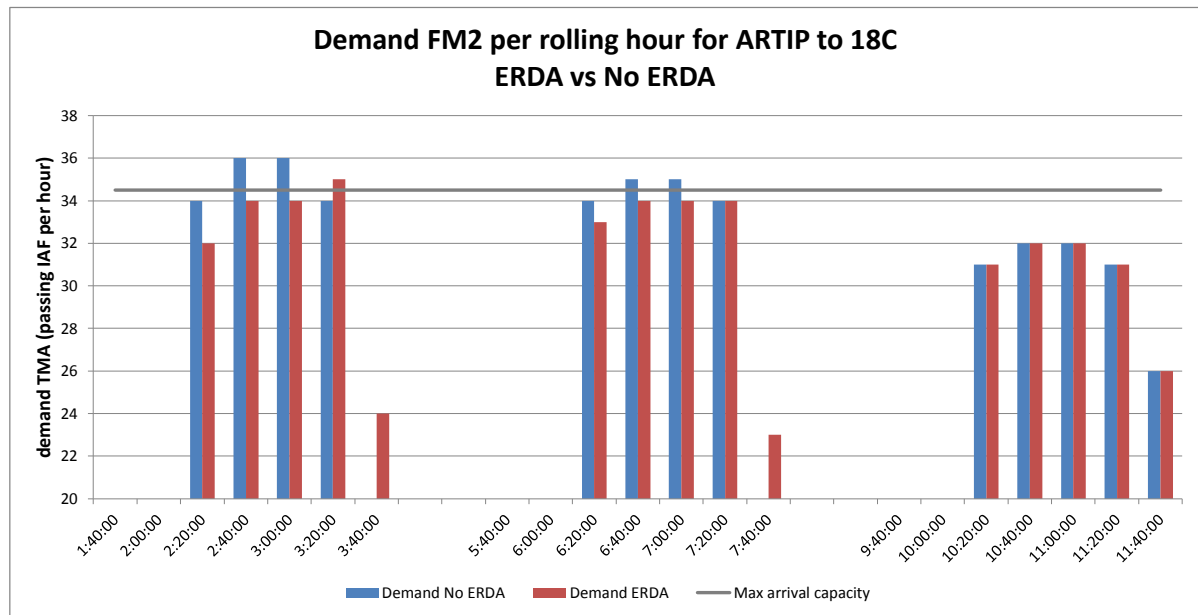


Figure 5.5: Fleet mix 2 demand per rolling hour for three arrival peaks at ARTIP to 18C. Both the demand with (red) and without (blue) En-Route Delay Absorption is given, together with the maximum arrival capacity based on the fleet mix order and required separation.

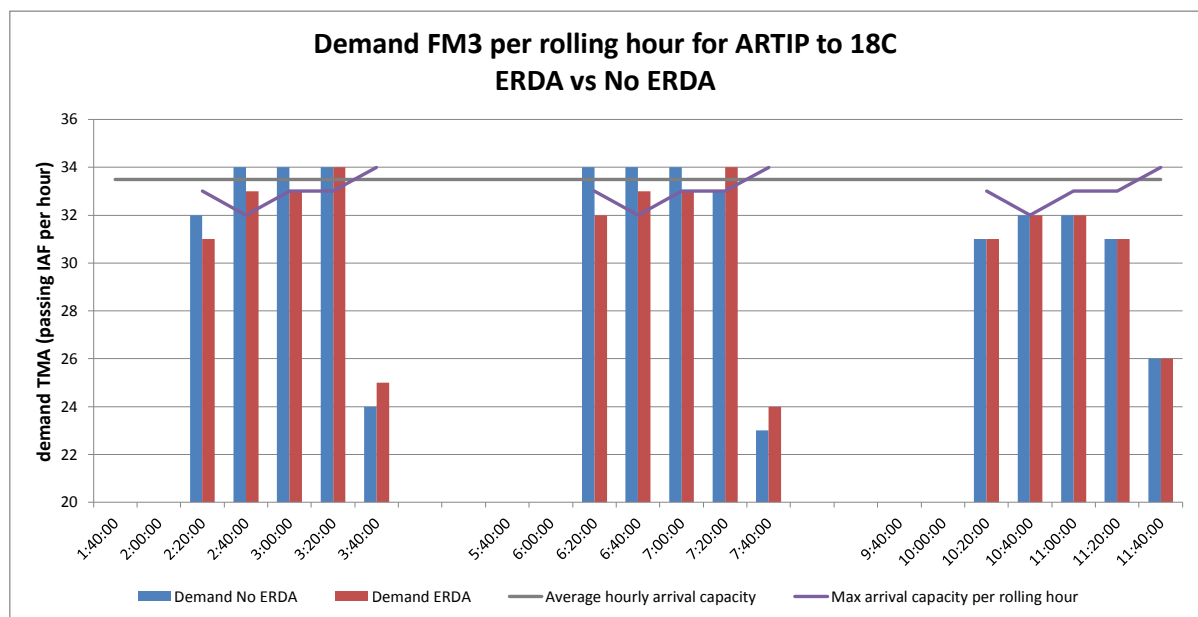


Figure 5.6: Fleet mix 3 demand per rolling hour for three arrival peaks at ARTIP to 18C. Both the demand with (red) and without (blue) En-Route Delay Absorption is given, together with the maximum arrival capacity based on the fleet mix order and required separation.

The demand per rolling hour for the three demand profiles with fleet mix 3 is given in figure 5.6. The average maximum arrival capacity for this fleet mix is lower than the ones for fleetmix 1 and 2. The third fleet mix has an average maximum arrival capacity of 33,5 aircraft per hour, based on the wake vortex separations. However, the actual arrival capacity per rolling hour for fleet mix 3 fluctuates more than the other two. To give a clear picture of the demand in relationship with the actual arrival capacity, a more accurate arrival capacity per rolling hour is also presented in the graph of fleet mix 3. Although 67 aircraft can land in two hours, resulting in an average arrival capacity of 33,5 aircraft

per hour, the actual arrival capacity per rolling hour shows a dip in the middle of the arrival peak. The small drop in capacity from 33 to 32 aircraft per rolling hour is a results of the fleet mix order were one medium aircraft is aligned after a super (A380) in combination with alternating medium aircraft landing after heavies instead of a combined group of heavies followed by a group of mediums. So there is a sequence of H-M-H-M-H-M aircraft in this third fleet mix order that reduces the capacity. If this sequence would have been reordered to a group of mediums landing after each other and a group of heavies, one extra airplane could have landed in that hour. This results in a decrease in throughput and an increase in delay, which will also be shown in the next section.

The graph in figure 5.6 reveals that the amount of aircraft passing the IAF is lower during the first inbound peak (32 and 34 aircraft per rolling hour) with this third fleet mix than the second fleet mix (34 and 36 aircraft per rolling hour). After close inspection on the trajectory logs of the simulation with FM 3, it appeared that the speeds of approximately 40 aircraft were reduced with 35 knots before they passed ARTIP. The speed reduction started to happen shortly before the third 20 minutes time period (2:40 hour). Also, some aircraft made a trajectory change in the ACC area to arrive later at the IAF. The reason for this speed reduction and trajectory change is caused by an AirTop simulation rule called 'waypoint in trail separation'. This rule will try to achieve a separation between the aircraft of minimal six NM when aircraft are passing the IAF, regardless of the wake vortex aircraft types. A demand of thirteen aircraft per 20 minutes apparently triggers the waypoint-in-trail rule, resulting in a decrease of planned demand. It is however strange to observe that the same demand profile triggers the waypoint-in-trail rule more often with a fleet mix 3 than a fleet mix of only mediums. To give a comparison: the number of aircraft affected by the waypoint-in-trail rule during the first inbound peak of the second fleet mix scenario was only fourteen. This change in speed and trajectory by the waypoint-in-trail rule resulted in a drop of demand from the planned thirteen arrivals at the IAF between 3:00 and 3:20 hour to only eleven. Although the demand restored to the planned number of twelve arrivals in the next 20 minutes, a demand of 34 aircraft per rolling hour is the result.

There is no significant difference in demand for the scenarios were aircraft enter the TMA at ARTIP and land on runway 36R instead of 18C. As an example, the graph of the demand for fleet mix 1 entering the TMA at ARTIP and landing on runway 36R is given in appendix C.

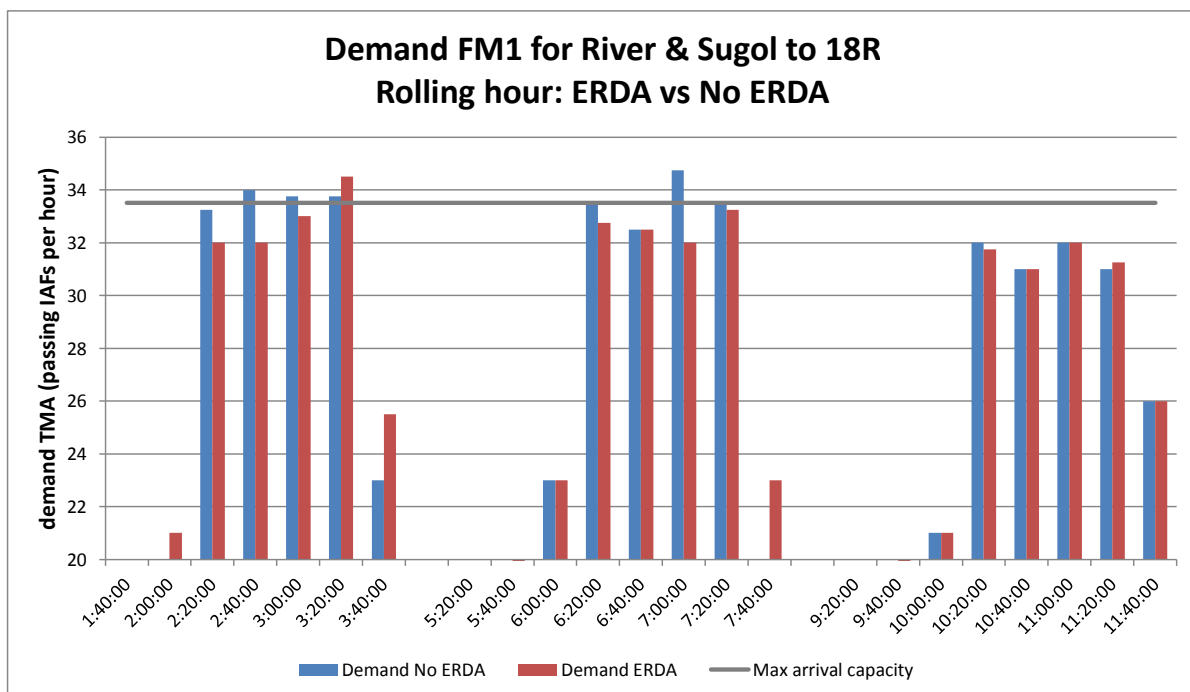


Figure 5.7: Fleet mix 1 demand per rolling hour for three arrival peaks at RIVER and SUGOL to 18R. Both the demand with (red) and without (blue) En-Route Delay Absorption is given, together with the maximum arrival capacity based on the fleet mix order and required separation.

For the scenarios where aircraft enter the TMA at RIVER and SUGOL and merge towards runway 18R, the demand per time period is somewhat different than the graphs shown previously. The reference times of aircraft in the simulation flight plans are defined by the amount of aircraft passing the threshold per 20 minutes time period and then the time each aircraft would pass the randomly assigned IAF is calculated based on the approach leg flight time. Because the flight time in the TMA is different for both approach legs, it can occur that an aircraft from SUGOL which is planned to land in front of the aircraft from RIVER, enters the TMA a time period later than the one coming from SUGOL. In other words, the demand profiles described in chapter 4.3.3 are not visible as such in the graph of figure 5.7.

Nonetheless, the first arrival peak still represents a high demand for arrivals such that the demand exceeds the capacity for a longer period of time. The third arrival peak has a low demand for arrivals below the maximum capacity and the second arrival peak has a demand that lies somewhere in between. At 7:00 hour, a high peak in demand appears for the non-ERDA case (blue bar), while ERDA caused a significant lower demand at the same time period. If this has an effect on the throughput, will be shown in the next section with figure 5.12. For completeness, the figures of demand for the remaining scenarios are given in appendix C.

5.1.2. Results of En-Route Delay Absorption with a single approach leg

First, the effect on throughput and delay with ERDA is shown separately for the three different fleet mixes that arrive at ARTIP and land on runway 18C. Next, the differences between the three fleetmixes is addressed shortly, followed by the final section that gives the difference between landings on runway 18C or 36R.

The effect on delay and throughput

The main research question of this project is to find out what the effect is of En-Route Delay Absorption on the landing throughput. The benefit of ERDA should be a reduction (or in the most optimal way, a disappearance) of the congestion delay in the TMA. In order to show both effects, the results of the different simulations regarding throughput and delay are presented in one graph.

Fleet mix 1

Figure 5.8 shows the throughput and delay for the first fleet mix entering the TMA at ARTIP and landing on runway 18C. The throughput is displayed as bars and the number of landings per rolling hour can be read on the left vertical axis. The average delay per aircraft is displayed as a line and is accompanied by a standard deviation to give an idea on the dispersion of the delay in that time period of the peak. The delay is related to the landing time and an average per 20 minutes is taken. The average delay is still given per 20 minutes and not per rolling hour, because there is a large difference in delay values between time periods, which would not be clearly visible when an average delay per hour would be given.

In figure 5.8, it can be observed that if an aircraft lands between 3:00 and 3:19:59 hours without ERDA (blue line), it would have endured an average delay in the TMA of 4 minutes and 33 seconds ($\sigma=15$ seconds). The effect of ERDA can clearly be observed: If the same aircraft lands in the same time period (3:00 hour) of arrival peak 1, but received together with the other aircraft an En-Route Delay Absorption instruction, it would only have encountered a delay of 47 seconds ($\sigma=10$ s) in the TMA (red line).

The maximum ERDA is limited to five minutes. During the first inbound peak, four aircraft required an en-route delay absorption above five minutes. As a result, some required additional spacing between those aircraft is left for the approach controller to resolve, which causes the delay in the TMA to rise to 1:03 minutes ($\sigma=10$ s) by the end of the peak. During the second inbound peak, a maximum required ERDA was kept under four minutes. The required ERDA decreases to three minutes for the last aircraft of the second inbound peak. If the predicted delay calculated by the ERDA algorithm can be absorbed en-route, which is the case for the second and third arrival peak, the delay in the TMA stays below one minute (red lines).

The delay propagation in each arrival peak occurs as expected. The first inbound peak without ERDA has a higher bunching effect (or peak in demand, see figure 5.4) and therefore, the maximum occurred delay is higher compared to the other two arrival periods. The difference in delay between ERDA and no ERDA for the third arrival period is not significantly large. This is not unexpected, because

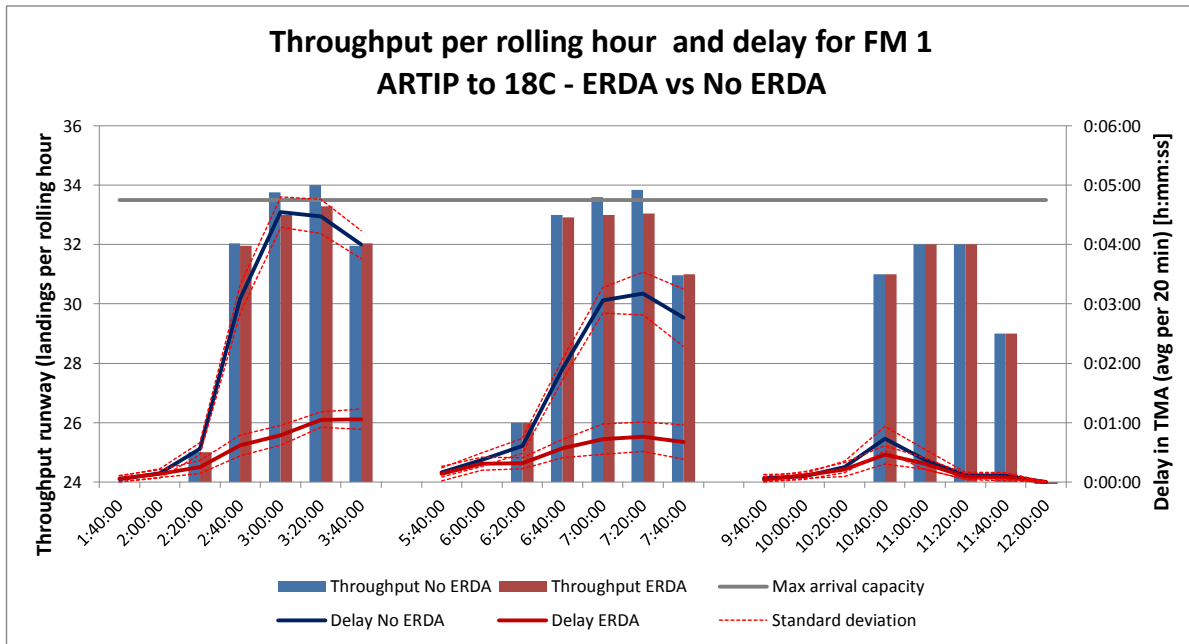


Figure 5.8: Fleet mix 1 throughput per rolling hour for three arrival peaks at ARTIP to 18C. Both the throughput with (red) and without (blue) En-Route Delay Absorption is given, together with the maximum arrival capacity based on the fleet mix order and required separation. The second vertical axis on the right side gives the average delay per aircraft per 20 minutes time period. The delay is shown with a standard deviation.

there is not much delay absorption to perform in the first place.

A small effect on the throughput can be observed in figure 5.8 for the first and second arrival period when En-Route Delay Absorption is applied. However, the decrease in throughput due to ERDA is relatively small. To give a clear indication on the effect of en-route delay absorption on the throughput, table 5.1 gives a detailed overview of the throughput values for the first two arrival periods that are displayed in figure 5.8. The difference in presenting the values per 20 minutes and per rolling hour is made clear by giving both. The throughput is an average over 25 simulation runs and therefore decimal numbers appear in the table. A standard deviation for the throughput is not given, because the variation is small (less than 0,5). From table 5.1, it is clear that for this scenario a decrease in runway throughput due to En-Route Delay Absorption is very small and can even be considered negligible.

Table 5.1: Detailed overview of the throughput per 20 minutes and rolling hour for the scenario of fleet mix 1 from ARTIP to runway 18C with and without ERDA. The top table represents the first arrival peak and the bottom table the second arrival peak.

Fleet mix 1							
Throughput \Time	1:40:00	2:00:00	2:20:00	2:40:00	3:00:00	3:20:00	3:40:00
20 min: No ERDA	4,0	10,0	11,0	11,0	11,8	11,2	9,0
20 min: ERDA	4,0	10,0	11,0	11,0	11,0	11,3	9,7
Rolling hour: No ERDA			25,0	32,0	33,8	34,0	32,0
Rolling hour: ERDA			25,0	32,0	33,0	33,3	32,0
Throughput \Time	5:40:00	6:00:00	6:20:00	6:40:00	7:00:00	7:20:00	7:40:00
20 min: No ERDA	4,0	11,0	11,0	11,0	11,6	11,2	8,2
20 min: ERDA	4,1	10,9	11,0	11,0	11,0	11,0	9,0
Rolling hour: No ERDA			26,0	33,0	33,6	33,8	31,0
Rolling hour: ERDA			26,0	32,9	33,0	33,0	31,0

The reason that the throughput does not decrease drastically, is because the inter-arrival time at the IAF between the aircraft is kept the same as the required wake vortex time separation. If one aircraft

arrives later at the IAF than the planned CTO, it will maintain a slightly higher speed or short flight path towards the glideslope to catch up. If the second aircraft is also later at the IAF than the planned CTO (let's say that both aircraft arrive 30 seconds later due to miscalculated headwind), it will not automatically lead to a decrease in runway throughput. The inter-arrival time at the IAF between both aircraft is not changed, because they both suffered the same (en-route) delay. En-route Delay Absorption will only help to diminish any bunching effect and optimise the inter-arrival separation. If the navigational equipment (on the ground or airborne) can guarantee an accurate time each aircraft can pass certain waypoints, the congestion delay in the TMA can be kept to a minimum.

Fleet mix 2

The effect on throughput and demand for the second fleet mix is graphically displayed in figure 5.9. The same trend found for the first fleet mix can be observed here. The first arrival peak has the highest delay, but this delay is not so high compared to the first fleet mix. This is because the arrival capacity for this fleet mix is higher and the demand stays the same. The highest delay occurs again at 3:00 hour and has an average value of 3:06 minutes ($\sigma=14$ s). The highest delay in the second arrival peak is 1:32 minutes ($\sigma=7$ s). All delays can be absorbed en-route and the average delay in the first and second arrival period does not rise above 32 seconds and a maximum standard deviation of ten seconds. The reason for a lower delay in the TMA can also be found in the homogeneous fleet mix. The approach speeds of the medium aircraft in this scenario do not divert much from each other. The simulation program could handle the speed solutions and vectoring problems much better.

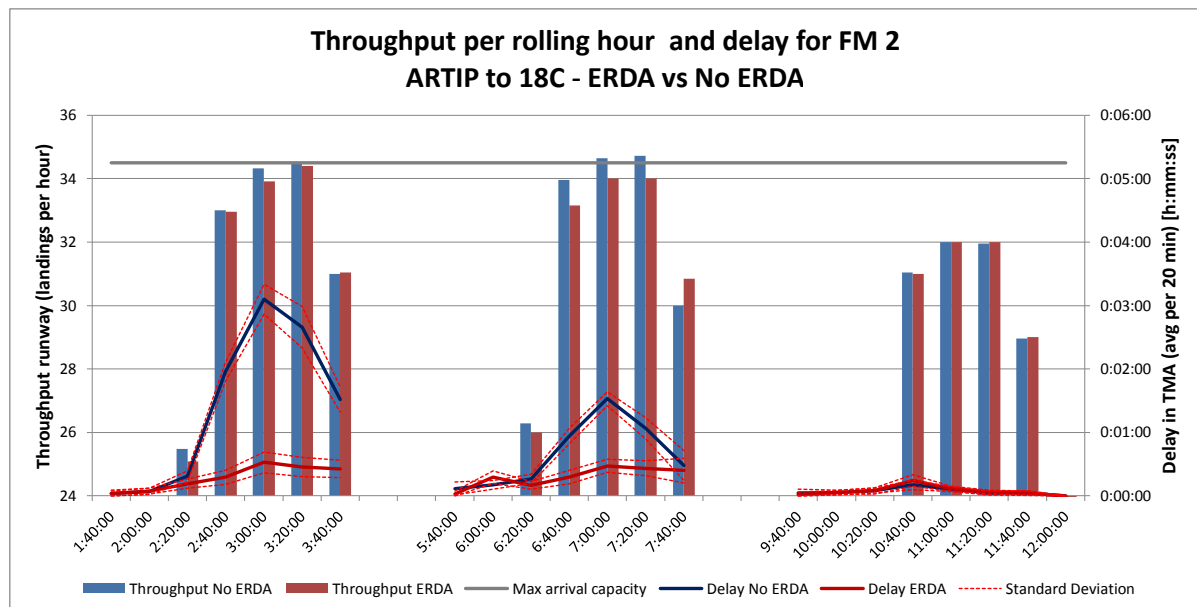


Figure 5.9: Fleet mix 2 throughput per rolling hour for three arrival peaks at ARTIP to 18C. Both the throughput with (red) and without (blue) En-Route Delay Absorption is given, together with the maximum arrival capacity based on the fleet mix order and required separation. The second vertical axis on the right side gives the average delay per aircraft per 20 minutes time period. The delay is shown with a standard deviation.

The difference in throughput between the ERDA and No ERDA scenario is again negligible. Both throughputs remain high and close to or slightly above the maximum declared capacity of 34 landings per hour.

The difference between the landing time of the ERDA and no ERDA scenario does not deviate much. The landing time of the last aircraft without ERDA is approximately one minute earlier than the last aircraft that did undergo an en-route delay instruction. However, this aircraft did not have to pay the cost of one extra minute at a low altitude in the TMA. The same holds for the last aircraft in the second arrival peak. The difference in landing time of the last aircraft between the two scenarios is approximately 30 seconds, because there was still half a minute of delay absorption required for the last airplane. In section 5.1.4, some additional research on the actual landing time differences between

ERDA and no ERDA is discussed.

Fleet mix 3

The third fleet mix results in a lower runway capacity than the second fleet mix and as described with figure 5.6, the actual runway capacity has a dip to 32 landings per hour in the beginning of the peak. This results in an average delay that is much higher compared to the other two fleet mixes, as can be seen in figure 5.10. The maximum delay when no ERDA is applied, reaches 5:57 minutes ($\sigma=18$ s) during the first arrival peak. Not all delay can be absorbed en-route during the first inbound peak and the delay in the TMA rises significantly above one minute in the scenario with ERDA (red line). The delay during the second inbound peak for the ERDA scenario behaves more constant throughout the peak.

The effect on throughput when En-Route Delay Absorption is applied, is the same for this fleet mix as with the others. The throughput does not decrease significantly in this simulation either. In fact, it is even increasing in the second hour of the first arrival peak. Most likely, this is because not all delay could be absorbed en-route by the end of the first inbound peak. The differences in throughput are very small and to have a good overview, the exact numbers are given in table 5.2.

Table 5.2: Detailed overview of the throughput per 20 minutes and rolling hour for the scenario of fleet mix 3 from ARTIP to runway 18C with and without ERDA. The top table represents the first arrival peak and the bottom table the second arrival peak.

Fleet mix 3							
Throughput \ Time	1:40:00	2:00:00	2:20:00	2:40:00	3:00:00	3:20:00	3:40:00
20 min: No ERDA	4,0	10,0	11,0	11,0	11,0	11,0	10,0
20 min: ERDA	4,0	10,0	10,4	10,8	11,7	11,0	10,0
Rolling hour: No ERDA			25,0	32,0	33,0	33,0	32,0
Rolling hour: ERDA			24,4	31,3	33,0	33,6	32,7
Throughput \ Time	5:40:00	6:00:00	6:20:00	6:40:00	7:00:00	7:20:00	7:40:00
20 min: No ERDA	4,2	10,8	11,0	11,0	11,0	11,0	9,0
20 min: ERDA	4,1	10,9	10,7	10,9	10,9	11,3	9,2
Rolling hour: No ERDA			26,0	32,8	33,0	33,0	31,0
Rolling hour: ERDA			25,7	32,5	32,5	33,1	31,4

The effect of different fleet mixes

The difference between the three fleet mixes has an effect on the actual runway capacity and this has a great impact on the delay propagation. More super and heavy aircraft mixed with medium ones (fleet mix 3) has a bigger (negative) impact on the runway throughput than the use of En-Route Delay Absorption. This research did not investigate the effect of resequencing the upcoming arrival stream with the aid of an AMAN system, but resequencing the order and swap some aircraft's place with another shows that the the runway arrival capacity will increase with one extra landing per hour.

Difference between landing on runway 18C or 36R

When the wind blows from a Northern direction, aircraft coming from ARTIP during an arrival peak are preferred to land on runway 36R (see chapter 3). The approach leg from ARTIP to runway 36R is longer than the one to 18C, so the flight time is longer as well. To see if a different (single) approach leg has an effect on the throughput and delay, the same scenarios and fleet mix orders previously described, are simulated with landings on runway 36R. The maximum arrival rate for this runway is kept the same, 34 landings per hour. The average shortest flight time for a jet aircraft from ARTIP to 36R is 1:25 minutes longer than towards runway 18C.

The throughput and delay for fleet mix 3 landing on runway 36R is displayed in figure 5.11. If this graph is compared with figure 5.10, only small differences in delay can be observed. The throughput between runway 36R and 18C for both ERDA and No ERDA scenarios are the same. The amount of delay for the 'No ERDA' scenario is the same for the first inbound peak, around six minutes. the maximum delay for the 'no ERDA' scenario increases slightly to 4,5 minutes in the second arrival peak when aircraft land on 36R, compared to the maximum delay of four minutes when aircraft land on runway 18C. There is also a slight increase in delay in the second arrival peak when ERDA is applied

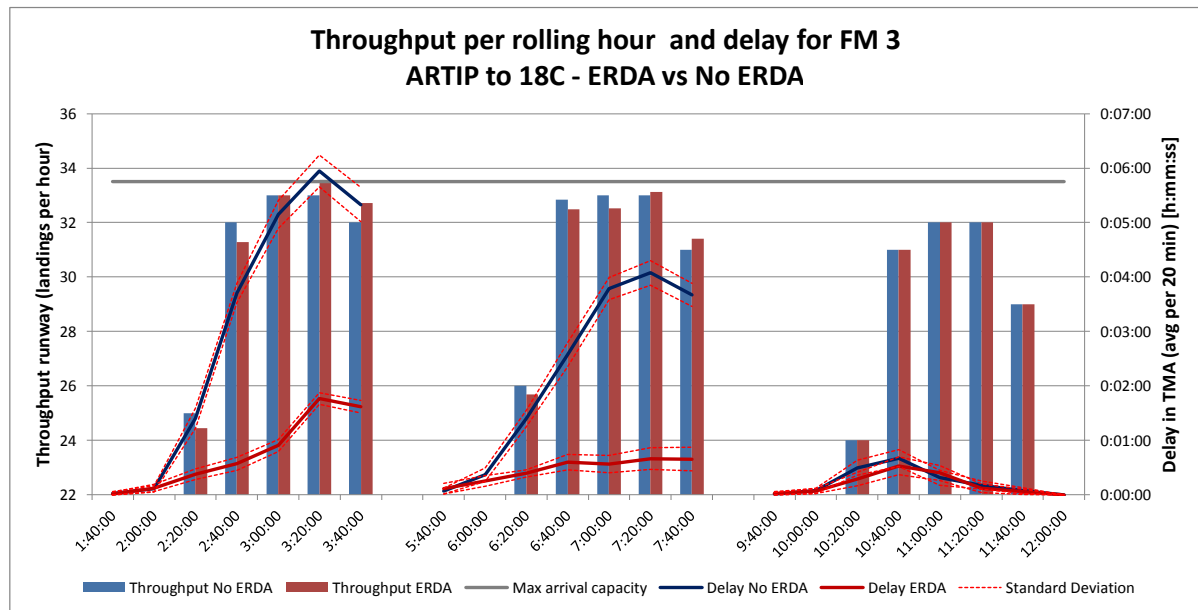


Figure 5.10: Fleet mix 3 throughput per rolling hour for three arrival peaks at ARTIP to 18C. Both the throughput with (red) and without (blue) En-Route Delay Absorption is given, together with the maximum arrival capacity based on the fleet mix order and required separation. The second vertical axis on the right side gives the average delay per aircraft per 20 minutes time period. The delay is shown with a standard deviation.

for landings on 36R compared to the scenario with ERDA when aircraft land on 18C. This is also the case for fleet mix 1 and 2 landing on runway 36R, of which the graphs are shown in appendix C .

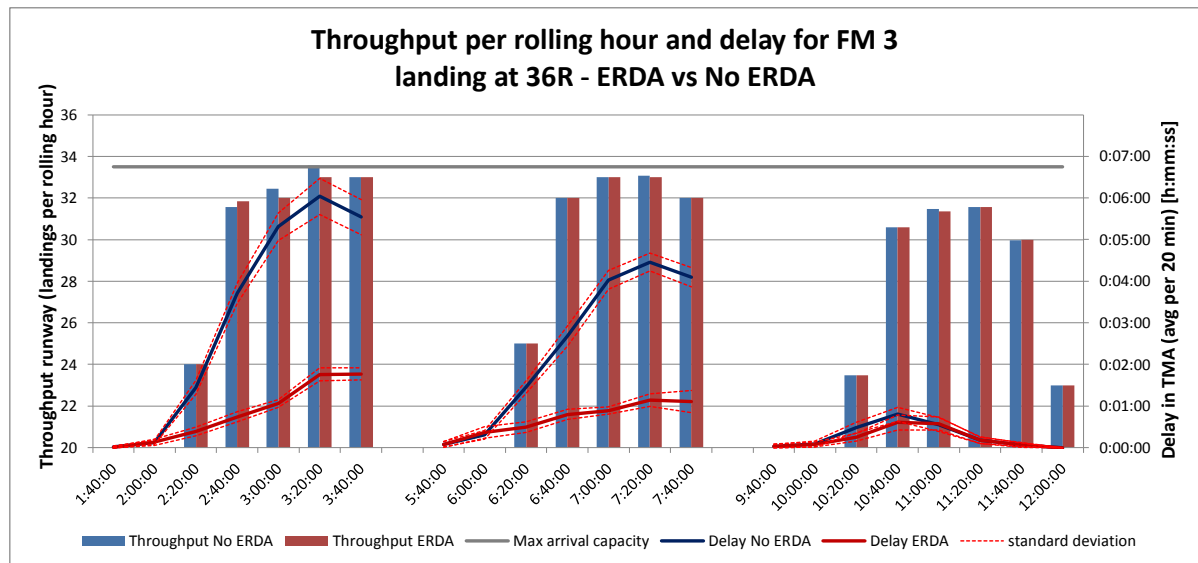


Figure 5.11: Fleet mix 3 throughput per rolling hour for three arrival peaks at ARTIP to 36R. Both the throughput with (red) and without (blue) En-Route Delay Absorption is given, together with the maximum arrival capacity based on the fleet mix order and required separation. The second vertical axis on the right side gives the average delay per aircraft per 20 minutes time period. The delay is shown with a standard deviation.

A possible explanation for this difference in delay between both approach paths could be the flight path length. The common flight path before the final approach fix is longer for the approach to runway 36R than the one used to land on 18C. If a slower aircraft is in front of a faster one, the faster aircraft has to add additional spacing (or time) in the vectoring area before the common flight path to prevent overtaking or a loss of separation on that path. In this case, the difference in length of both approach paths is not so big ,so the difference in delay is small as well. However, it is expected that an increase

in the length of the common approach path will increase the amount of delay, regardless of the use of ERDA. This can be important when fixed routes inside the TMA of Schiphol airport are implemented in the future.

5.1.3. Results of ERDA for two merging approach legs

When two approach legs merge in the TMA to one final approach path, the approach sequencing gets more complex. Aircraft on one approach leg must maintain enough spacing between them to allow other aircraft coming from a different approach leg to be merged on the common flight path. The accuracy of passing the IAF at the Controlled Time Over (CTO)¹ of both IAFs is very important in this situation, because the CTOs are related to each other. For example, if the ATO SUGOL of one aircraft deviates too much from the required CTO, but the ATO RIVER of another aircraft is exactly equal to the CTO, the planned separation between both aircraft at the merging point and on the final approach leg will be lost. During an inbound peak, this scenario can disrupt the planned sequence and result in additional delay in the TMA which was not foreseen. If aircraft already encountered delay absorption en-route, but have to endure the same amount of delay in the TMA that was predicted in the first place, the benefits of ERDA no longer holds.

In section 4.3.2, the range of accuracy in which aircraft have to pass their reference time (CTO at the IAF was determined to be ± 30 seconds. When the range of accuracy is different for one IAF than the other, it is referred to as an off-set between them. In the next section, the results are given for the simulation scenario when both fixes have the same range of accuracy for the reference time at the IAF, namely ± 30 seconds. Next, the outcome of those results are compared with the outcome of two simulation scenarios in which there is an off-set between the ATO accuracy of both IAFs.

Effect on throughput and delay with no off-set in ATO accuracy between both IAFs

The effect on the throughput and delay for fleet mix 1 is displayed in figure 5.12 in the same way as in the previous section. The maximum delay during the first arrival period has an average value of 4:50 minutes ($\sigma=15$ s) when no ERDA is applied and 1:01 minute ($\sigma=8$ s) when there is En-Route Delay Absorption. For the second arrival peak, the maximum delays are 3:05 minutes ($\sigma=13$ s) and 43 seconds ($\sigma=10$ s) for the scenario No ERDA and ERDA, respectively. The difference in delay in the third arrival peak is not significant and the maximum delay stays below one minute.

Also in this scenario with two approach legs, the throughput does not decrease when En-Route Delay Absorption is simulated. The values for the throughput in each arrival peak are similar to the ones for the single approach leg (and same fleet mix) presented in table 5.1 and figure 5.8. In fact, the results for the simulations of fleet mix 2 and 3 merging from two approach legs to one have the same outcome as the scenarios where a single approach leg is simulated. The graphs of the throughput and delay for these simulations can be found in appendix C.

The results of throughput and delay with ERDA are used as a reference in the next part, when the effect on throughput and delay with different off-sets is analysed.

Effect with an off-set between both IAFs

When aircraft arrive earlier or later at the IAF than the planned time of the AMAN system (due to e.g. a wrong wind prediction model) and have to merge from two approach legs to one runway, it could have a negative impact on the throughput and delay. The following simulations are performed with fleet mix 1 entering the TMA at RIVER or SUGOL and land on runway 18R:

- Off-set 1: The accuracy at RIVER is between -60 and -30 seconds (too early), at SUGOL between +30 and +60 seconds (too late).
- Off-set 2: The accuracy at RIVER is between +30 and +60 seconds (too late), at SUGOL between -60 and -30 seconds (too early).

The results of these simulations are presented in figure 5.13 and 5.14. The first graphs shows the throughput for the three different inbound peaks and compares the two off-sets with the throughput found earlier when there is no off-set. The second figure shows the corresponding delay. To have a clear view, the delay is presented in a different graph than the throughput and without the standard deviations ($\sigma_{max} = 11$ s).

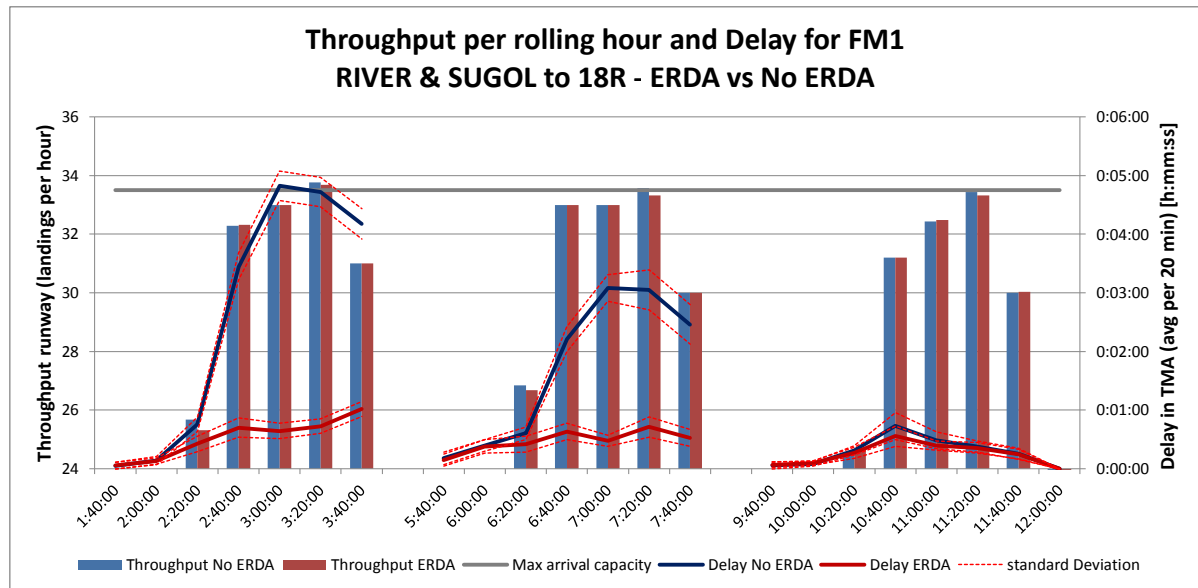


Figure 5.12: Fleet mix 1 throughput per rolling hour for three arrival peaks from RIVER & SUGOL to 18R. Both the throughput with (red) and without (blue) En-Route Delay Absorption is given, together with the maximum arrival capacity based on the fleet mix separation. The second vertical axis on the right side gives the average delay per aircraft per 20 minutes time period. The delay is shown with a standard deviation.

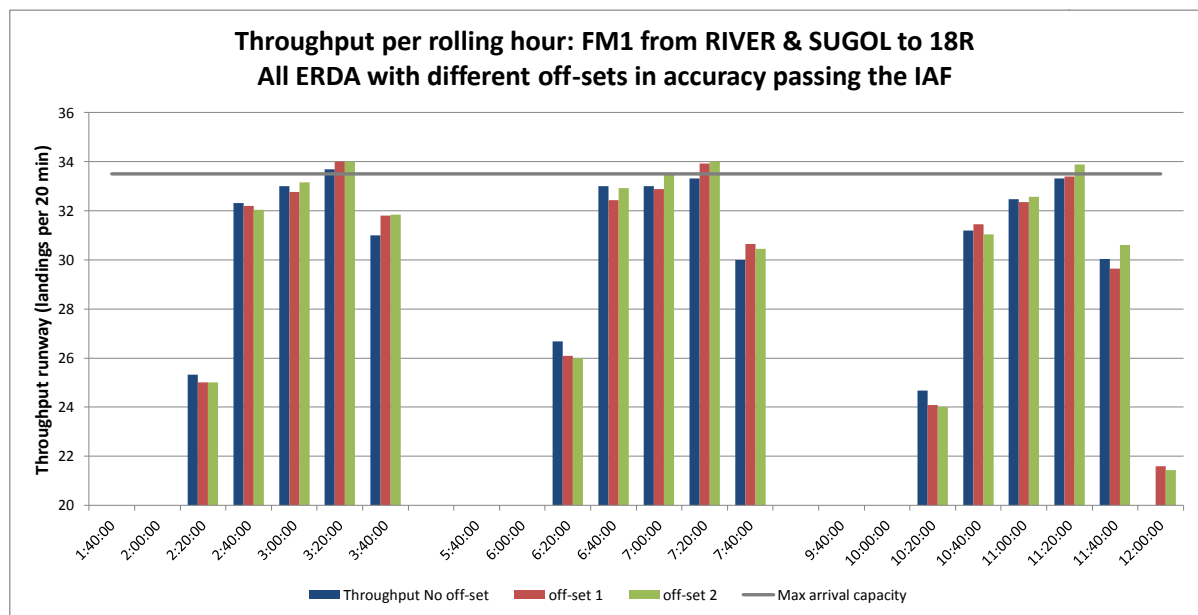


Figure 5.13: Throughput per rolling hour during three different inbound peaks with the two off-sets between RIVER and SUGOL and the reference throughput without off-set.

The different throughputs in figure 5.13 show no significant difference between them. The throughput in each rolling hour has the same value (rounded off to the closest integer number) as the throughput values found for the simulation where no ERDA was applied. It can be concluded that an off-set in passing the IAF has no effect on the throughput.

The results for delay, given in figure 5.14, show that the delay curve for off-set 1 and 2 is shifted upwards compared to the delay curve with the 'No off-set' scenario. The difference between the reference delay curve and off-set 1 is small and the standard deviations are actually overlapping, so it is hard to conclude that they differ significantly. Only at the end of the first and second inbound peak,

¹The time an aircraft has to be over a certain waypoint with a certain accuracy

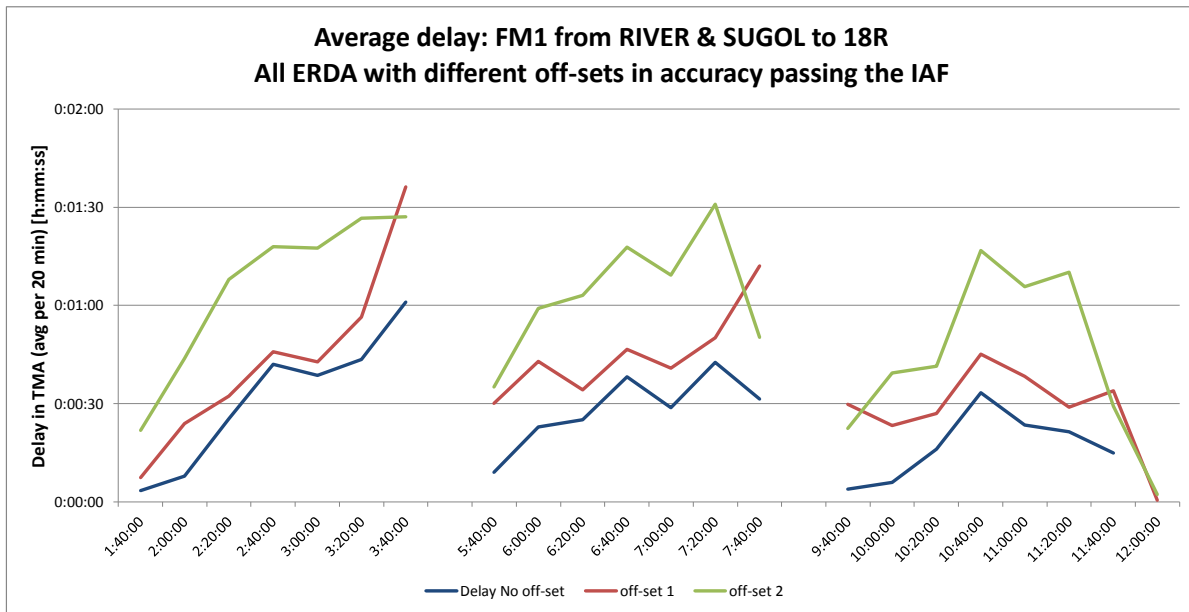


Figure 5.14: Delay curves for three different inbound peaks with the two off-sets between RIVER and SUGOL and the reference delay curve without off-set.

some difference in delay appear.

Apart from the delay at the end of the first and second arrival peak, only the delay curve of off-set 2 passes the 1 minute delay mark. Although there is an increase in delay when an off-set in accuracy between both IAFs occurs, the congestion delay is still below 1,5 minutes and the benefit of En-Route Delay Absorption is preserved. In section 5.2, more analysis is performed on scenarios where there is an off-set in ATO accuracy between two initial approach fixes with the simulations at Charles de Gaulle airport.

5.1.4. Discussion Schiphol airport simulation results

It is already briefly remarked during the presentation of the results of the second fleet mix, but the difference in actual landing time between an aircraft that endured congestion delay in the TMA and the one experienced En-Route Delay Absorption can be important for some stakeholders as well. If the total delay (the en-route delay imposed by the ERDA tool + some remaining delay in the TMA) is higher when ERDA is applied, stakeholders could be reluctant towards the use of it. The landing times from one simulation run of the first fleet mix are compared for both the ERDA and no ERDA case.

There is a maximum ERDA in the first inbound peak with fleet mix 1 of five minutes. The maximum delay when no ERDA is applied is approximately 4,5 minutes (see figure 5.8). So it is expected that the delay in the TMA is transferred to an earlier en-route phase and that the differences in actual landing time are minimal. The last ten aircraft of the first inbound peak with ERDA, still endured approximately 4 minutes of delay absorption en-route, but also face an average 1:03 minutes of delay in the TMA. The last ten aircraft of the first inbound peak without ERDA experienced on average between 4:00 and 4:28 minutes of congestion delay in the TMA. However, when no ERDA is applied, aircraft at the end of the peak arrived 1:26 minutes (± 10 s) earlier than the ones with ERDA.

The second inbound peak of figure 5.8 shows less difference in actual landing time between the two scenarios. Although three minutes of en-route delay absorption is required at the end of this inbound peak, the last ten aircraft land only 31 seconds (± 10 s) later than the ones without ERDA. But these aircraft have to accept on average congestion delays in the TMA between 2:46 and 3:10 seconds, while the ERDA aircraft only endure 40 to 46 seconds of congestion delay in the TMA.

It is up to the different stakeholders to decide if the benefits of En-Route Delay Absorption outweigh the possibility of a later arrival at the gate.

For the low demand peak (third inbound peak) of all three fleet mixes, no significant effect in demand (and therefore delay) can be observed, because there is no En-Route Delay Absorption needed. the

amount of aircraft arriving at the IAF per 20 minutes is spread out evenly, with a ATO accuracy of ± 30 seconds. However, large bunching effects at the FIR boundaries can still occur if e.g. ten aircraft arrive in the first ten minutes instead of evenly over 20 minutes. ERDA should easily be able to 'debunch' traffic when demand is low. Especially when the technique is used were the first aircraft gets an increased speed command and the last ones a speed decrease command, the throughput will be maintained.

The required amount of ERDA decreases by the end of the inbound peak when there is a decrease in demand (and the airport shift from inbound to outbound peak). Because the inbound peaks are limited in time, ERDA can be applied without a significant decrease in overall throughput during the inbound peak. It is not investigated what would happen in the case of a rolling hub and a constant demand close to the maximum arrival capacity for an extended period of time (compared to the operations at Heathrow airport).

It is not possible to automatically adjust the required ERDA in the used version of AirTop. The planned time over the IAFs must be adjusted through the flight plans and once the simulation is running, it cannot be modified in case additional delay in the TMA occurs. Therefore, it was not possible to include a random missed approach during the inbound peak. It was suggested by one of the operational experts at LVNL to investigate the effect of a missed approach when ERDA is applied. Such an event can occur during an inbound peak and will have a large impact on the further development of the inbound peak. The effect on cross border arrival management when a sudden change in runway capacity or demand occurs (a change in runway configuration, a missed approach, a pop-up flight, etc.), is worth investigating further. Preferable combined with a research on the workload of different air traffic controllers.

Although workload of the approach air traffic controllers is not measured in this research, the required area inside the TMA needed for vectoring manoeuvres with ERDA is considerably less than for the non-ERDA scenario. Figure 5.15 shows the difference between both. Although this picture primarily indicates that smaller vectoring manoeuvres are required with ERDA, it does not give an indication on the amount of speed reductions or other ATCO instructions required to separate the traffic. At this moment, it is unknown if an improved sequence of traffic prior to the TMA result in a decrease of workload for the APP controllers. The workload of controllers is an important factor used at LVNL for the maximum declared capacity of the runways [10]. If ERDA can decrease the overall workload of the APP controllers, an increase in maximum declared capacity could be considered.

However, if the workload of approach controllers would decrease, it will most likely increase the workload of ACC and upper area controllers [35]. A side effect of that increase in workload in the other airspaces could result in a decrease in the number of aircraft allowed towards the airport. So all airspaces and control areas along the trajectory need to experience at least an equal amount of workload when En-Route Delay Absorption is used, in order to make this arrival technique work.

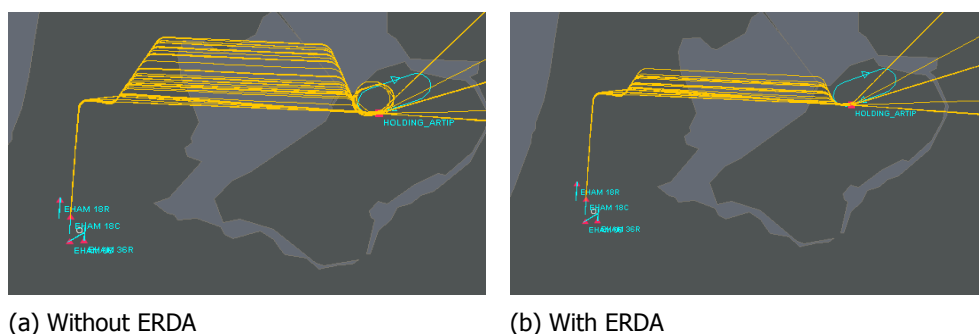


Figure 5.15: vectoring manoeuvres in the TMA for the second inbound peak of fleet mix 1 without (a) and with ERDA (b).

The results of throughput and delay when aircraft landed on runway 36R, shown in figure 5.11, revealed that there is a slight increase in delay for the ERDA scenario. One of the explanations could be that a longer common approach path (final approach path or fixed approach path for CDO) results in additional congestion delay if the arrival management system does not differentiate enough between different aircraft performance classes. Slower aircraft will always result in a decrease of runway effi-

ciency because gaps in the sequence occur due to an increase in distance between a faster leading aircraft and the slower trailing one. Furthermore, faster trailing aircraft have to slow down to prevent overtaking the slower leading one. Additional (time) spacing needs to be taken into account when faster aircraft in the sequence are entering the common flight path and slower aircraft have to merge that common flight path as late as possible. An exclusive approach path from an additional Initial Approach Fix towards a designated runway for general aviation and propeller aircraft could be a possible solution for Schiphol airport. This method of designated approach paths for propeller aircraft is used at Charles de Gaulle airport and could serve as an example. However, the TMA structure and size of CDG airport is different than the one at Schiphol airport, so additional research will have to be performed to see if this idea is applicable. The use of extra approach paths in the smaller TMA of Schiphol will increase the complexity and can create conflicts with other (outbound) air traffic paths.

The (estimated) flight time in the TMA is an important parameter for the ERDA algorithm and depends on aircraft performance and the reference approach flight path. Difference in aircraft performance or airline tactics can be an important parameter for the controlled time over the IAF, especially when future fixed arrival routes and Continuous Descent Operations (CDOs) limit the use of vertical separation in the TMA. The BADA files used for the simulations did not have much difference in approach profiles between aircraft. As a result, the flight times in the TMA between the different aircraft types did not deviate much as well. However, the question remains if the used BADA class 3 is accurate enough to represent the actual aircraft performance during the approach towards both airports.

One of the research objectives formulated in the beginning of the project, was to find a value for the amount of delay that was left for the TMA to absorb in order to maintain runway efficiency. The simulation results show that there is always a certain minimum delay in the TMA, which is mainly caused by the diversity in aircraft performance. When taking the assumptions of the simulations into account (good weather, certain accuracy in reaching the planned waypoint time, etc.), there is no need to maintain extra delay for the approach controller to absorb in order to guarantee a sufficient runway throughput. There will always be some deviation of the most optimal flight path for each aircraft in the TMA in order to fine-tune the arrival sequence, causing some congestion delay. This minimal delay in the TMA depends on length of the common approach path, the fleet mix order and the difference in aircraft performance. If the right inter-arrival times at the entrance of the TMA are achieved accurately enough, the runway efficiency will be maintained sufficiently. However, it does not mean that all congestion delay should be absorbed in an earlier en-route flight phase if it has a negative impact on ATCO's workload. It can be necessary to divide the expected amount of delay over all the different flight phases of the trajectory in order to find the best solution that serves the complete system and not just one or two individual aircraft.

5.2. Charles de Gaulle airport simulation results

Although both airports in this research have a similar approach in handling arrivals, there are also small differences that can change the outcome of the results. As explained in chapter 4, there were difficulties to get realistic simulation results when the same air traffic handling rules as Schiphol airport were applied. The simulation set-up is somewhat different and only one simulation is performed per scenario. Therefore, the results of the for Charles de Gaulle airport do not have a strong statistical strength, but they can still give a good indication of the effect on change in demand, delay and throughput when En-Route Delay Absorption techniques are applied.

In the next section the effect on the demand, delay and throughput for different distributions of aircraft passing the two Initial Approach Fixes is analysed. In chapter 5.2.2, the results of delay and throughput are given when there are different off-sets between both IAFs. This section ends with a discussion on the results of CDG.

5.2.1. Effect on demand, delay and throughput

The same order of presentation as for the results from Schiphol airport is used here. First, the change in demand and the variation in maximum arrival capacity of the fleet mix order are presented. Next, the effects on delay and throughput for the different scenarios are shown.

Demand and arrival capacity at CDG

When the wake turbulence time based separation rule in AirTop was used for the CDG simulation, too many unexpected conflicts occurred at the merging point of both approach legs. A stable simulation environment (where no aircraft would overtake another on the glideslope path) could only be achieved when the distance based wake turbulence separation rules were applied. An additional arrival buffer of 0,5 NM between each aircraft in the TMA helped to achieve an arrival rate of approximately 36 aircraft per hour. The actual simulated landing times and logged separation distances at the threshold revealed that the inter-arrival times between each wake turbulence class is similar to the calculated time based separation values.

In order to calculate the maximum arrival capacity for the simulated fleet mix order, the time based separation values are used. When an equal amount of aircraft during the inbound peak arrive at LORNI and MOPAR (50-50 distribution), the used fleet mix order allows 73 aircraft to land in 2 hours in perfect conditions. The same amount of aircraft can land for the 60-40 distribution scenario. There is a small decrease in maximum landing capacity due to a different order for the 70-30 and 30-70 percent distribution scenarios: 72 aircraft per hour.

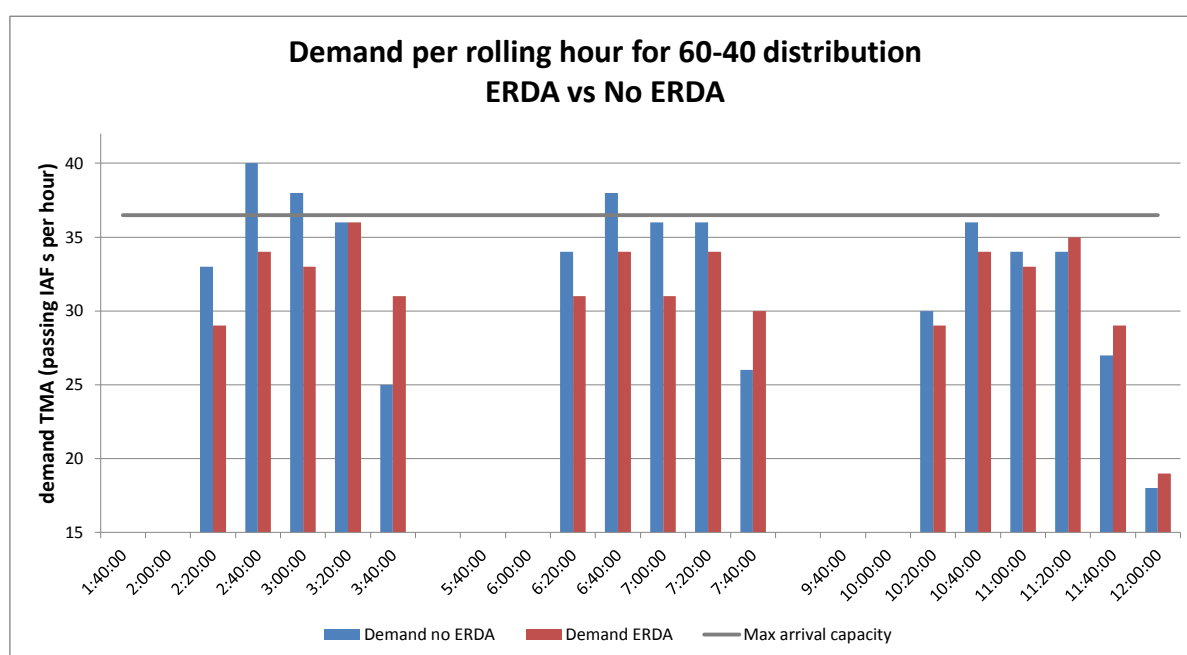


Figure 5.16: Demand per rolling hour for three inbound peaks at Charles de Gaulle and a distribution of arrivals between MOPAR and LORNI of 60 and 40 percent, respectively. Both the demand with (red) and without (blue) En-Route Delay Absorption is given, together with the maximum arrival capacity based on the fleet mix order and required separation.

The demand per rolling hour for the 60-40 distribution scenario is given in figure 5.16. The amount of aircraft passing both IAFs is higher than the maximum capacity in the first and second inbound peak when no ERDA is used. The bunching effect is higher in the first arrival peak, compared to the second one.

When ERDA is applied, the demand shows a drop at 3:00 and 7:00 hours, the busiest moments during the inbound peak. The exact reason for this drop is hard to determine. A combination of the fleet mix order (2 more heavies compared to the previous and next time period) and the distribution of aircraft entering the TMA at MOPAR or LORNI could be a possible explanation. Overall, the demand with ERDA stays well below the maximum arrival capacity. And the demand graphs for the other three distributions, which can be found in appendix C show the same result². An explanation for this decrease in demand must be found in the way the time based separation values are set. For each time interval between aircraft, eight seconds are added to compensate for the 0,5 NM arrival buffer. When the results of the simulations were analysed, it became clear that the time interval values already include

²The difference in demand for different distributions of arrivals at the IAFs is marginal. Therefore, the graphs for the demand are placed in the appendix in case the reader is interested in the specific demands per scenario.

the arrival buffer. When eight seconds of additional spacing are added, the maximum arrival capacity decreases to approximately 34 aircraft per hour.

Figure 5.17 shows the demand for the same 60-40 distribution, but now with adjusted ERDA settings for the intervals. The drop in demand at 3:00 and 7:00 hours is still there, which indicate that the fleet mix order can be a reason for that. But more important, the demand with ERDA is closer to the maximum arrival capacity. This will have an effect on the throughput and delay, shown in the next part.

Although the settings for ERDA are not used correctly, the results of these simulations are still presented because they clearly show the effect on the throughput when the wrong (dynamic) inter-arrival separation values are used in combination with En-Route Delay Absorption.

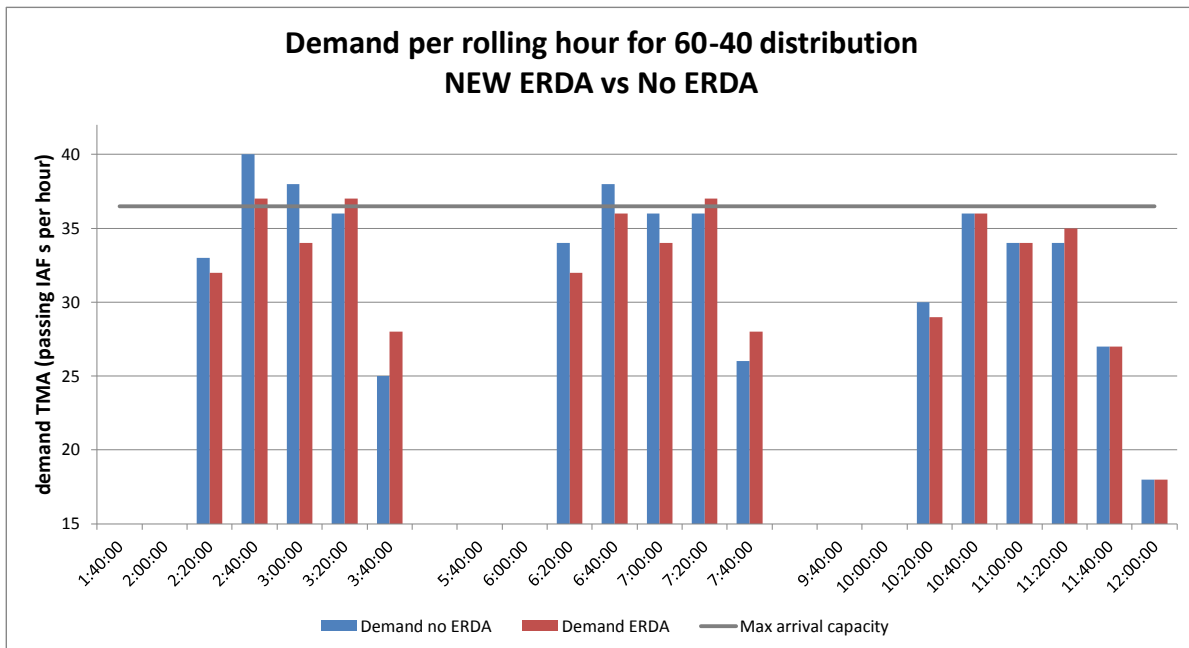


Figure 5.17: Demand per rolling hour with new inter-arrival time separation settings for ERDA.

Delay and throughput results

The effect in decreased throughput when the incorrect ERDA arrival-intervals are in place, can clearly be observed in figure 5.18. In this figure, the throughput and delay for the simulations with a distribution of 60 % arrivals at LORNI and 40 % at MOPAR is shown. The throughput remains at 34 landings per hour, which is substantially lower than the throughput when no ERDA is applied. It should be noted that due to the wrong interval times, the maximum delay that needed to be absorbed en-route increases to ten minutes. On the other hand, the delay in the TMA is on average only ten seconds (red line). The throughput for the first inbound peak without ERDA has a value of 38 landings per rolling hour, which is well above the maximum arrival capacity. After close inspection it appeared that for one medium aircraft no merging solution could be found and this aircraft landed at 3:23 hour, only seven seconds after the previous one. What happens when the simulation cannot find a separation solution is that it removes this aircraft (# 50 in the simulation flight plan sequence) from the arrival sequence and let it fly along the longest trajectory towards the runway. The aircraft that comes next in the sequence (# 51) gets the instruction to land with the required interval after aircraft # 49 and overtakes aircraft # 50. However, the landing of aircraft # 50 is still registered and taken into account for the throughput and delay values.

So the actual throughput is 37 landings per hour for the last two rolling hours in the first inbound peak with no ERDA. The corresponding delay will be higher, because the trailing aircraft after # 50 experienced less congestion and a small decrease in expected delay instead of an increase. If the delay propagation of the first arrival period is compared with the second one (blue line), the average delay already decreases from 3:20 hour onwards where the delay in the second arrival period keeps

increasing until 7:20 hours.

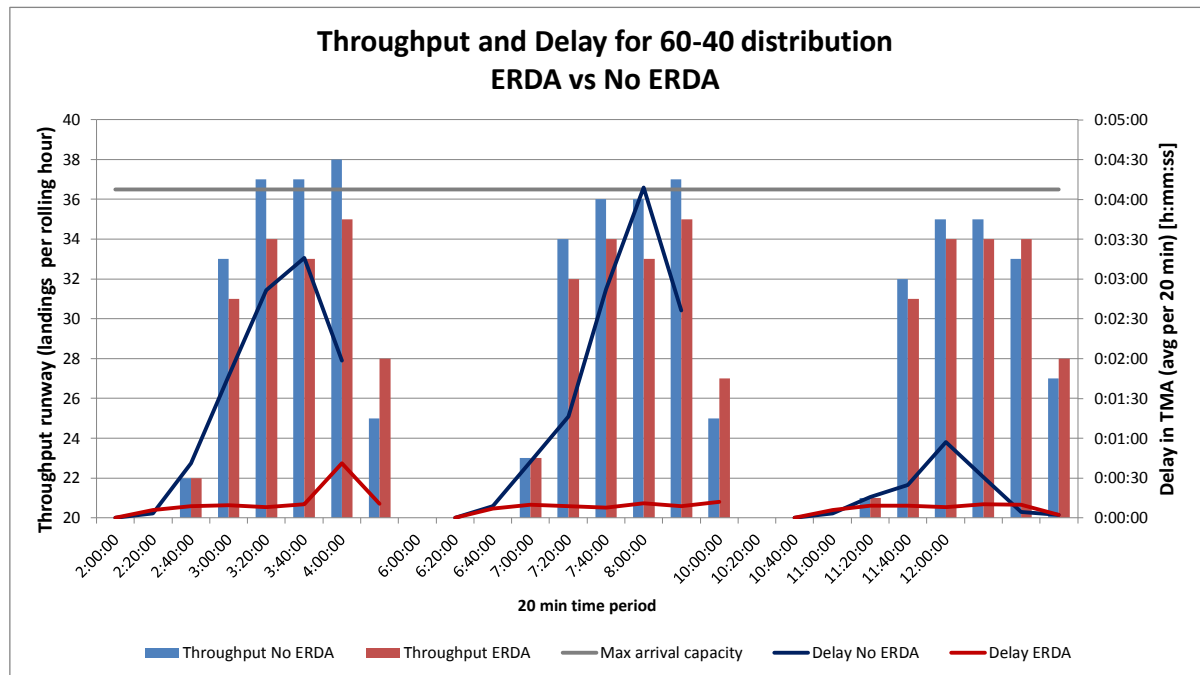


Figure 5.18: Throughput per rolling hour at CDG for the scenario with a 60-40 distribution. Both the throughput with (red) and without (blue) En-Route Delay Absorption is given, together with the maximum arrival capacity based on the fleet mix order and required separation. The second vertical axis on the right side gives the average delay per aircraft per 20 minutes time period.

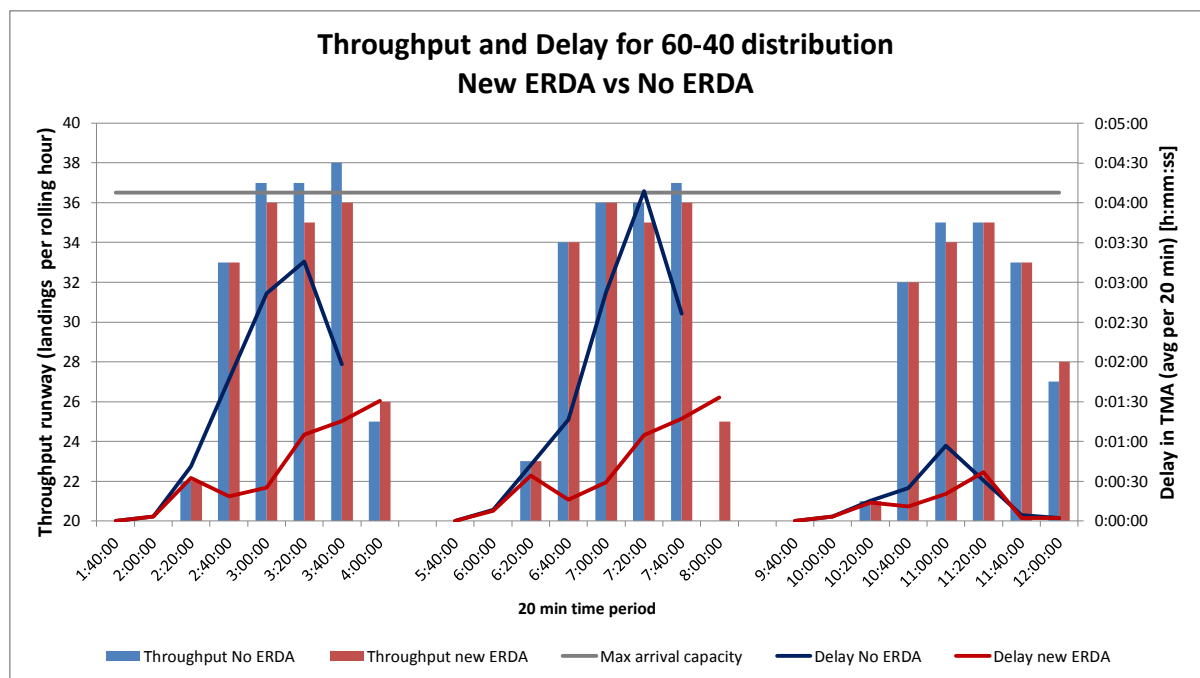


Figure 5.19: Throughput per rolling hour at CDG for the scenario with a 60-40 distribution and new ERDA interval settings. Both the throughput with (red) and without (blue) En-Route Delay Absorption is given, together with the maximum arrival capacity based on the fleet mix order and required separation. The second vertical axis on the right side gives the average delay per aircraft per 20 minutes time period.

Unfortunately, this problem of an airplane being deleted from the sequence also occurred in the other

scenarios with a different distribution. It always occurred in the first arrival period when no ERDA was applied. A possible explanation for this problem could be that the designed vectoring areas are too small for the amount of aircraft at that particular moment. But if a vectoring area is too small, the aircraft should go into a holding, which they did according to the data. The aircraft in question entered the TMA at both fixes, so it is hard to find a relation between the problem and the difference in approach legs. Although this problem has an impact on the throughput and delay results for the first inbound peak, the results for the second and third inbound peak can still be used.

Figure 5.19 displays the results for throughput and delay for the 60-40 distribution scenario and the new ERDA times. If these graphs are compared with the ones from figure 5.18, an increase of the overall throughput for the new ERDA scenario can be observed.

The exact amount of throughput for the second inbound peak is given in table 5.3. In total, the throughput is shifted by one aircraft from the 7:20 hour period towards the end of the inbound peak. The actual landing times between the scenario with and the scenario without ERDA are compared as well. The last ten aircraft with ERDA have a landing time that is on average 55 seconds later than the aircraft without en-route delay absorption.

The delay is significantly reduced in the second inbound peak from more than four minutes to 1,5 minute. Because only one simulation is performed, no standard deviation is given with the delay. The increase by the end of the inbound peak, both in the first and second one, is caused by the fact that the arrival sequence contains some alteration of mediums trailing heavy aircraft. This should not have an effect when correct arrival interval values are used. However, after close examination of the separation times at the threshold, the average trailing time of a medium landing after a heavy in this simulation is 2:18 minutes instead of the 2:00 minutes used for the ERDA adjusted arrival times. So each time a medium aircraft trails a heavy, additional delay needs to be found in the TMA to realize the correct separation.

Based on these results and findings, it can be stated that En-Route Delay Absorption decreases the congestion delay in the TMA without a negative impact on the runway efficiency. However, it is clear that the inter-arrival times have to be accurate and representative for the inbound fleet mix in order to make beneficial use of ERDA techniques. A more accurate inter-arrival time could also reduce the 55 seconds difference in total flight time between aircraft with- and without En-Route Delay Absorption.

Table 5.3: Detailed overview of the throughput per 20 minutes and rolling hour for the 60-40 distribution scenario with and without ERDA. The table represents the second inbound peak and the new inter-arrival time settings for ERDA.

Throughput \ Time	5:40:00	6:00:00	6:20:00	6:40:00	7:00:00	7:20:00	7:40:00	8:00:00
20 min: No ERDA	1	10	12	12	12	12	13	
20 min: ERDA New	1	10	12	12	12	11	13	1
Rolling hour: No ERDA			23	34	36	36	37	
Rolling hour: ERDA New			23	34	36	35	36	25

5.2.2. Effect when there is an offset between two IAFs

To test the effect on delay and throughput when aircraft with ERDA would arrive at the two IAFs with a different off-set to their planned time over the waypoint, a similar approach as with the scenario for Schiphol is used. Ten simulation runs per scenario are performed. When aircraft land on runway 27R of CDG airport, a Western wind blows and aircraft arriving at MOPAR endure a tailwind and aircraft arriving at LORNI encounter a headwind. The scenarios for the simulation are as follows:

- Off-set 1: The accuracy of passing MOPAR is between -20 and 0 seconds (too early), the accuracy at LORNI is between 0 and +20 seconds (too late).
- Off-set 2: The accuracy at MOPAR is between -40 and -20 seconds, at LORNI between +20 and +40 seconds.
- Off-set 3: The accuracy at MOPAR is between -70 and -50 seconds, at LORNI between +50 and +70 seconds.

The reference simulation is the ERDA simulation with the eight additional seconds. Although the maximum arrival capacity and throughput is decreased for this simulation, it should not be of influence to analyse the effect of an off-set between the IAFs. The ten runs were already performed and time prohibited to redo the simulations with new ERDA settings.

Figure 5.20 shows the different throughputs per rolling hour for the three different off-sets and the reference throughput. There is no significant difference in throughput to observe.

The different delay curves can be found in figure 5.21. The standard deviation is not given to keep a clear picture of the graphs, but the maximum standard deviation for all delay curves is eight seconds. There is only an increase in delay when the off-set is more than 50 seconds. So an accuracy of Controlled Time Over (CTO) the IAF of ± 30 to 40 seconds should be sufficient to use En-Route Delay Absorption. It is hard to conclude anything on the absolute value of delay, because the demand for landings is relatively lower than the maximum arrival capacity based on the fleet mix.

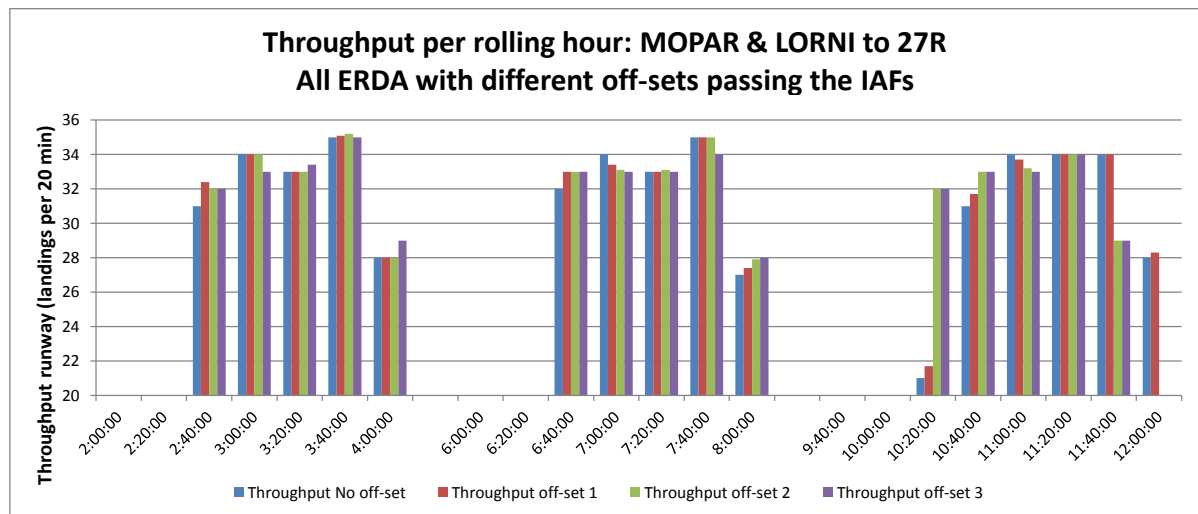


Figure 5.20: Throughput per rolling hour for the three off-sets between MOPAR and LORNI and the reference throughput without off-set.

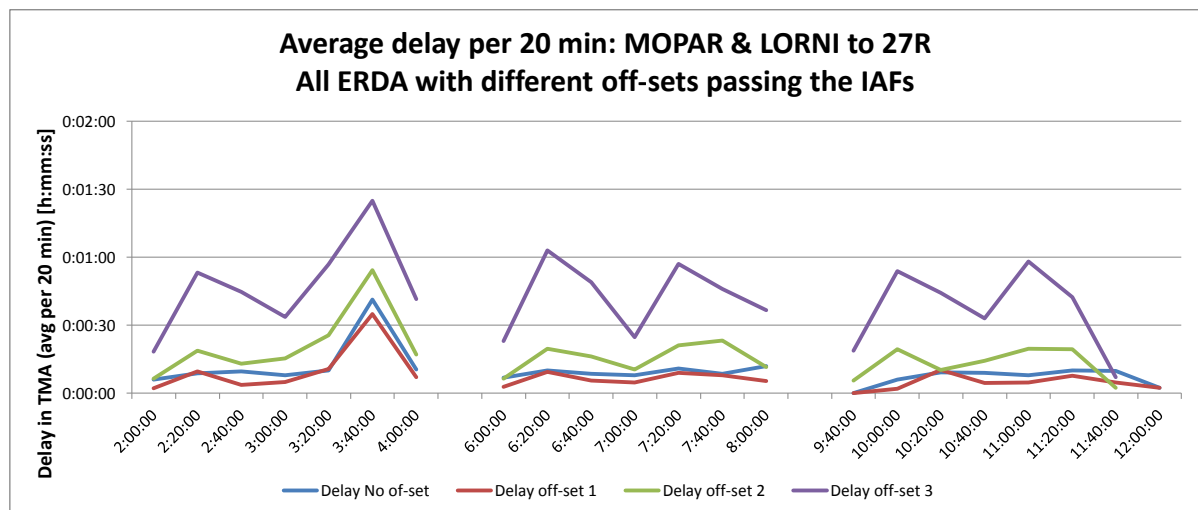


Figure 5.21: Delay curves for scenarios with the three off-sets between MOPAR and LORNI and the reference delay curve without off-set.

5.2.3. Discussion CDG airport simulation results

There is no significant difference to observe in the demand, throughput and delay results between the different distributions. Therefore, the results of all the different simulations with a change in distribution are omitted in the result section and put in the appendix. The additional time separation that was implemented in the ERDA scenarios accidentally showed some interesting changes in demand, throughput and delay. For that reason, the focus of the results section was shifted to examine the effect on throughput and delay when the wrong inter-arrival time separation values are used in the ERDA algorithm.

When the number of aircraft in the TMA is high and above the maximum runway capacity (see figure 5.17, where the demand in the first inbound peak reaches 40 aircraft per rolling hour), AirTop has difficulties with handling the traffic. This resulted in a loss of separation and corrupted values of throughput and delay. It is unclear so far what caused this problem, but it appeared in all four scenarios where the demand for arrivals was very high in a short period of time.

The question arises if this amount of demand (or bunching) is realistic. Flow management control most likely will prevent such high arrival peak from happening. The need for delay absorption higher than five minutes would also be unnecessary if a maximum demand of 38 aircraft per rolling for one period would not be exceeded. The maximum delay absorptions with the new ERDA interval settings were 5:08 minutes in the first inbound peak and 4:25 minutes in the second.

The difference in actual touchdown time when aircraft experience ERDA or not, can only be investigated for the second inbound peak and the scenario with new inter-arrival settings for ERDA. The first inbound peak has corrupted data due to a large loss of separation, as explained in the results section.

When aircraft had En-Route Delay Absorption in the second inbound peak, they arrived approximately one minute later at the end of the peak, compared to the aircraft that had no ERDA. The difference starts to build up after the first hour of and gradually increases towards one minute. Although there is no loss of separation, the separation time between aircraft at the threshold when no ERDA is applied, is often two or three seconds less. So in this perspective, the conclusion could be made that there is a decrease in runway efficiency. However, it is up to the different stakeholders to decide if the extra two or three minutes average delay inside the TMA are worth this small decrease of runway efficiency.

To determine the effect on throughput for CDG airport when ERDA is applied, only one simulation is performed per scenario. The reasoning for this decision was insufficient available data to verify the model accurately and the fact that too many conflicts appeared when the range of accuracy for the arrival time at the IAF was set to ± 30 seconds like with Schiphol airport. And this range of accuracy is the only variable suitable for variation to perform a Monte-Carlo simulation.

For the ERDA scenarios, the demand is lower and variation in the accuracy of arrival times could be executed. There are no conflicts or loss of separation in the simulations where an off-set between the arrival time at the two IAFs is carried out, except for off-set 3 (± 50 s and above). Per run, three to five minor conflicts occurred in the TMA when they merged on the final approach path, but the separation error was below 1 NM and no aircraft had a loss of separation at the threshold.

The inter-arrival separation times at the IAFs have a big influence on the throughput, demand and delay when En-Route Delay Absorption is used. A decent analysis of the current (and future) inbound peaks is needed to determine the right separation times at the waypoints of the approach trajectory. These separation times depend on aircraft performance, approach path lengths, separation standards at the threshold (in relationship with the maximum declared capacity) and other external factors (like strong headwind). If a dynamic time based separation technique at the threshold would be used with a link to En-Route Delay Absorption, additional thorough research on this subject is recommended.

6

Conclusions & Recommendations

The conclusions of this research are given in the following section and are related to the research questions described in chapter 2.1. Recommendations for Air Navigation Service Providers (ANSPs), other stakeholders and future research on this topic is given in section 6.2.

6.1. Conclusions

The conclusions of this research are split up in two parts. The first parts gives the answers to the research questions and the second part explains the remaining conclusions.

6.1.1. Conclusions related to the research questions

The purpose of this research is to investigate the effect of En-Route Delay Absorption (ERDA) on the runway throughput. Based on the simulation results presented in previous chapter, it can be concluded that en-route delay absorption can result in a small decrease of runway throughput, with a maximum of one aircraft per rolling hour. However, a decrease does not always occur, as shown in figure 5.11. By the end of the inbound peak, the actual landing time of an aircraft with ERDA is between 30 and 90 seconds later than the same aircraft with no ERDA. So the inbound peak is extended in time and shifted backwards with approximately one extra landing when ERDA is applied. The benefit of this technique is that aircraft have to spend considerably less time in the TMA of an airport.

The ideal Controlled Time Over (CTO) IAF for each aircraft in the landing sequence is based on the time separation between each aircraft type, the flight time along the approach path and the length of the common fixed approach path (e.g. the final path along the glideslope). During the simulations, the time separation between aircraft passing the IAF has the same value as the required time separation at the threshold. For the calculation of the flight times along the approach paths of Schiphol and Charles de Gaulle airport, a distinction is made between Jet and Turboprop engine aircraft, but a distinction between different approach speed categories is omitted. The simulation results of airports showed that, under the given assumptions, the difference in flight time between different aircraft performance within the same engine class did not pose a problem. When the distance between aircraft is too close due to differences in speed, vertical separation and a different route in the vectoring area can restore the required minimum separation distance. However, when fixed approach paths are used, the difference in speed and flight time of aircraft along the same trajectory can pose a separation problem or decrease the runway throughput.

It can be concluded that the ideal CTO IAF for each aircraft in the landing sequence can be calculated with the required time based separation at the threshold and an average flight time per aircraft category along the approach path. If the total flight time in the TMA between aircraft categories deviates more than one minute, it can be necessary to use different approach paths to the final approach fix for each aircraft category, in order to maintain safety and sufficient runway throughput.

The results from CDG show that a wrong setting of time based separation at the IAF in the order of five to ten seconds already has a significant impact on the runway throughput and decreases it by two

landings per rolling hour throughout the inbound peak. So the answer on research question 9, 'which parameter(s) used in the simulations have a significant effect on the runway throughput and delay', is that the interval time between aircraft at the IAF and a correct calculation of it has a significant effect on both. The effect on delay with a wrong determination of the interval time can be observed in figure 5.18 and 5.19 in the previous chapter. There is a difference in average delay up to 1,5 minutes when the incorrect separation values in the ERDA algorithm are used.

The results presented in chapter 5.1.1 show that there is a linear relationship between the amount of delay and the ratio demand per runway capacity. This answers research question 5: 'What is the development of the delay in time when demand exceeds capacity?'. If the demand for arrivals in the TMA is close to or exceeds the runway capacity for a certain period of time, the amount of average delay grows linearly in time. However, the results only show a clear linear growth of delay when the demand is constant for an extensive period of time. The effect on delay for certain demand/capacity ratios for a shorter period of time is not investigated. The simulation results of Schiphol airport in chapter 5.1.2 and 5.1.3 reveals that delay increases rapidly to an average of three minutes when the demand per rolling hour exceeds the capacity by one aircraft. It is however recommended to do more thorough research on the development of delay when AMAN is used, if knowledge of the exact relationship between demand and delay is desirable.

The amount of aircraft that can be offered to the TMA of an airport in relationship to the maximum runway capacity (see R.Q. 4) depends on the separation between the aircraft. Depending on the accuracy of delivering aircraft at the IAF, the maximum runway throughput can still be achieved with a low amount of delay in the TMA. However, there will always be a minimum amount of delay left in the TMA to be absorbed, which is part of the final sequencing and lining up for the runway. Under good weather conditions, the average delay in the TMA can be kept under one minute if ERDA is used. Research question 6, 'what is the margin of the demand such that no unacceptable delay occur?', it is not really applicable anymore. The margin is smaller than one aircraft, which is physically impossible. If one extra aircraft in a certain amount of time arrives at the IAF, it immediately results in an increase of delay. A good example is given in figure 5.10, where the delay increases rapidly in the first inbound peak of the ERDA scenario, when not all delay could be absorbed en-route.

6.1.2. Other conclusions

The definition of runway pressure, described at the beginning of this report in chapter 2.4, suggests that there is a minimum amount of delay that should be left for the APP controller to absorb, in order to guarantee sufficient runway throughput. From the results of this research, it can be concluded that there will always be a minimum amount of delay that needs to be absorbed in the TMA to optimize the landing sequence. However, the minimum amount of delay in the TMA is a consequence of the difference in flight time between aircraft types and the range of accuracy of the ATO IAF. But a minimum amount of delay is not required to maintain sufficient runway throughput. On the other hand, there will always be a minimum amount of delay during an inbound peak in order to fine-tune the landing sequence of all different aircraft types. If the term 'runway pressure' is the right one to relate this minimum amount of delay in the TMA during an inbound peak, is another question.

During the simulation set-up and initial testing of the environment, it became clear that a good analysis of the (approach) procedures at an airport is important to create a realistic simulation. Every airport and air traffic control centre has its own identity and a different way of handling traffic. The difference in details makes it harder to develop a general simulation model that can be applied for multiple airports. Furthermore, the amount of delay that can be left in the TMA or can be absorbed in earlier flight phase strongly depends on the capacity of each airspace sector. This capacity depends on many more parameters than the ones taken into account during the simulations. Workload, outbound or transition traffic and amount of radio transmissions are such parameters, to name a few.

The flight time calculated by the simulation is based on the BADA aircraft files version 3.12. The verification with the reference flight times calculated by the Trajectory Predictor (TP) of Schiphol airport shows that the difference in calculated optimal flight time is at most 47 seconds for a flight time of 12,5

minutes. This is a difference of six percent. Furthermore, the current aircraft data files used by the TP of Schiphol airport is not as accurate and up to date as expected for several aircraft types used during the verification. Therefore, it can be stated that the used BADA files are accurate enough to represent realistic aircraft performance during these simulations.

The data from Charles de Gaulle airport's Air Traffic Management (ATM) system was too limited to make any useful verification of the simulation model with actual traffic.

6.2. Recommendations

The required amount of ERDA decreases by the end of the inbound peak when there is a decrease in demand. Because the inbound peaks are limited in time, ERDA can be applied without a significant decrease in overall throughput during the inbound peak. It is not investigated what would happen in the case of a continuous or rolling hub and a constant demand close to the maximum arrival capacity for an extended period of time (like to the operations at e.g. Heathrow airport).

It is recommended to investigate the development of delay during inbound peaks when demand is regulated by flow control and arrival management systems. This recommendation is based on the findings presented in chapter 5.1.1, where a linear relationship between delay and the demand/capacity ratio was found instead of an expected exponential growth of delay.

Because the used version of AirTOP did not have an Arrival Management (AMAN) and flow control module that allowed CTO IAF to be changed during the simulations, no missed approach or any other unexpected event could be simulated. For future research, it is recommended to test the effect of ERDA when pop up flights, missed approaches and other events occur during an inbound peak with an upgraded version of AirTOP.

The simulations did not take into account any wind. New time based separation concepts change the separations at the threshold dynamically, based on available meteo data [18]. Because the time based separation values are an important parameter for the AMAN and ERDA algorithms, it is suggested to take dynamic time based separation into account in any future research.

A final recommendation for future research on this topic is to investigate the effect on the workload of all controllers involved with ERDA. In that case, a possible distribution of the total delay among different parts of the flight can be investigated.

Bibliography

- [1] F. Knottenbeld, *Cover picture*, (2015).
- [2] DSNA & NATS, *Benefits from the xman heathrow live trials*, (2015).
- [3] EUROCONTROL, *Cross-border arrival management (xman)*, (2015).
- [4] G. Regniaud, *Delay sharing strategy*, (2013), [internal document LVNL].
- [5] J. van der Klugt, *Calculating capacity of dependent runway configurations*, Master's thesis, Faculty of Aerospace Engineering, TU Delft (2012).
- [6] AirTOp, *Atc fast time simulator and air traffic optimizer*, (2015).
- [7] Commercial Aviation Safety Team (ICAO), *Phase of flight definitions*, (2013).
- [8] EUROCONTROL, *Eurocontrol atm lexicon*, (2015).
- [9] LVNL, *(dutch) voorschriften dienst verkeersleiding*, (2015), [internal document].
- [10] S&P Performance department LVNL, *(dutch) overzicht en onderbouwing van uurcapaciteit van acc-sectoren en mainport schiphol v2.5.0*, (2014), [internal document].
- [11] LVNL, *Over ons*, (2015).
- [12] LVNL, *Operations and instructions manual*, (2015), [internal document].
- [13] Luchtvaartnieuws, *Airbus a380 china southern airlines op schiphol geland*, (2015).
- [14] SKYbrary Aviation Safety, *Approach speed categorisation*, (2015).
- [15] Boeing, *Airport reference code and approach speeds for boeing airplanes*, (2011).
- [16] FAA, *Safo 12007:re-categorization (recat) of faa wake turbulence separation categories at specific airports*, (2013).
- [17] EUROCONTROL, *Wake vortex*, (2015).
- [18] C. Morris, J. Peters, and P. Choroba, *Validation of the time based separation concept at london heathrow airport*, Tenth USA/Europe Air Traffic Management Research and Development Seminar (ATM2013) (2013).
- [19] T. Gerz, F. Holzäpfel, and D. Darracq, *Commercial aircraft wake vortices*, Progress in Aerospace Sciences **38** (2002).
- [20] SKYbrary Aviation Safety, *Airbus a380 wake vortex guidance*, (2015).
- [21] R. C. Nelson, *Trailing vortex wake encounters at altitude - a potential flight safety issue?* AIAA Atmospheric Flight Mechanics Conference **1** (2006).
- [22] ICAO, *Doc 7488 manual of the icao standard atmosphere*, (1993).
- [23] Schiphol Group, *Traffic review 2014*, (2015).
- [24] Air France - KLM, *Klm on airport*, (2015).
- [25] F. Poldy, *Airport Runway Capacity and Delay: Some Models for Planners and Managers*, Tech. Rep. (Australian government, 1982).

- [26] T. Guest, *A Matter of Time: Air Traffic Delay in Europe. Volume 2*, Tech. Rep. (EUROCONTROL, 2007).
- [27] W. Vermeersch, *Literature study runway pressure research*, (2015), unpublished.
- [28] N. T. Thomopoulos, *Fundamentals of Queing Systems*, 1st ed. (Springer, 2012).
- [29] R. de Neufville and A. Odoni, *Airport Systems: Planning, Design and management* (Mc Graw Hill, 2013).
- [30] G. Guadagni, S. Ndreca, and B. Scoppola, *Queueing systems with pre-scheduled random arrivals*, *Mathematical Methods of Operational Research* **73** (2011).
- [31] M. V. Caccavale, A. Iovanella, C. Lancia, G. Lulli, and B. Scoppola, *A model of inbound air traffic: The application to heathrow airport*, *Journal of AirTransport Management* (2013).
- [32] EUROCONTROL, *The european ais database*, (2015).
- [33] N. Hasevoets and P. Conroy, *AMAN Status Review 2010*, Tech. Rep. (EUROCONTROL, 2010).
- [34] EUROCONTROL, *Base of aircraft data (bada)*, (2015).
- [35] L. M. C. Adriaens, *MUAC En Route Delay Absorption Capabilities for Schiphol Inbounds*, Master's thesis, Faculty of Aerospace Engineering, TU Delft (2015).
- [36] Air Traffic Control the Netherlands, *Ais the netherlands*, (2015).
- [37] S&P Strategy department LVNL, *Masterplan atm systeem 2013-2025 v2*, (2013), [internal document].
- [38] S&P Strategy & Operations department LVNL, *(dutch) ops visie & strategie richtjaar 2025 v1.0*, (2013), [internal document].



Additional Schiphol airport information

In this appendix, the reference flight times used in the simulation of Schiphol airport can be found. The three different fleet mixes and landing sequence are given in section A.2. The map with the Standard Arrival Routes towards Schiphol airport is shown at the end of this appendix.

A.1. Reference flight times of the simulation

The calculation of the flight times in the TMA of Schiphol airport by the Trajectory Predictor (TP) is described in chapter 3.1.7. The parameters like speed profiles of the different aircraft and approach path length are used to create a model for the simulations. AirTOP calculates for each aircraft along an active approach path a reference flight time. This is the shortest or most optimal path towards the runway with normal speed settings. These reference flight times are used in the simulation to calculate the delay and an overview is given in table A.1. The table contains the minimum, maximum and average optimal flight times of all jet and turboprop aircraft of the used fleet mix for Schiphol airport. It is clear that the deviation in flight time between aircraft from the same class is limited to approximately 15 seconds. The difference in flight time between classes is the largest for the trajectory from RIVER to runway 18R with more than one minute difference.

Table A.1: Simulation reference flight times along four different approach paths for jet and turboprop aircraft.

Jet	ARTIP - 18C	Jet	ARTIP - 36R	Jet	RIVER - 18R	Jet	SUGOL 18R
avg	0:11:52	avg	0:13:17	avg	0:14:46	avg	0:10:33
min	0:11:38	min	0:13:03	min	0:14:33	min	0:10:19
max	0:12:07	max	0:13:32	max	0:15:01	max	0:10:50
Turboprop		Turbo-Props		Turboprop		Turboprop	
avg	0:12:33	avg	0:14:00	avg	0:15:57	avg	0:11:26
min	0:12:27	min	0:13:53	min	0:15:41	min	0:11:11
max	0:12:38	max	0:14:06	max	0:16:12	max	0:11:37

As mentioned in chapter 3.1.7, the comparison with the calculated reference flight time of the simulation and the reference flight used by the acTP of the AAA system is somewhat harder to make due to the different speed profiles and more complex used parameters. However, if a rough comparison is made, the reference flight times of the simulation are close to the reference flight times of the real acTP presented in table A.2. The largest difference between both reference flight times is on the approach path between ARTIP and runway 36R, but the difference stays below one minute for both engine type aircraft.

Table A.2: Reference flight times calculated by the TP of the AAA system at Schiphol. The flight times are based on data from 28 May and 3 June 2014.

TP calculations	ARTIP - 18C		ARTIP - 36R		RIVER - 18R		SUGOL 18R
Jet	0:11:32	Jet	0:12:30	Jet	0:14:35	Jet	0:10:09
Turboprop	0:12:50	Turbo-Props	0:13:15	Turboprop	0:15:20	Turboprop	0:11:20

A.2. Fleet mix, landing sequence and capacity

The three different fleet mixes and landing sequence order used in the simulations of Schiphol airport are given in table A.3 and A.4. The tables contain the wake vortex category (MT stands for Medium Turboprop aircraft), aircraft type, minimum separation which takes into account maximum arrival rate of 34 aircraft per hour and the total number of landings as integer number per different time period.

A.3. STAR routes Schiphol airport

The different Standard Arrival Routes (STARs) towards Schiphol airport are given in figure A.1.

Table A.3: The landing sequence order with minimum separations for fleet mix 1 and 2.

Fleet mix 1	WTC	Type	Separation	Counting	Per 20 min	Rolling hour	Fleet mix 2	Type	Separation	Counting	Per 20 min	Per rolling hour
1	M	E190					M	A321				
2	M	E190	0:01:45	0:01:45			MT	DH8D	0:01:45	0:01:45		
3	M	B738	0:01:45	0:03:30			M	CRJ9	0:01:45	0:03:30		
4	M	B738	0:01:45	0:05:15			M	E190	0:01:45	0:05:15		
5	M	E190	0:01:45	0:07:00			M	E190	0:01:45	0:07:00		
6	M	A320	0:01:45	0:08:45			M	E190	0:01:45	0:08:45		
7	H	B744	0:01:45	0:10:30			M	E190	0:01:45	0:10:30		
8	M	B733	0:02:00	0:12:30			M	E190	0:01:45	0:12:15		
9	H	B744	0:01:45	0:14:15			M	A319	0:01:45	0:14:00		
10	M	E190	0:02:00	0:16:15			M	A320	0:01:45	0:15:45		
11	M	B738	0:01:45	0:18:00			M	B738	0:01:45	0:17:30		
12	M	B733	0:01:45	0:19:45	12		M	A319	0:01:45	0:19:15	12	
13	M	A319	0:01:45	0:21:30			M	E190	0:01:45	0:21:00		
14	M	E190	0:01:45	0:23:15			M	E190	0:01:45	0:22:45		
15	M	F70	0:01:45	0:25:00			M	B737	0:01:45	0:24:30		
16	MT	DH8D	0:01:45	0:26:45			M	B738	0:01:45	0:26:15		
17	M	A320	0:01:45	0:28:30			M	E190	0:01:45	0:28:00		
18	M	B738	0:01:45	0:30:15			M	B737	0:01:45	0:29:45		
19	M	B739	0:01:45	0:32:00			M	F70	0:01:45	0:31:30		
20	H	A310	0:01:45	0:33:45			M	B738	0:01:45	0:33:15		
21	M	A319	0:02:00	0:35:45			M	B737	0:01:45	0:35:00		
22	H	A333	0:01:45	0:37:30			M	B737	0:01:45	0:36:45		
23	M	B738	0:02:00	0:39:30	11		M	CRJ9	0:01:45	0:38:30	11	
24	H	B763	0:01:45	0:41:15			MT	AT45	0:01:45	0:40:15		
25	M	F70	0:02:00	0:43:15			M	B738	0:01:45	0:42:00		
26	M	B733	0:01:45	0:45:00			M	F70	0:01:45	0:43:45		
27	M	B738	0:01:45	0:46:45			M	E190	0:01:45	0:45:30		
28	H	B77W	0:01:45	0:48:30			M	E190	0:01:45	0:47:15		
29	M	CRJ9	0:02:00	0:50:30			M	F70	0:01:45	0:49:00		
30	M	B738	0:01:45	0:52:15			M	B737	0:01:45	0:50:45		
31	H	B772	0:01:45	0:54:00			M	E190	0:01:45	0:52:30		
32	M	F70	0:02:00	0:56:00			M	B737	0:01:45	0:54:15		
33	M	A321	0:01:45	0:57:45			M	CRJ9	0:01:45	0:56:00		
34	MT	AT45	0:01:45	0:59:30	11	34	M	A319	0:01:45	0:57:45		
35	M	E190	0:01:45	1:01:15			M	A321	0:01:45	0:59:30	12	35
36	M	E190	0:01:45	1:03:00			M	E190	0:01:45	1:01:15		
37	M	B738	0:01:45	1:04:45			M	E190	0:01:45	1:03:00		
38	MT	DH8D	0:01:45	1:06:30			M	E190	0:01:45	1:04:45		
39	M	B738	0:01:45	1:08:15			M	E190	0:01:45	1:06:30		
40	M	E190	0:01:45	1:10:00			M	F70	0:01:45	1:08:15		
41	H	B744	0:01:45	1:11:45			M	F70	0:01:45	1:10:00		
42	M	A320	0:02:00	1:13:45			M	B737	0:01:45	1:11:45		
43	M	B733	0:01:45	1:15:30			MT	DH8D	0:01:45	1:13:30		
44	H	B744	0:01:45	1:17:15			MT	AT45	0:01:45	1:15:15		
45	M	E190	0:02:00	1:19:15	11	33	M	E190	0:01:45	1:17:00		
46	M	B738	0:01:45	1:21:00			M	E190	0:01:45	1:18:45	11	34
47	M	B733	0:01:45	1:22:45			M	B737	0:01:45	1:20:30		
48	M	A319	0:01:45	1:24:30			M	E190	0:01:45	1:22:15		
49	M	E190	0:01:45	1:26:15			M	B737	0:01:45	1:24:00		
50	H	A310	0:01:45	1:28:00			M	B737	0:01:45	1:25:45		
51	H	A333	0:01:40	1:29:40			M	B738	0:01:45	1:27:30		
52	H	B763	0:01:40	1:31:20			M	A320	0:01:45	1:29:15		
53	M	F70	0:02:00	1:33:20			M	E190	0:01:45	1:31:00		
54	M	A320	0:01:45	1:35:05			M	B737	0:01:45	1:32:45		
55	M	B738	0:01:45	1:36:50			M	CRJ9	0:01:45	1:34:30		
56	M	B739	0:01:45	1:38:35	11	33	M	A319	0:01:45	1:36:15		
57	M	A319	0:01:45	1:40:20			M	B738	0:01:45	1:38:00		
58	M	B738	0:01:45	1:42:05			M	B737	0:01:45	1:39:45	12	35
59	MT	AT45	0:01:45	1:43:50			M	B738	0:01:45	1:41:30		
60	H	B77W	0:01:45	1:45:35			M	B738	0:01:45	1:43:15		
61	M	F70	0:02:00	1:47:35			M	E190	0:01:45	1:45:00		
62	M	B733	0:01:45	1:49:20			M	F70	0:01:45	1:46:45		
63	M	B738	0:01:45	1:51:05			M	CRJ9	0:01:45	1:48:30		
64	M	CRJ9	0:01:45	1:52:50			M	CRJ9	0:01:45	1:50:15		
65	M	B738	0:01:45	1:54:35			M	E190	0:01:45	1:52:00		
66	H	B772	0:01:45	1:56:20			M	E190	0:01:45	1:53:45		
67	M	F70	0:02:00	1:58:20	11	33	M	B737	0:01:45	1:55:30		
68	M	A321	0:01:45	2:00:05			M	B737	0:01:45	1:57:15		
									0:01:45	1:59:00	11	34
			Average per hour	33.5					Average per hour	34.5		

Table A.4: The landing sequence order with minimum separations for fleet mix 3 and the resequence of that fleet mix.

Fleet mix 3	Type	Separation	Counting	Per 20 min	Per rolling hour	Resequence	FM3	Separation	Counting	Per 20 min	Per rolling hour
M	B737					M	B737				
M	A320	0:01:45	0:01:45			M	A320	0:01:45	0:01:45		
M	A321	0:01:45	0:03:30			M	A321	0:01:45	0:03:30		
M	E190	0:01:45	0:05:15			M	E190	0:01:45	0:05:15		
H	B777	0:01:45	0:07:00			H	B777	0:01:45	0:07:00		
M	A318	0:02:00	0:09:00			M	A318	0:02:00	0:09:00		
M	A319	0:01:45	0:10:45			M	A319	0:01:45	0:10:45		
M	A318	0:01:45	0:12:30			M	A318	0:01:45	0:12:30		
M	B737	0:01:45	0:14:15			M	B737	0:01:45	0:14:15		
M	E190	0:01:45	0:16:00			M	E190	0:01:45	0:16:00		
M	A319	0:01:45	0:17:45			M	A319	0:01:45	0:17:45		
M	A319	0:01:45	0:19:30	12		M	A319	0:01:45	0:19:30	12	
M	A320	0:01:45	0:21:15			M	A320	0:01:45	0:21:15		
S	A388	0:01:45	0:23:00			S	A388	0:01:45	0:23:00		
M	B737	0:03:00	0:26:00			H	A330	0:02:20	0:25:20		
H	A330	0:01:45	0:27:45			M	B737	0:02:00	0:27:20		
M	A320	0:02:00	0:29:45			M	A320	0:01:45	0:29:05		
M	A320	0:01:45	0:31:30			M	A320	0:01:45	0:30:50		
M	E190	0:01:45	0:33:15			M	E190	0:01:45	0:32:35		
H	A330	0:01:45	0:35:00			H	A330	0:01:45	0:34:20		
H	B777	0:01:40	0:36:40			H	B777	0:01:40	0:36:00		
M	A318	0:02:00	0:38:40	10		H	A330	0:01:40	0:37:40		
M	A321	0:01:45	0:40:25			H	B787	0:01:40	0:39:20	11	
H	A330	0:01:45	0:42:10			M	A318	0:02:00	0:41:20		
M	A319	0:02:00	0:44:10			M	A321	0:01:45	0:43:05		
H	B787	0:01:45	0:45:55			M	A319	0:01:45	0:44:50		
M	A320	0:02:00	0:47:55			M	A320	0:01:45	0:46:35		
M	A321	0:01:45	0:49:40			M	A321	0:01:45	0:48:20		
H	B747	0:01:45	0:51:25			H	B747	0:01:45	0:50:05		
M	E190	0:02:00	0:53:25			M	E190	0:02:00	0:52:05		
M	A321	0:01:45	0:55:10			M	A321	0:01:45	0:53:50		
M	E190	0:01:45	0:56:55			M	E190	0:01:45	0:55:35		
M	A319	0:01:45	0:58:40	11	33	M	A319	0:01:45	0:57:20		
M	E190	0:01:45	1:00:25			M	E190	0:01:45	0:59:05	11	34
H	B787	0:01:45	1:02:10			H	B787	0:01:45	1:00:50		
M	A319	0:02:00	1:04:10			M	A319	0:02:00	1:02:50		
M	B737	0:01:45	1:05:55			M	B737	0:01:45	1:04:35		
M	A321	0:01:45	1:07:40			M	A321	0:01:45	1:06:20		
M	E190	0:01:45	1:09:25			M	E190	0:01:45	1:08:05		
M	A320	0:01:45	1:11:10			M	A320	0:01:45	1:09:50		
M	A319	0:01:45	1:12:55			M	A319	0:01:45	1:11:35		
M	A318	0:01:45	1:14:40			M	A318	0:01:45	1:13:20		
M	E190	0:01:45	1:16:25			M	E190	0:01:45	1:15:05		
H	B777	0:01:45	1:18:10	11	32	H	B777	0:01:45	1:16:50		
M	A320	0:02:00	1:20:10			M	A320	0:02:00	1:18:50	11	33
M	E190	0:01:45	1:21:55			M	E190	0:01:45	1:20:35		
S	A388	0:01:45	1:23:40			S	A388	0:01:45	1:22:20		
H	B777	0:02:20	1:26:00			H	B777	0:02:20	1:24:40		
H	A330	0:01:40	1:27:40			H	A330	0:01:40	1:26:20		
M	E190	0:02:00	1:29:40			M	E190	0:02:00	1:28:20		
M	A321	0:01:45	1:31:25			M	A321	0:01:45	1:30:05		
M	E190	0:01:45	1:33:10			M	E190	0:01:45	1:31:50		
M	E190	0:01:45	1:34:55			M	E190	0:01:45	1:33:35		
M	A318	0:01:45	1:36:40			M	A318	0:01:45	1:35:20		
M	B737	0:01:45	1:38:25	11	33	M	B737	0:01:45	1:37:05		
M	A319	0:01:45	1:40:10			M	A319	0:01:45	1:38:50	11	33
H	A330	0:01:45	1:41:55			H	A330	0:01:45	1:40:35		
H	B747	0:01:40	1:43:35			H	B747	0:01:40	1:42:15		
M	A321	0:02:00	1:45:35			M	A321	0:02:00	1:44:15		
M	A320	0:01:45	1:47:20			M	A320	0:01:45	1:46:00		
M	B737	0:01:45	1:49:05			M	B737	0:01:45	1:47:45		
H	A330	0:01:45	1:50:50			H	A330	0:01:45	1:49:30		
M	A321	0:02:00	1:52:50			M	A321	0:02:00	1:51:30		
M	A319	0:01:45	1:54:35			M	A319	0:01:45	1:53:15		
M	A320	0:01:45	1:56:20			M	A320	0:01:45	1:55:00		
M	A320	0:01:45	1:58:05			M	A320	0:01:45	1:56:45		
M	A318	0:01:45	1:59:50	12	34	M	A318	0:01:45	1:58:30	11	33
M	A319	0:01:45	2:01:35			M	A319	0:01:45	2:00:15		
Average per hour			33.5			Average per hour			33.5		

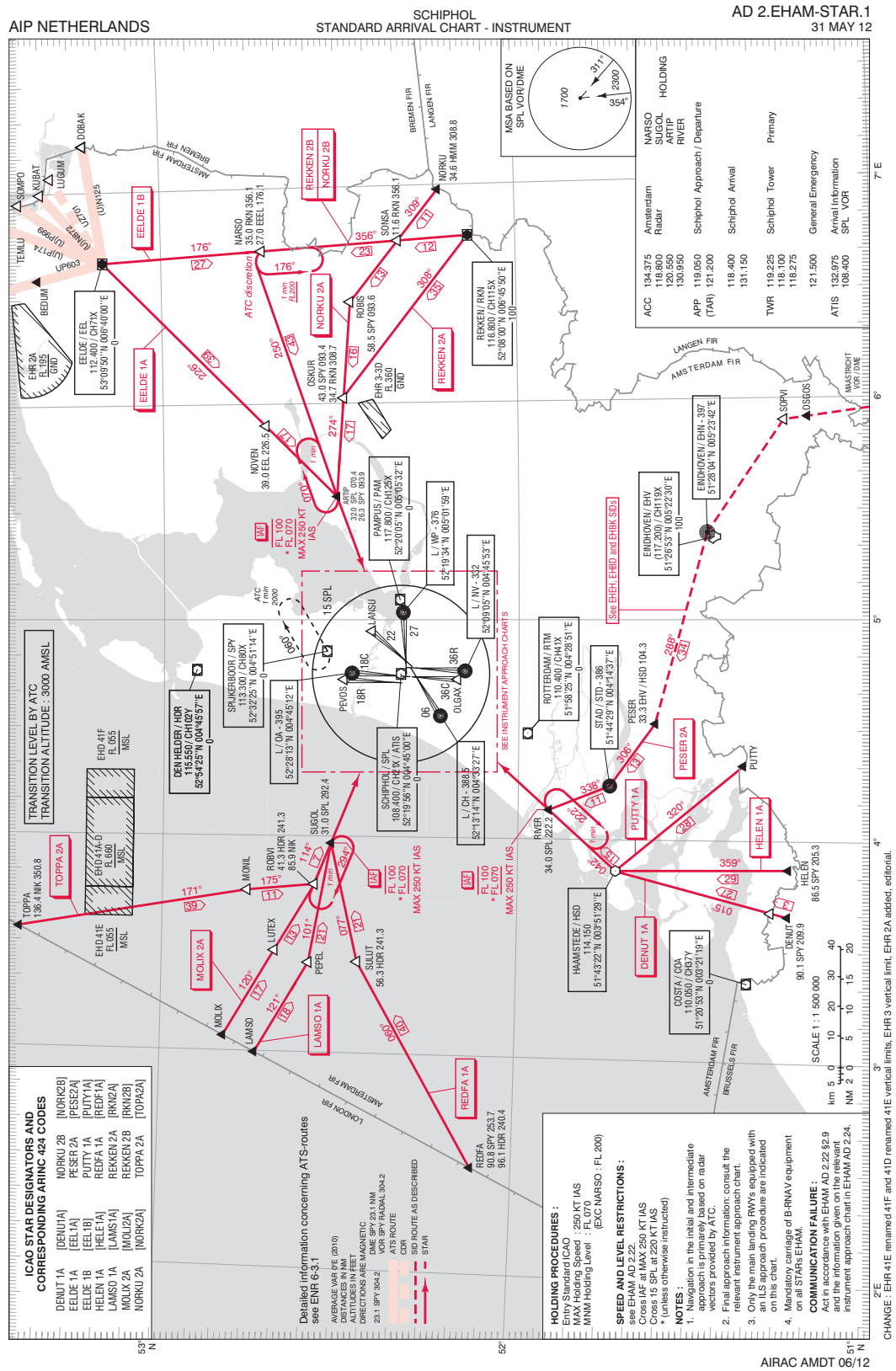


Figure A.1: STARs overview for arrivals towards Schiphol airport [36].

B

Additional Charles de Gaulle airport Information

The airspace sectors around Charles de Gaulle airport and the routes towards the different IAFs of CDG are shown in figure B.1. The routes in the upper area start around 300 NM from CDG, but the length does not have an influence on the outcome of the simulations. It is just mentioned to give the reader an idea of the scale.



Figure B.1: Airspace sectors used in the simulation model and the routes towards CDG.

Fleet mix used with the simulations

There is only one fleet mix used for the simulations of CDG airport. This fleet, shown in table B.1, mix is based on the the actual fleet mix in the winter of 2014 and provided by DSNA, the French air traffic

control operator.

Table B.1: Aircraft type specification for the simulations at CDG airport

for 36 A/C per hour per runway		Specification	
A380	1	A388	1
Heavy	8	A330	3
Medium	27	B777	3
No Turboprops		B787	1
		B747	1
		A318	3
		A319	5
		A320	6
		A321	4
		B737-serie	3
		E190	4
		RJ85	2

Table B.2 shows the landing sequence used for the simulations with a 60-40 ratio of arrivals at LORNI and MOPAR, respectively.

Table B.2: Fleet mix landing sequence for CDG airport simulations with the minimum separation values for a maximum arrival rate of 36 landings. Based on these values, 36 landings per hour cannot be achieved with this fleet mix order.

Fleet mix	60-40 dist.	Type	Separation	Counting	Per 20 min	Per rolling hour	Part 2	WTC	Type	Separation	Counting	Per 20 min	Per rolling hour
1	Medium	E190_2					37	Medium	A321_6	0:01:40	1:04:00		
2	Medium	A321_1	0:01:40	0:01:40			38	Medium	B738_2	0:01:40	1:05:40		
3	Heavy	A332_3	0:01:40	0:03:20			39	Medium	A320_11	0:01:40	1:07:20		
4	Medium	RJ85_2	0:02:00	0:05:20			40	Heavy	A332_4	0:01:40	1:09:00		
5	Medium	A321_2	0:01:40	0:07:00			41	Medium	A319_9	0:02:00	1:11:00		
6	Medium	A320_2	0:01:40	0:08:40			42	Medium	A319_8	0:01:40	1:12:40		
7	Heavy	B772_2	0:01:40	0:10:20			43	Heavy	A332_5	0:01:40	1:14:20		
8	Medium	E190_3	0:02:00	0:12:20			44	Heavy	B772_4	0:01:40	1:16:00		
9	Medium	B738_1	0:01:40	0:14:00			45	Medium	A319_10	0:02:00	1:18:00		
10	Medium	A319_4	0:01:40	0:15:40			46	Medium	E190_6	0:01:40	1:19:40	12	34
11	Medium	RJ85_1	0:01:40	0:17:20			47	Heavy	B772_6	0:01:40	1:21:20		
12	Heavy	B772_3	0:01:40	0:19:00	12		48	Medium	A318_4	0:02:00	1:23:20		
13	Medium	A318_2	0:02:00	0:21:00			49	Medium	E190_5	0:01:40	1:25:00		
14	Heavy	A332_2	0:01:40	0:22:40			50	Medium	A321_5	0:01:40	1:26:40		
15	Medium	E190_4	0:02:00	0:24:40			51	Heavy	B772_5	0:01:40	1:28:20		
16	Medium	A320_1	0:01:40	0:26:20			52	Heavy	B748_2	0:01:40	1:30:00		
17	Heavy	A332_1	0:01:40	0:28:00			53	Medium	B734_2	0:02:00	1:32:00		
18	Medium	A318_3	0:02:00	0:30:00			54	Medium	A320_12	0:01:40	1:33:40		
19	Medium	A321_4	0:01:40	0:31:40			55	SuperHeavy	A388_2	0:01:40	1:35:20		
20	Medium	B734_1	0:01:40	0:33:20			56	Heavy	A332_6	0:02:20	1:37:40		
21	Medium	B733_1	0:01:40	0:35:00			57	Medium	RJ85_4	0:02:00	1:39:40	11	34
22	Medium	E190_1	0:01:40	0:36:40			58	Medium	A320_10	0:01:40	1:41:20		
23	Medium	A320_5	0:01:40	0:38:20	11		59	Medium	A319_6	0:01:40	1:43:00		
24	Medium	A318_1	0:01:40	0:40:00			60	Medium	A319_7	0:01:40	1:44:40		
25	Heavy	B788_1	0:01:40	0:41:40			61	Medium	A321_8	0:01:40	1:46:20		
26	Medium	A321_3	0:02:00	0:43:40			62	Medium	E190_8	0:01:40	1:48:00		
27	Heavy	B748_1	0:01:40	0:45:20			63	Medium	A318_6	0:01:40	1:49:40		
28	Medium	A319_3	0:02:00	0:47:20			64	Medium	A320_9	0:01:40	1:51:20		
29	Medium	A319_5	0:01:40	0:49:00			65	Medium	A321_7	0:01:40	1:53:00		
30	Medium	A320_4	0:01:40	0:50:40			66	Medium	B733_2	0:01:40	1:54:40		
31	SuperHeavy	A388_1	0:01:40	0:52:20			67	Medium	A320_8	0:01:40	1:56:20		
32	Medium	A320_6	0:03:00	0:55:20			68	Medium	E190_7	0:01:40	1:58:00		
33	Heavy	B772_1	0:01:40	0:57:00			69	Heavy	B788_2	0:01:40	1:59:40	12	35
34	Medium	A319_1	0:02:00	0:59:00	11	34	70	Medium	A318_5	0:02:00	2:01:40		
35	Medium	A320_3	0:01:40	1:00:40			71	Medium	RJ85_3	0:01:40	2:03:20		
36	Medium	A319_2	0:01:40	1:02:20			72	Medium	A320_7	0:01:40	2:05:00	3	
											Average per hour		34.5

C

Overview additional results

In this appendix, the remaining graphs and figures from the results in chapter 5 are given. The first section shows the graphs for the results of Schiphol airport and section C.2 the remaining results of CDG airport.

C.1. Remaining results of Schiphol airport

The following figures show the results for demand, throughput and delay of the different scenarios for the Schiphol airport simulations, which are not shown in chapter 5. The remaining graphs for demand are shown first in figures C.1 and C.2.

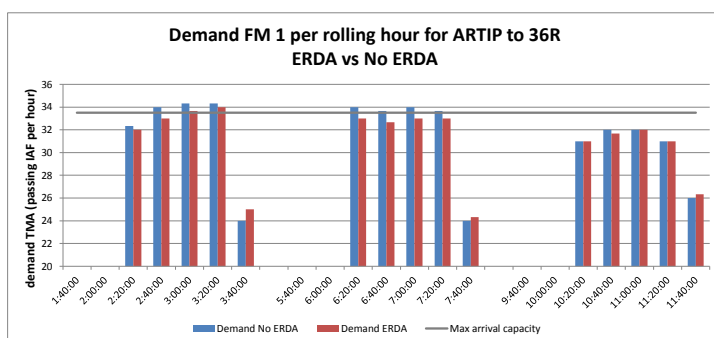
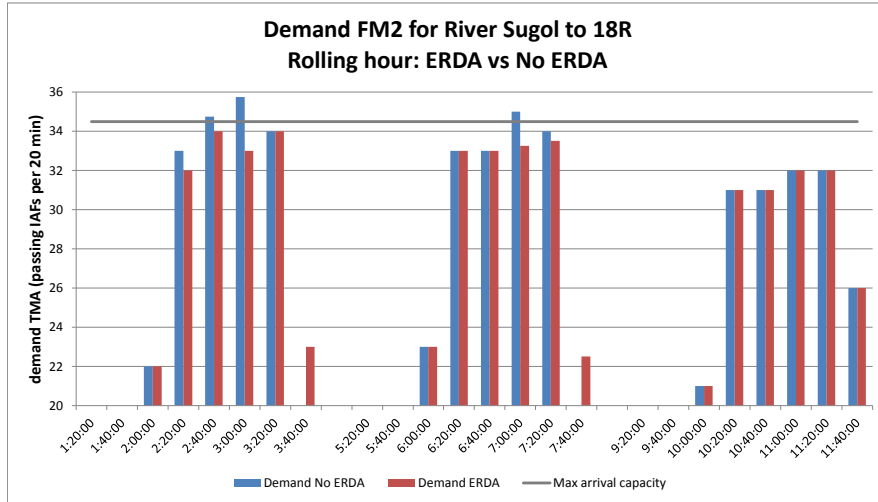
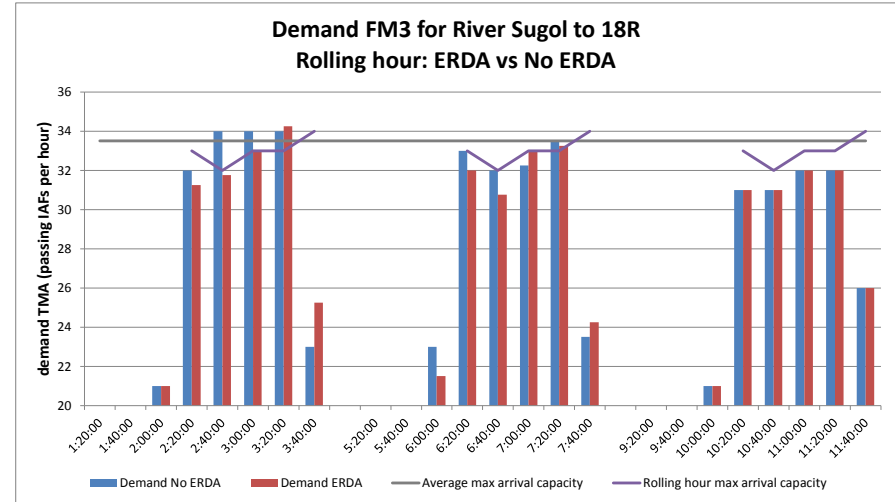


Figure C.1: Demand for the three inbound peaks of the scenario with traffic from ARTIP to 36R and with fleet mix 1.



(a)



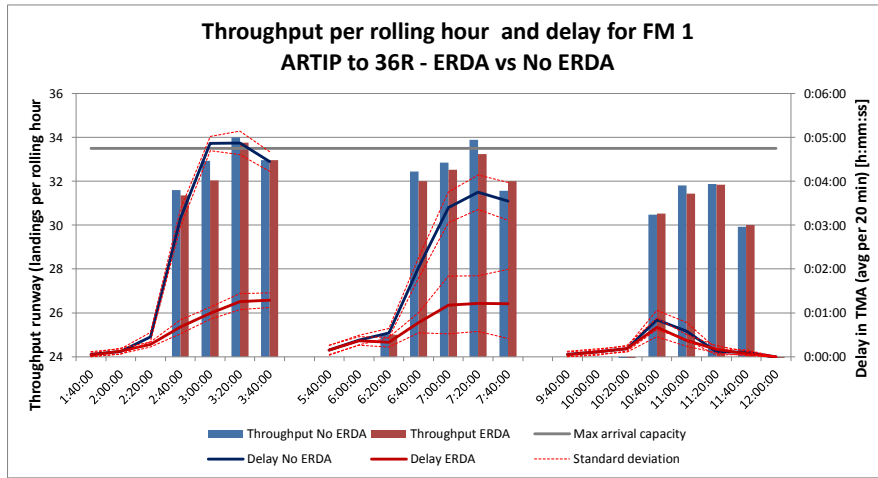
(b)

Figure C.2: Demand for the three inbound peaks of the scenarios with traffic from RIVER and SUGOL to 18R. For fleet mix 2 (a) and 3 (b).

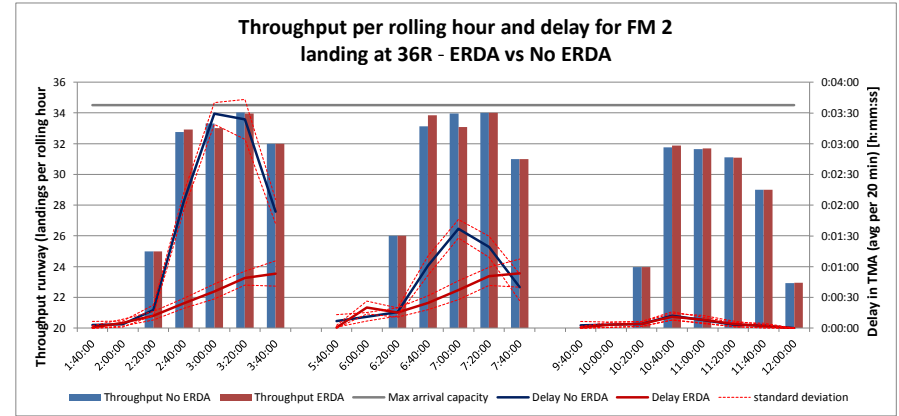
The results for the throughput and delay for the scenarios with traffic from ARTIP to runway 36R and from RIVER/SUGOL to 18R are given in figures C.3 and C.4.

C.2. Remaining results of CDG airport

Figure C.5 shows the results for the throughput and delay for two different distributions of arrivals at IAFs LORNI and MOPAR.

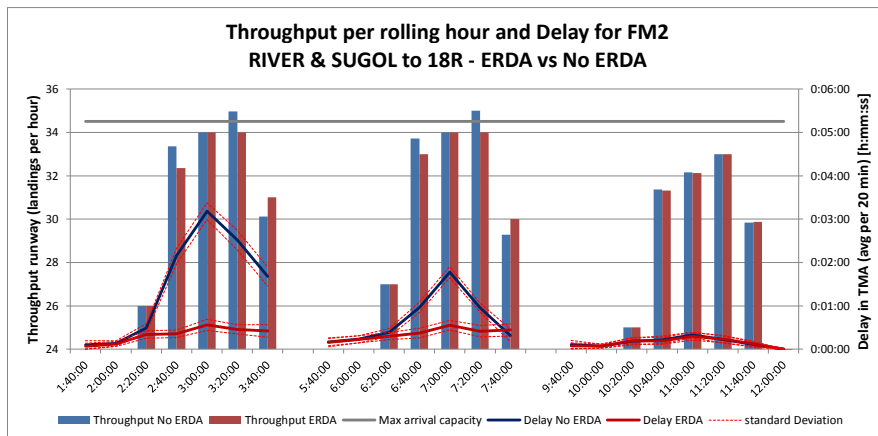


(a)

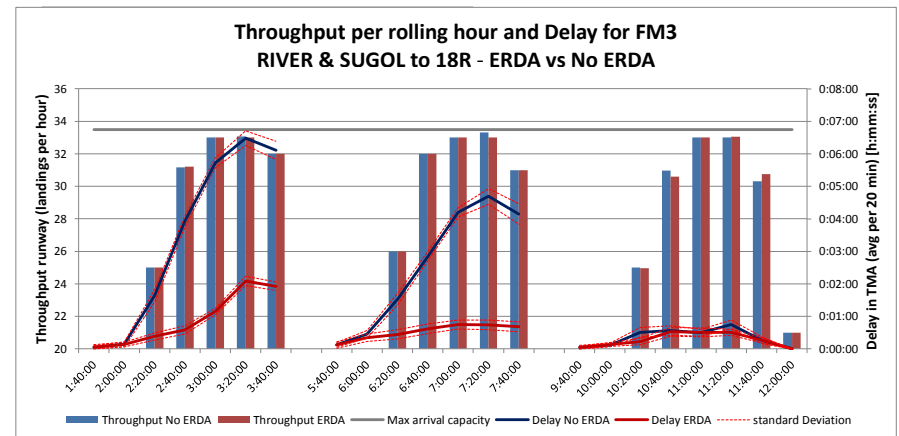


(b)

Figure C.3: Throughput and delay for the three inbound peaks of the scenarios with traffic from ARTIP to 36R, for fleet mix 1 (a) and 2 (b).

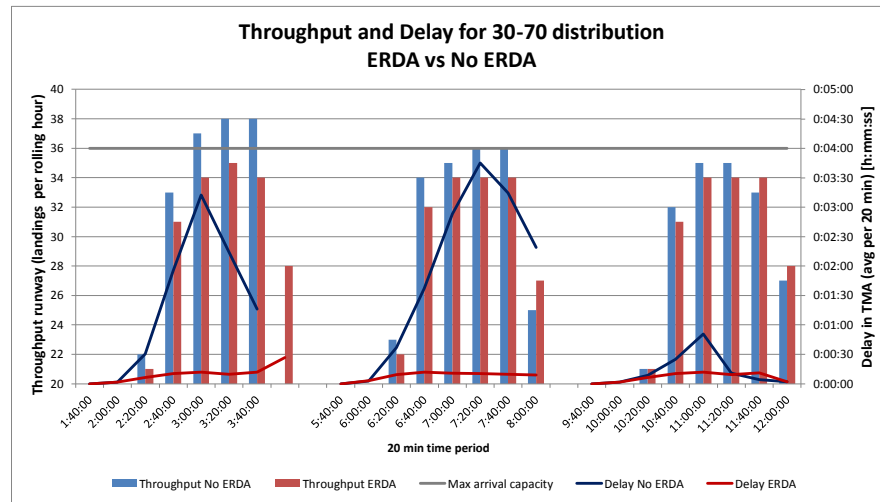


(a)

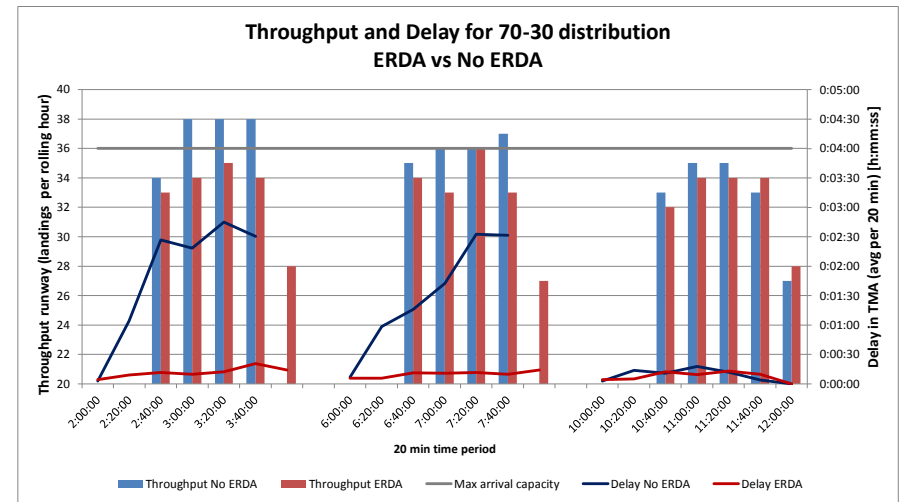


(b)

Figure C.4: Throughput and delay for the three inbound peaks of the scenarios with traffic from RIVER and SUGOL to 18R, for fleet mix 2 (a) and 3 (b).



(a)



(b)

Figure C.5: Throughput and delay for the three inbound peaks of the scenarios with different distributions of arrivals at LORNI and MOPAR.

Acronyms

AAA	Amsterdam Advanced ATM system	EAT	Estimated Approach Time
ACC	Area Control Centre	ETA	Estimated Time of Arrival
AIP	Aeronautical Information Publication	ETO	Estimated Time Over
AMAN	Arrival Management	FAF	Final Approach Fix
ANSP	Air Navigation Service Provider	FIR	Flight Information Region
APLN	Arrival Planner	FL	Flight Level
APP	Approach (control centre)	IAF	Initial Approach Fix
ATA	Actual Time of Arrival	IAS	Indicated Air Speed
ATC	Air Traffic Control	ICAO	International Civil Aviation Organisation
ATCO	Air Traffic Controller	IFR	Instrument Flight Rules
ATM	Air Traffic Management	ILS	Instrument Landing System
ATO	Actual Time Over	LIV	Landing Interval Ratio
BADA	Base of Aircraft Data	LVNL	Air Traffic Control the Netherlands
CDA	Continuous Descent Approach	MRS	Minimum Radar Separation
CDG	Charles de Gaulle airport	MUAC	Maastricht Upper Airspace Control Centre
CDO	Continuous Descent Operation	SARA	Speed And Route Advisor
CFMU	Control Flow Management Unit	STAR	Standard Arrival Route
CTA	Control Area	TMA	Terminal Manoeuvring Area
CTO	Controlled Time Over	TP	Trajectory Predictor
ERDA	En-Route Delay Absorption	XMAN	Cross-border Arrival Management